On the Role of Chloroplast Plastoglobule Lipoprotein Particles in Vitamin E Biosynthesis

A dissertation submitted to the
UNIVERSITY OF NEUCHATEL
for the degree of
Doctor of Natural Sciences

Presented by PIERRE-ALEXANDRE VIDI
from the Institute of Botany, Laboratory of Plant Physiology

Accepted on the recommendation of
Prof. Felix Kessler, thesis director
Prof. Jean-Marc Neuhaus
Prof. Samuel Zeeman
Prof. Danny Schnell
the 10 July 2006

Keywords: Chloroplasts, plastoglobules, lipid bodies, plastoglobulins, tocopherol cyclase, vitamin E.

Mots-clefs: Chloroplastes, plastoglobules, corps lipidiques, plastoglobulines, tocophérol cyclase, vitamin E.

Université de Neuchâtel

IMPRIMATUR POUR LA THESE

On the Role of the Chloroplast Plastoglobules Lipoprotein Particles Vitamin E Biosynthesis

Pierre-Alexandre VIDI

UNIVERSITE DE NEUCHATEL

FACULTE DES SCIENCES

La Faculté des sciences de l'Université de Neuchâtel,
sur le rapport des membres du jury

MM. F. Kessler (directeur de thèse),
J.-M. Neuhaus,
S. Zeeman (ETH Zürich)
et D. Schnell (Uni. of Massachusetts USA)

autorise l'impression de la présente thèse.

Neuchâtel, le 11 septembre 2006 Le doyen :

J.-P. Derendinger

UNIVERSITE DE NEUCHATEL
FACULTE DES SCIENCES
Secrétariat-décanat de la faculté
Rue Emile-Argand 11 - CP 158
CH-2009 Neuchâtel

Faculté des Sciences
■ Rue Emile-Argand 11 ■ CP 158 ■ CH-2009 Neuchâtel
■ Téléphone : +41 32 718 21 00 ■ Fax : +41 32 718 21 03 ■ E-mail : secretariat.sciences@unine.ch ■ www.unine.ch

Contents

Abstract

Chloroplasts contain lipoprotein particles termed plastoglobules. Plastoglobules are generally believed to have little function beyond lipid storage. However, increased plastoglobule size and number has been correlated with oxidative stress conditions indicating dynamic behaviour. Structural proteins from the PAP/fibrillin family are associated with plastoglobules and are upregulated under various environmental stresses. We have identified AtPGL35 as an *Arabidopsis thaliana* plastoglobule marker protein, and shown that its upregulation under oxidative stress conditions parallels increase of plastoglobule size in chloroplasts.

In order to discover new components and functions of plastoglobules, proteins from purified Arabidopsis plastoglobules have been identified by tandem mass spectrometry. The identified peptides belonged to PAP/fibrillins and to known metabolic enzymes including the tocopherol cyclase (AtVTE1), catalysing the penultimate step of α-tocopherol (Vitamin E) biosynthesis. In addition, plastoglobules were shown to be a major site of α-tocopherol accumulation. The data presented suggest that the cyclase reaction is the only step of the α-tocopherol biosynthesis pathway occurring in plastoglobules. Association of AtVTE1 with plastoglobules indicates that these lipid-bodies are not mere storage sites for tocopherols but that they are involved in their synthesis.

Plants are emerging as cost-effective alternatives for the production of recombinant proteins. Extraction and purification of transgene products are however obstacles for so-called molecular farming. We propose to take advantage of the low-density of plastoglobules for efficient recovery of recombinant proteins. As a proof-of-concept, the yellow fluorescent protein (YFP), fused to an Arabidopsis PAP/fibrillin, was targeted to plastoglobules and purified by a simple gradient flotation centrifugation procedure. Accumulation of the recombinant protein had no apparent effect on plant viability. These results identify plastoglobules as a promising sub-organellar compartment for molecular farming.

Résumé

Les chloroplastes contiennent des corps protéo-lipidiques connus sous le nom de plastoglobules. Les plastoglobules ont longtemps été considérés comme des sites de stockage de lipides. Cependant, des études ont montré que leur nombre et leur volume augmente dans des situations de stress oxydatif. Ces structures ont donc un comportement dynamique. Des protéines structurelles appartenant à la famille des PAP/fibrillines, sont associées aux plastoglobules et leur expression est positivement régulée par plusieurs types de stress environementaux. Nous avons identifié AtPGL35, une protéine marqueur pour les plastoglobules dans la plante *Arabidopsis thaliana*, et montré que la synthèse de cette protéine est induite par divers stress oxydatifs. En parallèle, des observations microscopiques ont montré une augmentation de la taille des plastoglobules dans des chloroplastes exposés à un stress oxydatif.

Dans le but de découvrir de nouveaux composants et de nouvelles fonctions des plastoglobules, un extrait protéique issu de plastoglobules purifiés a été analysé par spectrométrie de masse. Les peptides identifiés appartenaient à des PAP/fibrillines ainsi qu'à des enzymes dont la tocopherol cyclase (AtVTE1), catalysant la pénultième étape de la biosynthèse de l'α-tocopherol (la vitamine E). De plus, un fort enrichissement en tocophérols a été mesuré dans les plastoglobules. Des résultats suggérant que AtVTE1 est la seule enzyme de la voie de synthèse des tocophérols à être localisée dans les plastoglobules sont présentés. La présence de AtVTE1 en association avec les plastoglobules indique que ces corps lipidiques ne sont pas uniquement des sites de stockage, mais qu'ils participent à la synthèse de la vitamine E.

Actuellement, les protéines recombinantes destinées à la médecine et à l'industrie sont principalement produites par des microorganismes ou des cultures de cellules animales. Dans l'optique de limiter les coûts de production et les risques liés aux pathogènes dans les systèmes animaux, les plantes ("l'agriculture moléculaire") représentent une alternative intéressante. Si la production de matériel végétal est peu coûteuse, les étapes de purifications sont un obstacle pour cette technologie. Afin de simplifier les procédures de purification, nous proposons de tirer parti de la faible densité des plastoglobules pour une première étape d'enrichissement. Comme preuve de principe, nous avons généré des plantes exprimant la protéine fluorescente jaune (YFP) fusionnée une PAP/fibrilline. La protéine chimérique a été localisée dans les plastoglobules des plantes transgéniques et a pu être fortement enrichie par une simple cen-

trifugation sur gradient. L'accumulation de la protéine recombinante n'a pas eu de conséquence néfaste apparente pour les plantes. Ces résultats démontrent que les plastoglobules représentent un site d'adressage prometteur pour l'agriculture moléculaire.

List of abbreviations

α-TTP	α-tocopherol transport protein
γ-TMT	γ-tocopherol methyl transferase
% (v/v)	ml/100ml
% (w/v)	g/100ml
E. coli	*Escherichia coli*
ABA	abscissic acid
ABC	ATP-binding cassette
ADRP	adipocyte differentiation-related protein
AOS	allene oxide synthase
ARC	accumulation and replication of chloroplasts
At	*Arabidopsis thaliana*
ATP	adenosine triphosphate
BCP32	*Brassica campestris* 32kDa polypeptide
bp	base pairs
CAB	chlorophyll a/b binding protein
CAD2	CADMIUM-SENSITIVE2
CaMV	cauliflower mosaic virus
CCD	carotenoid cleavage dioxygenase
cDNA	complementary DNA
CDSP34	chloroplastic drought-induced protein of 34kDa
CFP	cyan fluorescent protein
ChrB, C	chromoplast protein B, C
CLA1	CLOROPLASTOS ALTERADOS 1
CTAB	cetyltrimethylammonium bromide
DEPC	diethyl pyrocarbonate
DGAT	diacylglycerol acyltransferase
DMPQ	2,3-dimethyl-6-phytyl-1,4-benzoquinone
DNA	desoxyribonucleic acid
dNTP	desoxy nucleotide triphosphate
DTT	1,4-dithio-DL-threitol
EDTA	ethylenediamine-N,N,N',N'-tetraacetic acid
EST	expressed sequence tag
FBA	fructose-bis-phosphate aldolase
FDH	formate dehydrogenase

FITC	fluorescein isothiocyanate
FR	far red
gDNA	genomic DNA
GFP	green fluorescent protein
GGDP	geranylgeranyldiphosphate
GS	goat serum
HGA	homogentisic acid
His_6	hexahistidinyl-tag
HPPD	4-hydroxyphenylpyruvate dioxygenase
HPT	HGA phytyltransferase
$_{ihp}$RNA	intron-containing self-complementary hairpin RNA
JA	jasmonic acid
kb	kilo base pairs
kDa	kilo Dalton
LB	T-DNA left boarder or Luria-Bertani
LR-white	London Resin-white
MES	2(N-Morpholino)ethanesulfonic acid
MPQ	2-methyl-6-phytyl-1,4-benzoquinone
mRNA	messenger RNA
MS	Murashige and Skoog
Ni-NTA	nickel-nitrilotriacetic acid
NP-40	Nonidet P-40
NPQ	non-photochemical quenching
OCS	octopin synthase gene (from A. tumefaciens)
PAP	plastid lipid associated protein
PCR	polymerase chain reaction
PG1	plastoglobulin 1
PGL	plastoglobulin
phytyl-PP	phytyldiphosphate
pptR	phosphinothricin-resistant
pptS	phosphinothricin-sensitive
PQH2	plastoquinone
PSII	photosystem II
pSSU	precursor of the RSSU
RB	T-DNA right boarder
RGD	arginin - glycin - aspartic acid
RLSU	RuBisCO large subunit
RNA	ribonucleic acid
RNAi	RNA interference
ROS	reactive oxygen species
rRNA	ribosomal RNA
RSSU	RuBisCO small subunit
RT	room temperature
RT-PCR	reverse transcription-PCR
RuBisCO	ribulose-1,5-bisphosphate carboxylase oxygenase
SDS	sodium dodecyl sulfate

SDS-PAGE	SDS-polyacrylamide gel electrophoresis
SXD	sucrose export deficient
TAG	triacylglycerol
TAP	tocopherol associated protein
T-DNA	transfer DNA
TEM	transmission electron microscopy
TIC	translocon at the inner chloroplast membrane
TOC	translocon at the outer chloroplast membrane
tricine	N-tris(hydroxymethyl)methylglycine
Tris	tris(hydroxymethyl)aminomethane
TX-114	triton X-114
UTR	untranslated region
UV	ultra violet
VAR1	VARIEGATED1
VIPP	vesicle-inducing protein in plastids
VTC1	VITAMIN C DEFICIENT1
VTE1-5	VITAMIN E DEFICIENT 1-5
wt	wild type
YEB	yeast extract broth
YFP	yellow fluorescent protein

Upper case, italic	gene, wild type allele (e.g. *AtPGL35*)
Lower case, italic	mutant allele (e.g. *pgl35-4*)
Upper case	protein (e.g. AtPGL35)

Chapter 1

Introduction

1.1 Plastids are highly versatile plant organelles

1.1.1 An overview of plastid types

Plastids form a group of plant-specific organelles. They are seen as the result of an ancient endosymbiotic event where a cyanobacterial ancestor invaded a primitive eukaryotic cell (McFadden, 1999). All plastid types initially derive from proplastids, which are small undifferentiated organelles abundant in meristematic tissues. As suggested by the etymology of their name, plastids (from *plassein*, the Greek for 'to mould' or 'shape') are highly plastic organelles, both in structure and function. The fate of plastids is not definitive and interconversions of plastid types occur during plant development or in response to environmental constrains (Thomson and Whatley, 1980). The best studied plastid differentiation process is the biogenesis of chloroplasts in greening tissues. Upon illumination, thylakoid granum and stroma lamellae are rapidly assembled and the synthesis of photosynthetical proteins is upregulated (Bauer *et al.*, 2001). Conversely, prolonged darkness periods induce the formation of etioplasts which are characterised by tubular membrane arrays known as prolamellar bodies (Amrani *et al.*, 1994). In roots, seeds or tubers, plastids differentiate into storage compartments and accumulate starch (amyloplasts) lipids (elaioplasts) or proteins (Whatley, 1983; Thomson and Whatley, 1980; Newcomb, 1967). Elaioplasts also accumulate in the tapetum, a cell layer facing the anther's locules. In the late stages of pollen maturation, tapetum cells undergo lysis, releasing their lipid content which participates in the formation of the pollen coat (Piffanelli *et al.*, 1998). In maturing fruits and petals, chloroplasts differentiate into chromoplasts. During this process, thylakoid membranes disintegrate, and carotenoid pigments massively accumulate in fibrillar or globular structures, conferring the colourful appearance to the tissues (Lichtenthaler, 1969; Vishnevetsky *et al.*, 1999). Similarly, leucoplasts in white petals originate from chloroplast redifferentiation (Pyke and Page, 1998).

Differentiation of plastids into specialised plastid types is essential for con-

ferring to tissues their functions in metabolism, storage or pollinator attraction. Plastid interconversions require: i) Important changes in the protein assortment achieved through *de novo* protein synthesis in the organelle as well as import of cytosolic precursors (Marano *et al.*, 1993; Bauer *et al.*, 2001) and ii) remodelling of plastid architecture, notably of lipidic structures including internal thylakoid membranes and lipid bodies (Sprey and Lichtenthaler, 1966; Lichtenthaler, 1969).

1.1.2 Compartmentalisation of chloroplasts

The chloroplast is the hallmark organelle in green tissues. It is the site of photosynthesis which allows plants to grow photoautrophically, i.e. harvest solar energy and use CO_2 as a source of carbon. The structure of chloroplasts has been extensively studied by electron microscopy (Staehelin, 1986). The boundary of the organelle is delimited by a double membrane, termed the envelope. The inside of chloroplasts is composed of an aqueous matrix, the stroma, and of an extended membrane system, the thylakoids. Thylakoid membranes are arranged in stacks, the grana, interconnected by stromal lamellae. Starch granules and lipid bodies, referred to as osmiophilic bodies or plastoglobules, are also structures commonly observed in the stroma. The latter are presented in the next section.

Distinct metabolic processes are associated with the different chloroplast compartments. A number of enzymatic reactions, notably involved in lipid biosynthesis, are localised to the inner membrane of the envelope (Joyard *et al.*, 1998). Transporters, regulating influx and efflux of metabolites, also mostly localise to the inner membrane, the outer membrane being largely permeable to small molecular weight compounds. The stroma encompasses a large number of hydrophilic proteins (e.g. the highly abundant enzymes from the Calvin cycle), multiple copies of plastidic DNA, as well as complete transcription and translation machineries. The photosystems, which consist of photosynthetic pigments and proteins, are embedded in the thylakoid membranes. Similar to mitochondria cristae, thylakoid lamellae allow the formation of a proton gradient utilised by the F_1F_0 ATPase to drive ATP synthesis.

1.2 Plastoglobules are ubiquitous plastid lipid bodies

Analysis of chloroplast ultrastructure by electron microscopy has revealed the presence of lipid bodies ('osmiophilic globuli') in the stroma (Greenwood *et al.*, 1963; Lichtenthaler and Sprey, 1966; Thomson and Platt, 1973). The diameter of these bodies, hereafter termed plastoglobules, ranges from 30 nm to 5 μm and varies in different species and plastid types (Lichtenthaler, 1968).

1.2.1 Lipid composition of plastoglobules

The main components of chloroplast plastoglobules are triacylglycerols (TAG) and prenylquinones Plastohydroquinone and tocopherols (vitamin E) are the major prenylquinone constituents while phylloquinone (vitamin K) is present in slight amounts. (Legget Bailey and Whyborn, 1963; Greenwood *et al.*, 1963; Lichtenthaler and Sprey, 1966; Steinmüller and Tevini, 1985; Tevini and Steinmüller, 1985). Traces of chlorophylls and carotenoids (β-carotene, lutein) have also been detected in plastoglobule fractions (Greenwood *et al.*, 1963; Lichtenthaler and Sprey, 1966) but have been considered as thylakoid contamination by Steinmüller and Tevini (1985). Similarly, glyco- and phospholipids have been identified in plastoglobule preparations but their genuine association with plastoglobules has been questioned (Steinmüller and Tevini, 1985).

The lipid composition of plastoglobules from non-green plastids is markedly different from that of chloroplasts. Plastoglobules from gerontoplats in senescing leaves, e.g., accumulate carotenoid esters, oxidised prenylquinones and free fatty acids (Tevini and Steinmüller, 1985). Carotenoid esters are also the major constituents of chromoplast plastoglobules and fibrils (Deruère *et al.*, 1994).

Variations in lipid composition suggest that plastoglobules are highly dynamic structures and that their functions evolve during plastid differentiation.

1.2.2 Protein content of plastoglobules

Early biochemical studies identified nitrogen in purified chloroplast lipid bodies, suggesting the presence of associated proteins (Legget Bailey and Whyborn, 1963). Steinmüller and Tevini (1985) also detected proteins in purified plastoglobules but considered them as thylakoid contamination. This view changed since several groups demonstrated the presence of proteins in carotenoid fibrils of bell pepper fruit chromoplasts and in chloroplast plastoglobules (Deruère *et al.*, 1994; Pozueta-Romero *et al.*, 1997; Wu *et al.*, 1997; Ting *et al.*, 1998; Kessler *et al.*, 1999). These proteins range in size from 30 to 38 kDa and belong to the so-called PAP/fibrillin family. PAP/fibrillins are seen as structural proteins and the corresponding literature is reviewed in section 1.3.

Although PAP/fibrillins are the most abundant peptides in fibrils and plastoglobules, SDS-PAGE analysis indicated that at least a dozen different proteins associate with plastid oil-bodies (Wu *et al.*, 1997; Kessler *et al.*, 1999). Recently, the proteome of Arabidopsis plastoglobules has been unravelled independently by Ytterberg et al. (2006) and by our group (Vidi *et al.*, 2006; see Table 4.2 on page 85). In addition to proteins from the PAP/fibrillin family, enzymes belonging to various biochemical pathways were detected. Fructose-bis-phosphate aldolase (FBA) isoforms, an epoxycarotenoid dioxygenase (CCD4), the allene oxide synthase (AOS), the tocopherol cyclase (VTE1), putative lipid-modifying enzymes, as well as proteins with ATP-binding cassette (ABC) domains were identified in both studies.

1.2.3 Common features of lipid bodies and their associated proteins

In plants, animals and microorganisms, lipid bodies have functions as diverse as energy storage, structural lipid storage, lipid transport and lipid metabolism (Murphy, 2001). Common themes exist between lipid bodies. They consist of a hydrophobic core surrounded by a monolayer of amphiphatic lipids. Peripherally associated proteins are found in most types of lipid bodies and are more or less tightly bound to their surface. Such an architecture was proposed for chromoplast fibrils (Knoth *et al.*, 1986; Deruère *et al.*, 1994), and chloroplast plastoglobules (Kessler *et al.*, 1999).

Proteins associated with lipid bodies have highly diverse physicochemical properties and topologies, reflecting various modes of association with the lipidic structures. In desiccation tolerant seeds, oil bodies are coated with oleosins. A central hydrophobic domain in the proteins, often referred to as "proline knot motif" is essential for their association with oil bodies (Hsieh and Huang, 2004). Interestingly, association of the hepatitis C virus core protein with cytosolic lipid droplets in mammalian cells requires a proline-containing domain similar to that of oleosins (Hope *et al.*, 2002). In mammalian cells, and in certain conditions, caveolins accumulate on the surface of cytoplasmic lipid droplets. Using deletion constructs, Ostermeyer *et al.* (2004) demonstrated requirement of a hydrophobic domain for lipid droplet targeting. Hydrophobic domains were also shown to play important roles in targeting and anchoring perilipin to lipid droplets in adipocytes (Subramanian *et al.*, 2004). Apolipoproteins which associate with lipoproteins contain amphipathic α-helices and β-strands, the apolar surfaces interacting with acyl chains of surface lipids and polar surfaces facing the aqueous environment (Segrest *et al.*, 2001). Although hydrophobic sequences are essential for targeting and anchoring a variety of lipid body proteins, no obvious consensus sequence could be defined, suggesting different modes of protein-lipid association.

If several lipid body proteins are characterised by hydrophobic domains, others lack large apolar regions. Adipophilin (also termed Adipocyte Differentiation-related Protein, ADRP), which localises at the periphery of cytosolic lipid bodies in mammalian cells, has no obvious lipid-binding motif (hydrophobic domains or amphiphatic α-helices; Murphy, 2001) and discontinuous stretches of the protein are necessary for targeting to lipid bodies (Targett-Adams *et al.*, 2003).

Lipid body proteins with highly diverse structures and properties have similar functions. They are generally thought to prevent coalescence of lipid bodies with neighbouring lipophilic structures. In addition, certain lipid body proteins including ADRP induce the formation and regulate the size of the lipid bodies (Imamura *et al.*, 2002; Fukushima *et al.*, 2005).

1.2.4 Proposed functions of plastoglobules

In chloroplasts, plastoglobules are associated with thylakoid membranes (Kessler *et al.*, 1999; Austin *et al.*, 2006), suggesting that they play a role in thylakoid

membrane function, possibly as a reservoir for certain lipids (Lichtenthaler, 1968). Indeed, plastoglobules enlarge during thylakoid disassembly in senescing chloroplasts (Lichtenthaler, 1968; Tuquet and Newman, 1980; Ghosh *et al.*, 2001; Keskitalo *et al.*, 2005). Their accumulation in senescing rosette leaves of Arabidopsis correlates temporally with the activation of diacylglycerol acyltransferase 1 (AtDGAT1) and with enhanced synthesis of TAGs (Kaup *et al.*, 2002). Dismantling of thylakoid membranes during senescence allows remobilisation of energy for seed production. TAG accumulating in plastoglobules must therefore leave plastids in order to be converted into sugars through β-oxidation and the glyoxylate cycle. Evidence gained from ultrastructural analysis of senescing plastids indicated that plastoglobules are released from gerontoplasts through a blebbing process (Guiamet *et al.*, 1999; Keskitalo *et al.*, 2005).

Plastoglobules may also be involved in the formation of thylakoid membranes in de-etiolating plastids. After exposure to light, the number of plastoglobules was shown to decrease in barley etioplasts while prolamellar bodies were converted into thylakoid lamellae (Sprey and Lichtenthaler, 1966). Plastoglobules in etioplasts may therefore represent a lipid reservoir allowing the rapid formation of thylakoids in greening tissues.

Plastoglobules have also been implicated in chloroplast to chromoplast transition. During chromoplast differentiation, plastoglobules enlarge (Lichtenthaler, 1968) and accumulate esterified isoprenoids (Steinmüller and Tevini, 1985). In certain species, plastoglobules elongate to form fibrillar structures (Thomson and Whatley, 1980; Vishnevetsky *et al.*, 1999).

Although roles of plastoglobules in chromoplast differentiation and in thylakoid formation and dismantling have been defined, their functions in mature chloroplasts remain largely unknown.

1.3 PAP/fibrillins: proteins associated with plastid lipid bodies

1.3.1 Discovery of PAP/fibrillins

Studies on fruit ripening in bell pepper resulted in the identification of chromoplast proteins strongly upregulated during fruit maturation (Hadjeb *et al.*, 1988; Newman *et al.*, 1989). A major peptide of 35 kDa was identified independently by tree groups and designated ChrB (Newman *et al.*, 1989), fibrillin (Deruère *et al.*, 1994) or PAP (Pozueta-Romero *et al.*, 1997). A homologous protein (ChrC) was subsequently identified in cucumber flowers (Vishnevetsky *et al.*, 1996). Expression of fibrillin and ChrC was first proposed to be restricted to chromoplast-containing tissues such as fruits and corollas (Deruère *et al.*, 1994; Vishnevetsky *et al.*, 1996). However Pozueta-Romero and colleagues detected fibrillin in leaves and expression of a fibrillin homolog in citrus leaves was reported (Moriguchi *et al.*, 1998). Moreover, homologous proteins were identified in leaves from pea (PG1; Kessler *et al.*, 1999) and turnip (PAP1-3; Kim *et al.*, 2001), as well as in anthers from rapeseed (BCP32; Ting *et al.*, 1998), indicat-

ing that PAP/fibrillin proteins are not chromoplast-specific and associate with various types of lipid bodies.

1.3.2 PAP/fibrillins are proteins of ancient origin

PAP/fibrillin homologues from a large number of plant species including pea (PG1), bell pepper (fibrillin), potato (CDSP34), tobacco, turnip (PAP1-3), citrus (CitPAP), rice and maize are present in the database. Several cyanobacterial proteins contain a PAP/fibrillin motif. Related proteins are however absent from bacterial, animal and fungal genomes.

The broad distribution of PAP/fibrillins and their presence in cynobacteria indicate an ancient origin of the protein family. Phylogenetic analysis further suggested that plant and cyanobacterial PAP/fibrillins evolved from a single cyanobacterial ancestor and that most of them diverged after the endosymbiotic event leading to chloroplasts (Laizet *et al.*, 2004).

1.3.3 Structural functions of PAP/fibrillins

Immunogold-electon microscopy studies have shown that fibrillin and PG1 associate at the periphery of plastoglobules (Deruère *et al.*, 1994; Pozueta-Romero *et al.*, 1997; Kessler *et al.*, 1999). The proteins do not share sequence homology with known enzymes. Moreover, Deruère and collaborators (1994) could reconstitute fibrils *in vitro* by adding purified fibrillin to chromoplast lipids. Overexpressing fibrillin in tobacco lead to an increase in plastoglobule number and to the formation of plastoglobule clusters (Rey *et al.*, 2000). The role of PAP/fibrillins is therefore probably mainly structural, maintaining the shape of oil-bodies and preventing their coalescence. PAP/fibrillins may also be involved in the formation of plastoglobules and in the disassembly of photosynthetic membranes during senescence or chloroplast to chromoplast transition.

Several PAP/fibrillins were shown to associate with thylakoid membranes (Eymery and Rey, 1999; Monte *et al.*, 1999; Rey *et al.*, 2000) and a role in the modulation of photosynthetic activity was proposed (Monte *et al.*, 1999).

1.4 Plastoglobules may participate in adaptation to oxidative stress

1.4.1 A network of antioxidants protects chloroplast membranes

Adverse conditions like drought, high salinity or high light intensity lead to the formation of reactive oxygen species, notably in chloroplasts. If they accumulate, ROS cause oxidative damage including lipid peroxidation, denaturation of proteins as well as damage to nucleic acids. Controlling the redox homeostasis is therefore essential for maintaining an active metabolism. Hydrophilic antioxidants (glutathione and ascorbate) and lipophilic antioxidants (xanthophylls and

tocopherols) are present in chloroplasts and effectively scavenge ROS (Foyer and Noctor, 2005). A number of studies have shown that their concentrations strongly increase during oxidative stress, improving the capacity to scavenge the radicals (e.g. Collakova and DellaPenna, 2003; Havaux *et al.*, 2005; Munne-Bosch and Alegre, 2000, 2003).

Arabidopsis mutants with reduced levels of antioxidants are available. The *npq1* mutant is deficient in violaxanthin deepoxidase and hence in zeaxanthin biosynthesis (Niyogi *et al.*, 1998). *vtc1* (Conklin *et al.*, 1996) and *cad2* (Howden *et al.*, 1995; Cobbett *et al.*, 1998) have reduced levels of ascorbate and glutathione, respectively, and *vte1* plants lack tocopherols (Porfirova *et al.*, 2002).

1.4.2 Tocopherols act as lipid antioxidants in plastids and accumulate in plastoglobules

Tocopherols are known to protect membrane lipids from oxidative damage by scavenging radicals and by quenching ROS (reviewed in Munne-Bosch, 2005; Schneider, 2005). Tocopherols were recently shown to prevent photoinactivation of the photosystem II (Havaux *et al.*, 2005). They also protect seed storage lipids from oxidation (Sattler *et al.*, 2004). Moreover, a strong increase in tocopherol synthesis accompanies chloroplast-to-chromoplast differentiation in pepper fruits (Lichtenthaler, 1969; Camara *et al.*, 1982). During this process, chromoplasts acquire their colour by massively accumulating carotenoids. Tocopherol probably protects the pigments as well as lipids from envelope membranes against photo-oxidative degradation. In chloroplasts, absence of tocopherols is accompanied by an increased photoinhibition under conditions of photo-oxidative stress (Porfirova *et al.*, 2002; Maeda *et al.*, 2005). When reduction of tocopherols and glutathione (Kanwischer *et al.*, 2005) or zeaxanthin (Havaux *et al.*, 2005) contents were combined, stronger photoinhibition was observed, indicating that photoprotection is guaranteed by a network of antioxidants, including tocopherols.

Tocopherols have been detected in all chloroplast membranes and notably in plastoglobules (Lichtenthaler and Sprey, 1966; Lichtenthaler and Peveling, 1967; Munne-Bosch and Alegre, 2002). In these studies, a strong enrichment in prenylquinones was observed in plastoglobules compared to total chloroplast extracts. Moreover, comparison of various plastid types revealed a positive correlation between plastoglobule abundance and prenylquinone contents. Recently, tocopherol measurements in Arabidopsis chloroplast membrane fractions showed that around 50% of the tocopherol pool is localised in plastoglobules, representing a 25 fold enrichment with regard to thylakoids (Vidi *et al.*, 2006). To date, however, the function of tocopherols in chloroplast plastoglobules is not known.

1.4.3 Morphological studies have implicated plastoglobules in plant stress response

Enlarged plastoglobules have been described in chloroplasts under conditions resulting in oxidative stress such as drought (Eymery and Rey, 1999; Rey *et al.*, 2000), hypersalinity (Locy *et al.*, 1996), nitrogen starvation (Bondada and Syvertsen, 2003), and growth in presence of heavy metals (e.g. Duret *et al.*, 1986; Panou-Filotheou *et al.*, 2001). In aloe plants exposed to strong sunlight and drought stress, accumulation in leaves of the red carotenoid rhodoxanthin paralleled transformation of chloroplasts into plastoglobule-rich chromoplasts (Merzlyak *et al.*, 2005). Studies on spruce and aspen trees have also identified swelling of plastoglobules as part of the physiological response to elevated ozone concentrations (e.g. Oksanen *et al.*, 2001; Ebel *et al.*, 1990).

Ageing also seems to affect plastoglobule morphology. Older broad bean leaves had significantly larger plastoglobules than younger ones (Greenwood *et al.*, 1963). The same observation was made in rhododendron leaves (Nilsen *et al.*, 1988). Since levels of reactive oxygen species are known to raise with time in plastids (Munne-Bosch and Alegre, 2002), swelling of plastoglobules in older chloroplasts may represent a response to the increase of ROS concentration.

1.4.4 Several PAP/fibrillins are upregulated by oxidative stress

Upregulation of several PAP/fibrillins has been observed as a consequence of various treatments generating reactive oxygen species (see Table 1.1). These include drought, cold, salt and high light stresses. Based on the localisation of potato CDSP34 to thylakoid membranes (Pruvot *et al.*, 1996a), Gillet and collaborators (1998) proposed a model in which the protein would associate with thylakoid lipids, hence stabilising the photosynthetic membranes and protecting them from oxidative damage.

Supporting a role of PAP/fibrillins in stress response, deregulation of these proteins was shown to affects plant growth and stress tolerance. Overexpression of pepper fibrillin in tobacco enhanced growth under high light intensities as well as drought tolerance (Rey *et al.*, 2000). In contrast, antisense potato plants with reduced levels of C40.4 displayed stunted growth and reduced tuber yield (Monte *et al.*, 1999). Interestingly, xanthophyll content was reduced in C40.4 antisense plants, indicating a possible link between plastoglobules and carotenoid synthesis. Recently, Yang *et al.* (2006) could show a correlation between maximal photochemical efficiency of photosystem II (Fv/Fm) and levels of an Arabidopsis fibrillin homologue in light stress conditions. Reduction of Fv/Fm values is regarded as photoinhibition of PSII (Bailey *et al.*, 2002). These results therefore strengthen the view that PAP/fibrillins directly or indirectly protect the photosynthetic apparatus.

Taken together, these observations identify increases in plastoglobule size and number, as well as upregulation of PAP/fibrillins as responses to environmental stress. How plastoglobules mediate stress tolerance is however unknown

and understanding of the molecular events underlying these physiological responses is lacking.

1.5 Aim of this work

Numerous studies on chloroplast ultrastructure (cited above) have shown that plastoglobules are involved in diverse physiological responses including senescence, chloroplast-to-chromoplast transition and adaptation to oxidative stress. With the exception of the well documented chromoplast differentiation in ripening fruits, the molecular basis of these processes are largely unknown. Due to the availability of its genome sequence (*The Arabidopsis Genome Initiative*, 2000) and of large mutant populations (Bouche and Bouchez, 2001), *Arabidopsis thaliana* has become the plant model organism of choice for molecular genetic studies. We therefore decided to use Arabidopsis leaves as a model system to study the function of plastoglobules.

As an entry point for the study of plastoglobules and their associated proteins, the first task of this thesis was to identify homologs of PG1 in Arabidopsis and to analyse their expression. To establish the model system and to further investigate the function of plastoglobules, a second aim was to identify a reliable Arabidopsis plastoglobule marker protein and to determine whether oxidative stress leads to changes in plastoglobule morphology in Arabidopsis, as observed for other species.

Analysis of low-density chloroplast membrane fractions recently suggested association of the tocopherol cyclase AtVTE1 with plastoglobules. The third goal of this work was to confirm localisation of AtVTE1 to plastoglobules.

Proteins associated with plastoglobules or related fibrils in pea chloroplasts and bell pepper chromoplasts have been documented. However, the mode of association of these proteins with plastid lipid bodies is unknown. An objective of this study was to address whether localisation of PAP/fibrillins to plastoglobule rely on targeting determinants in their amino acid sequences and to use this knowledge for targeting recombinant proteins to plastoglobules as a strategy for molecular farming.

Table 1.1: Induction of PAP/fibrillin expression by treatments generating oxidative stress.

PAP/fibrillin	**Species**	**Treatment**	**Reference**[a]
FIBRILLIN (FIB)	Bell pepper	Drought	1
		Wounding	1
	Arabidopsis	High light	2,3
FIB promoter	Tobacco	Drought	1
		Wounding	1
		Methyl viologen	1
	Tomato	Drought	4, 5
		Cold	5
		High light	5
		High salinity	5
		Wounding	1, 5
		Methyl viologen	1
		Hydrogen peroxide	5
		Biotic stress [b]	6
		Ageing	6
CDSP34	Potato	Drought	6-10
		Cold	8
		High light	6, 9
		High salinity	8
		Methyl viologen	6
		Hydrogen peroxide	6
		γ irradiation	6
CDSP34-related	Tomato	Drought	6
	Tobacco	Drought	6
	Arabidopsis	Drought	6
	Craterostigma	Drought	6
	Barley	Drought	6
	Tobacco	High light	10
	Tomato	Biotic stress [c]	6

[a] 1. Chen *et al.*, 1998; 2. Yang *et al.*, 2006 3. Giacomelli *et al.*, 2006 4. Kuntz *et al.*, 1998; 5. Manac'h and Kuntz, 1999; 6. Langenkamper *et al.*, 2001; 7. Pruvot *et al.*, 1996a 8. Pruvot *et al.*, 1996b 9. Gillet *et al.*, 1998 10. Rey *et al.*, 2000

[b] *Erwinia chrysanthemi*, strain 3739

Chapter 2

Results

2.1 Characterisation of Arabidopsis plastoglobulins

2.1.1 Homology searches identify 13 plastoglobulin genes in the Arabidopsis genome

Previous work in pea and bell pepper led to the identification of highly conserved proteins associated with plastoglobules (Kessler *et al.*, 1999; Pozueta-Romero *et al.*, 1997). Pea PG1 and bell pepper fibrillin both represent major plastoglobule proteins and belong to the so-called PAP/fibrillin family. We have used sequence homology search to identify Arabidopsis homologues of PG1. Thirteen genes, coding for proteins ranging from 24 to 45 kDa, were identified (Fig. 2.1). The same set of genes was also identified by Laizet *et al.* (2004). Expressed sequence tags (ESTs) for all the corresponding genes are present in the database (The Arabidopsis Information Resource, http://www.arabidopsis.org/), ruling out the presence of pseudogenes in the family. All 13 proteins contain a PAP/Fibrillin Pfam motif (PF04755) and possess a predicted chloroplast transit peptide. Because PAP and FIB have already been defined by the International Arabidopsis Community as standing for phosphatidic acid phosphatase and fibrillarin respectively, we propose to abbreviate Arabidopsis PAP/fibrillins as PGL (plastoglobulin) and to differentiate between them using the predicted molecular weight of their precursors.

Multiple sequence alignment of AtPGL amino acid sequences (Fig. 2.1A) identified two conserved regions. The first domain (residues 116-151 of AtPGL35) is characterised by abundant prolines (NPTPxP) and a conserved glycin-leucin/arginin-tryptophan stretch. The second domain, located at the C-termini, includes a RGD cell adhesion motif (D'Souza *et al.*, 1991).

Phylogenetic analysis of Arabidopsis plastoglobulins (Fig. 2.1B) revealed three pairs of closely related AtPGLs (*AtPGL35* and *-33*; *AtPGL30* and *-34*; *AtPGL25* and *-29*). The corresponding genes are located on highly similar

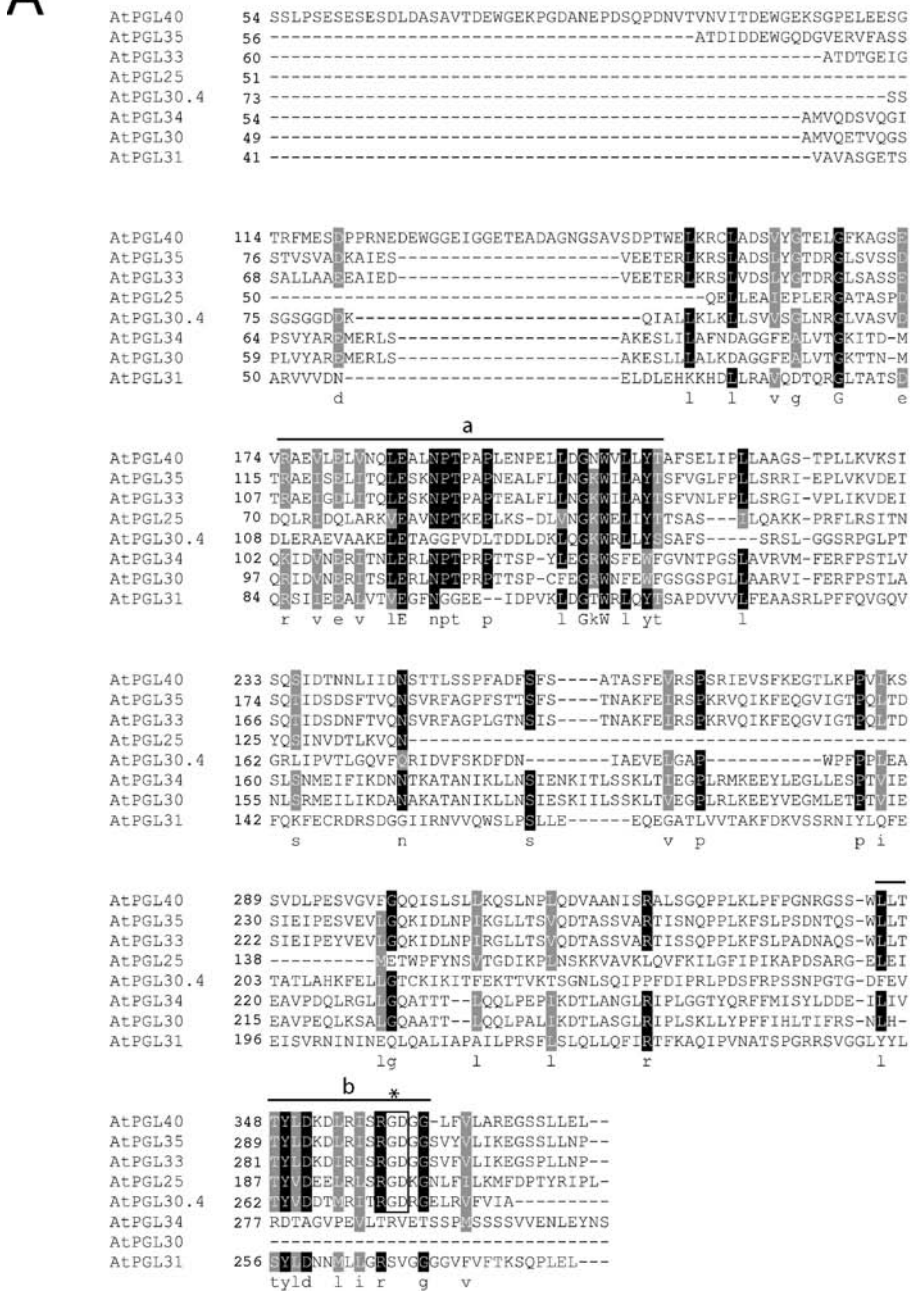

Figure 2.1: The Arabidopsis plastoglobulin family (see caption on page 13).

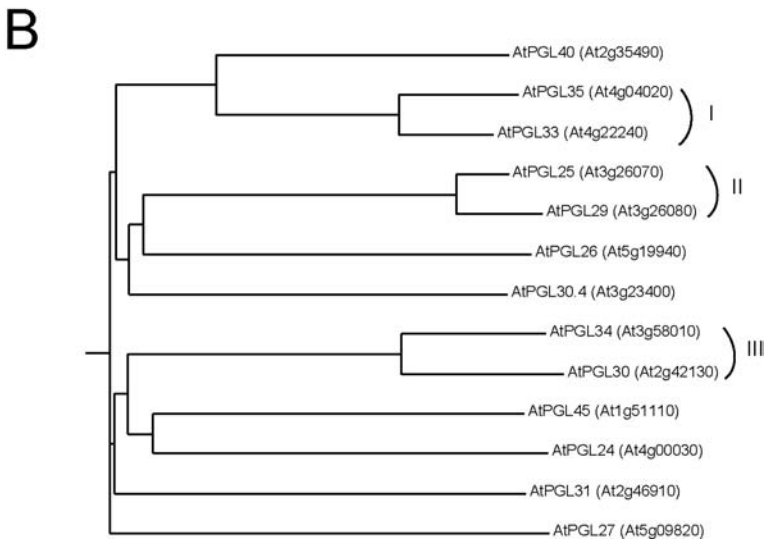

Figure 2.1: The Arabidopsis plastoglobulin family (continued). **A**, Multiple sequence alignment of Arabidopsis plastoglobulins (PGLs). Amino acid sequences from AtPGLs identified in the proteome of plastoglobules (see section 1.2.2 on page 3) were aligned using ClustalW. Transit peptides were predicted using the TargetP software and removed from the protein sequences. The alignment was formatted with the BOXSHADE 3.21 software. Conserved regions (a and b), as well as RGD motifs (star) are highlighted. Residues identical in at least 6 sequences are shaded. Identical residues are in black and conserved substitutions are in grey. Consensus amino acid residues are shown below the alignment. **B**, Phylogenetic analysis of Arabidopsis plastoglobulins. A phylogenetic tree was generated using dendrograms generated by ClustalW and the Phylodendron software. AGI gene codes are indicated in bracket. Duplicated gene groups are indicated with roman numbers.

chromosome fragments, indicating recent gene duplication events (http://www-.tigr.org/tdb/e2k1/ath1/Arabidopsis_genome_duplication.shtml).

Several Arabidopsis PGLs (AtPGL45, -40, -35, -33, -30.4 and -25) have been identified in proteomic studies of thylakoids (Friso *et al.*, 2004; Kleffmann *et al.*, 2004). This is not surprising since plastoglobules are often found in close contact with thylakoid membranes in electron microscopy studies (Kessler *et al.*, 1999; Austin *et al.*, 2006). With the exception of AtPGL45, these proteins were also identified by Ytterberg *et al.* (2006) and our group (Vidi *et al.*, 2006; see Table 4.2) in the proteome of plastoglobules.

2.1.2 Arabidopsis plastoglobulins have overlapping but distinct expression patterns

In a first attempt to characterise Arabidopsis plastoglobulins, we analysed publicly available microarray data using the Genevestigator toolbox (Zimmermann *et al.* 2004; https://www.genevestigator.ethz.ch/at/). Microarray probesets were found for all Arabidopsis PGLs except *AtPGL33* and *AtPGL29* . Probesets for *AtPGL35* and *-25* were non-unique, i.e. represented two (or more) closely related genes. Since AtPGL35 and -33 share a high degree of similarity (84%), transcripts from both genes probably hybridise to the same probeset. The same is true for AtPGL25 and -29 which share 76% similarity.

All AtPGL genes for which probesets were available were expressed above background levels, at least in leaves and cotyledons (data not shown). The different plastoglobulins showed overlapping but distinct patterns of expression (Fig. 2.2). *AtPGL25* transcript, for example, was over-represented in siliques, *AtPGL27*, *-30* and *-45* were mostly expressed in pedicels and, unlike most plastoglobulins, *AtPGL31* was expressed in pollen grains. Interestingly, a single plastoglobulin (*AtPGL24*) showed highest signals in senescing leaves. Comparing microarray data from three replicate experiments revealed a 1.9 fold higher expression of *AtPGL24* in senescing compared to adult rosette leaves. With some exceptions, plastoglobulin transcripts were present predominantly in green tissues. Most Arabidopsis plastoglobulins were expressed in leaves and cotyledons. In contrast, lowest messenger levels were generally observed in pollen, seeds and roots. These observations suggest that members of the plastoglobulin family play a role in chloroplast function. However, the presence of transcripts of certain AtPGLs in non-photosynthetic tissues (e.g. *AtPGL34* in roots) suggests that these proteins are involved in the metabolism of multiple plastid types. Moreover, high transcript levels of certain AtPGLs in petals (containing mostly leukoplasts) parallels the high levels of fibrillin detected in ripening fruit chromoplasts (Deruère *et al.*, 1994), and suggests association with non-photosynthetic lipid structures.

Expression of *AtPGL35*, which is a close homologue to pea PG1, was further studied. To analyse the spatial distribution of *AtPGL35* transcripts, Arabidopsis plants were grown on soil under 16h light conditions for 4 weeks. RNA extracted from different organs was then used for Northern blot analysis. *AtPGL35* transcripts were detected using a [^{32}P]-labelled probe synthesised from *AtPGL35*

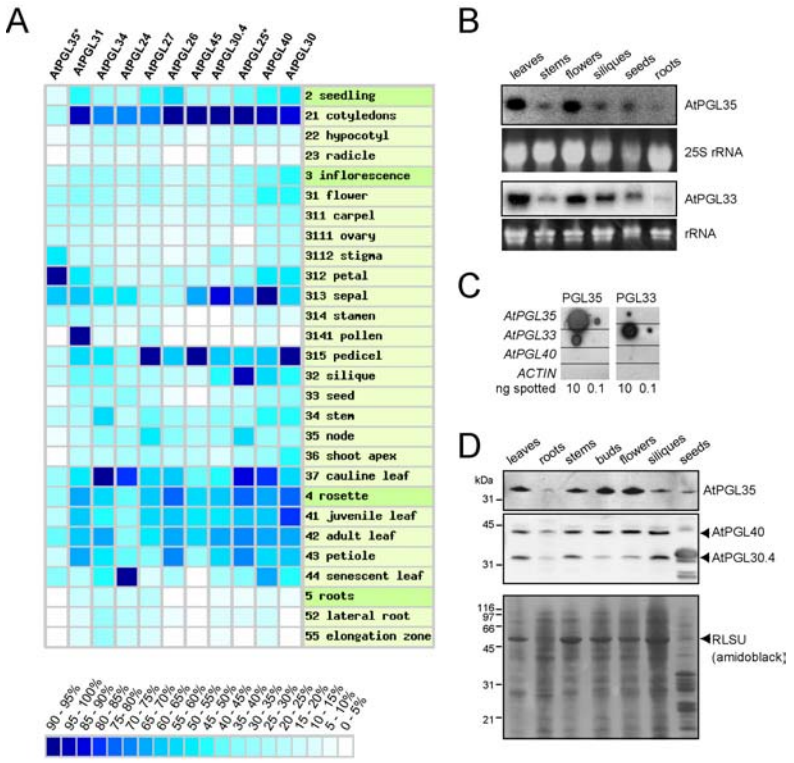

Figure 2.2: Spatial expression patterns of Arabidopsis plastoglobulins. **A**, Expression profile of AtPGLs in different organs and developmental stages. Public microarray data were analysed using the Genevestigator software. The blue-white heat map reflects signal intensity values. All gene-level profiles were normalised for colouring such that for each gene the highest signal intensity obtained a value of 100% (dark blue) and absence of signal obtained a value of 0% (white). Probesets for genes labelled with a star are non-unique. **B**, Northern analysis of the distribution of *AtPGL35* and *AtPGL33* transcripts in plant organs. RNA extracted from rosette leaves (leaves), stems, flowers, siliques, seeds or roots was used for acrylamide gel electrophoresis followed by Northern blotting. *AtPGL35* and *AtPGL33* mRNAs were detected using gene specific [^{32}P]-labelled probes. Ribosomal RNA (rRNA) indicates comparable loading amounts. **C**, Spot tests of probes specificity. Coding sequences from *AtPGL35*, *-33*, *-40* and *ACTIN* were amplified by PCR and 10 or 0.1 ng were spotted on nylon membranes. Membranes were hybridised with probes specific to *AtPGL35* (PGL35) or *AtPGL33* (PGL33). **D**, Western blot analysis of the distribution of AtPGL35, -40 and -30.4 in plant organs. Total protein extracts (25 μg) of rosette leaves (leaves), roots, stems, flower buds (buds), flowers, siliques or seeds were analysed by Western blotting using antibodies specific to AtPGL35, AtPGL40 and AtPGL30.4. The amidoblack-stained membrane is shown. Position of the large subunit of RuBisCO (RLSU) is indicated.

coding sequence template. As shown in Fig. 2.2B, *AtPGL35* transcripts were predominantly detected in rosette leaves and in flowers. Transcript abundance was lower in stems, siliques and seeds and was close to detection limit in roots. The results are in accordance with the microarray data. The latter suggest strongest expression of *AtPGL35* in petals. Since whole flowers were used for Northern analysis (vs. isolated petals or other floral organs for microarray analysis), transcripts from petals were diluted with mRNAs from other floral organs in the Northern experiment. Expression of *AtPGL33*, which shares high sequence similarity with *AtPLG35*, was also monitored by Northern blot (Fig. 2.2B). The distribution of *AtPGL33* and *-35* transcripts was very similar, with highest levels in leaves and flowers. Using a dot blot experiment, cross-hybridisation of the probes was estimated to 1% (Fig. 2.2C).

To determine if PGL protein and RNA levels correlate, plant organs were used for Western blot analysis. Total proteins were isolated from rosette leaves, roots, stems, flower buds, flowers, siliques or seeds as described (Rensink *et al.*, 1998). Proteins were resolved by SDS-PAGE, blotted to nitrocellulose membrane and AtPGL35, -40 or -30.4 were detected using specific antibodies (Fig. 2.2D). The α-AtPGL35 antibody decorated a single protein in the different extract with an apparent mass of 32 kDa. The predicted molecular weight of mature AtPGL35 (residues 56-318) is 29 kDa. A shift between predicted and apparent mass was also observed for AtPGL40 (37/43 kDa) and AtPGL30.4 (23/32 kDa) and similar differences were reported for homologous proteins (Ting *et al.*, 1998). The slightly acidic character of AtPGL35 and -40 (theoretical pI 4.6 and 4.3) could account for this difference. AtPGL30.4, however, showed the largest discrepancy between predicted and apparent mass and has a predicted isoelectric point of 5.9. Post-translational modifications of the proteins may also account for the observed behaviour on SDS-PAGE.

AtPGL35 was mostly detected in green tissues as well as in flowers or flower buds. Weak signals were detected in roots and seeds. This result is in good agreement with microarray and Northern data. AtPGL40 and -30.4 showed a similar distribution to that of AtPGL35. AtPGL30.4, however, was less abundant in flowers and flower buds. In seeds, strong signals were given by anti-AtPGL30.4 and -40 antibodies. These corresponded in size to abundant 12S cruciferin proteins (Hou *et al.*, 2005) and may therefore have resulted from unspecific cross-reactions. Alternatively, these could reflect presence of AtPGL degradation products in seeds. To exclude the possibility that AtPGLs were degraded during preparation of the protein extract, seed protein were extracted directly in SDS sample buffer as described (Hennig *et al.*, 2002). Similar results were obtained (data not shown) indicating that protein degradation had not occurred during sample preparation.

2.1.3 Several Arabidopsis plastoglobulins are regulated by light

The observation that most AtPGLs are predominantly expressed in green tissues (Fig. 2.2A) suggests that plastoglobulins may be regulated by light. To verify

this hypothesis, AtPGL transcript levels in etiolated seedlings and in seedlings exposed to white light for 4 hours were compared using the Genevestigator Digital Northern toolbox (Zimmermann *et al.*, 2004). Data for AtPGL genes for which signal values were significantly higher than background are shown in Fig. 2.3A. At least *AtPGL26*, *-30.4* and *-45* were induced by the treatment. Transcripts from *AtPGL45* accumulated more than six fold after light treatment. This is comparable with the upregulation of the chlorophyll a/b binding protein (CAB, AT1G29910). *AtPGL30.4* was two-fold upregulated already 45 minutes after illumination.

To verify whether light treatment also triggers accumulation of PGL proteins, Arabidopsis plants were grown for 8 days in the dark or in a 16h/8h light/dark regime. As expected, protein levels of the CAB and of the large subunit of RuBisCO (RLSU) were higher in de-etiolated seedlings (Fig. 2.3B). AtPGL35 and AtPGL30.4 were more abundant in light-grown compared to etiolated seedlings, indicating that not only PGL transcripts but also protein levels increased after exposure to light. In contrast, light treatment had little or no impact on the expression of other AtPGLs, notably *AtPGL34* and *AtPGL40*, suggesting involvement of the proteins in general plastid metabolism. The observation that these proteins are also expressed in roots (Fig. 2.2), supports this idea.

At least two models could account for the observed accumulation of several AtPGLs in light conditions. In a first model, photoreceptors sensing the light would act positively on AtPGL transcription. The control of a large set of genes related with chloroplast metabolism is mediated by phytochomes, photoreceptors absorbing red and far red (FR) light (Schafer and Bowle, 2002). In an alternative model, oxidative stress in chloroplasts caused by illumination may indirectly trigger accumulation of AtPGLs. Indeed, several studies have shown accumulation of plastoglobulins in environmental conditions resulting in oxidative stress (see Table 1.1). To distinguish between these two models, accumulation of AtPGL transcripts after exposure to white, red or far red light was compared using a digital Northern (Fig. 2.3C). All plastoglobulin genes which were strongly induced by white light responded to FR light. Furthermore, *AtPGL26* and *-30.4* were also upregulated by red light. Longer wave length light have lower energy content and FR light is not or little absorbed by photosynthetical pigments. FR light is therefore expected to cause only little photooxydative stress in plastids. These preliminary results therefore strongly suggest a direct effect of light on the transcription of several AtPGL genes.

2.1.4 AtPGL35 as an Arabidopsis plastoglobule marker protein

Studying plastoglobules required a reliable marker protein for this chloroplast compartment. We chose AtPGL35, which shares a high degree of similarity with the pea plastoglobulin PG1, as a candidate marker protein for Arabidopsis plastoglobules. Although PG1 and the closely related pepper fibrillin were shown to associate with plastoglobules (Kessler *et al.*, 1999; Pozueta-Romero

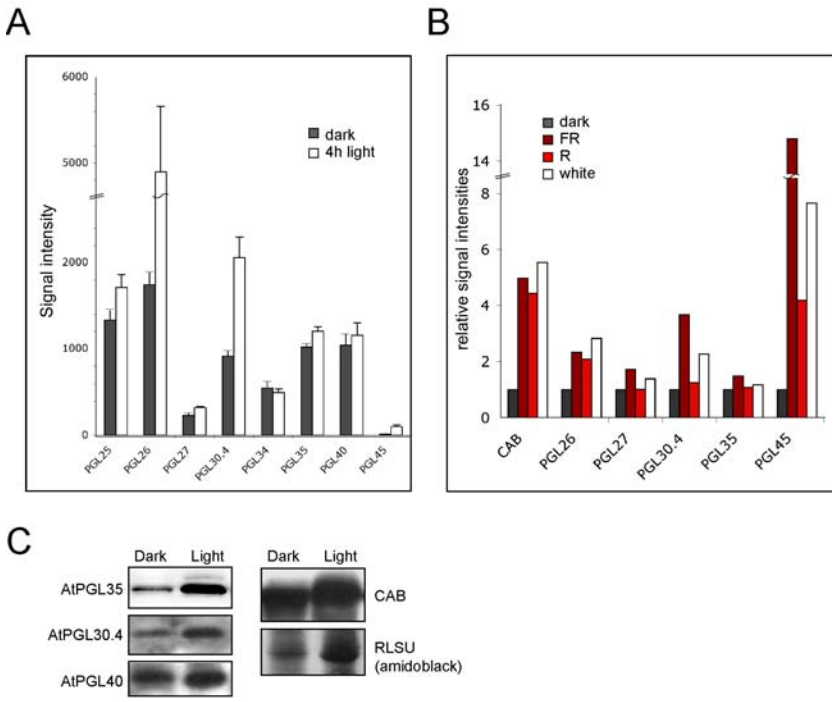

Figure 2.3: Induction of Arabidopsis PGLs by light. **A**, Digital northern showing relative transcript abundance in etiolated seedlings (grey bars) and after exposure to white light during 4h (white bars). Values of signal intensities were retrieved from public microarray datasets using the Genevestigator Digital Northern toolbox. Means and standard errors from 3 replicate experiments are shown. **B**, Digital northern showing the effect of 4h red (R) and far red (FR) light treatment on AtPGL transcript abundance. Means from 3 replicate experiments were calculated and relative values are shown (for each gene, signal value for the dark treatment was set to 1). **C**, Western blot analysis of etiolated and light grown seedlings. Plants were grown for 8 days in the dark or in a 16h/8h light/dark regime (light) on half MS medium. Total proteins (20 μg) were used for SDS-PAGE, Western transfer and immunoblot analysis. AtPGL40, AtPGL35, AtPGL30.4 and CAB were detected using specific antibodies.

et al., 1997), other laboratories have reported localisation of potato C40.4 and CDSP34 PAP/fibrillins to chloroplast stroma or thylakoid membranes (Monte *et al.*, 1999; Rey *et al.*, 2000). In order to determine the subcellular localisation of AtPGL35, we used immunolocalisation approaches. Affinity purified antibodies against AtPGL35 recognised a single band in a total protein extract of Arabidopsis leaves (Fig. 2.4A), indicating that artefacts caused by unspecific hybridisation were unlikely.

Immunogold-electron microscopy was first used to localise AtPGL35 in ultrathin sections prepared from Arabidopsis leaves (Fig. 2.4B). When sections were incubated with anti-AtPGL35 antibodies, labelling was restricted to chloroplasts. Gold particles were detected at the periphery of negatively stained plastoglobules but were absent from thylakoid or envelope membranes. No labelling was found in control experiments where anti-AtPGL35 antibody were omitted (data not shown). To obtain independent evidences for the localisation of AtPGL35, immunofluorescence experiments were performed with protoplasts. Fixed protoplasts were incubated with anti-AtPGL35 antibodies followed by FITC-coupled secondary antibodies. Fluorescein was subsequently detected by confocal laser scanning microscopy. FITC signals overlapped with chloroplasts in merged fluorescent and bright-field images, demonstrating localisation of AtPGL35 in chloroplasts (Fig. 2.4C). Furthermore, a dot-like fluorescent pattern was observed, consistent with labelling of plastoglobules. Control experiments using antibodies against AtTOC159 (At3g46740) and CAB (chlorophyll a/b binding protein) resulted in rim-like fluorescence at the envelope or fluorescence at the thylakoids, respectively. When protoplasts were incubated with the fluorescein-labelled secondary antibody in absence of primary antibodies, only low levels of background fluorescence were detected.

Taken together, the data indicate that, at least in leaves, AtPGL35 localises to plastoglobules. The protein is therefore an adequate plastoglobule marker in leaf preparations.

2.1.5 Plastoglobulins may have diverse molecular functions

Overexpressing different AtPGL-GFP fusion constructs lead to distinct fluorescent patterns

To confirm localisation of AtPGL35 to plastoglobules, we engineered constructs encoding C-terminal green fluorescent protein (GFP) fusions under the control of the CaMV 35S promoter. The constructs were used to transform Arabidopsis protoplasts and GFP fluorescence was monitored by confocal scanning laser microscopy (Fig. 2.5). AtPGL35 is predicted to possess a transit peptide (amino acids 1 to 54) responsible for chloroplast targeting (TargetP, http://www.cbs.dtu.dk/services/TargetP/). In agreement with the prediction, a GFP fusion to residues 1-74 from AtPGL35 ($AtPGL35_{1-74}$) gave a fluorescence pattern which widely overlapped with chlorophyll autofluorescence, indicating targeting to chloroplasts. Moreover, shifts between peak GFP and

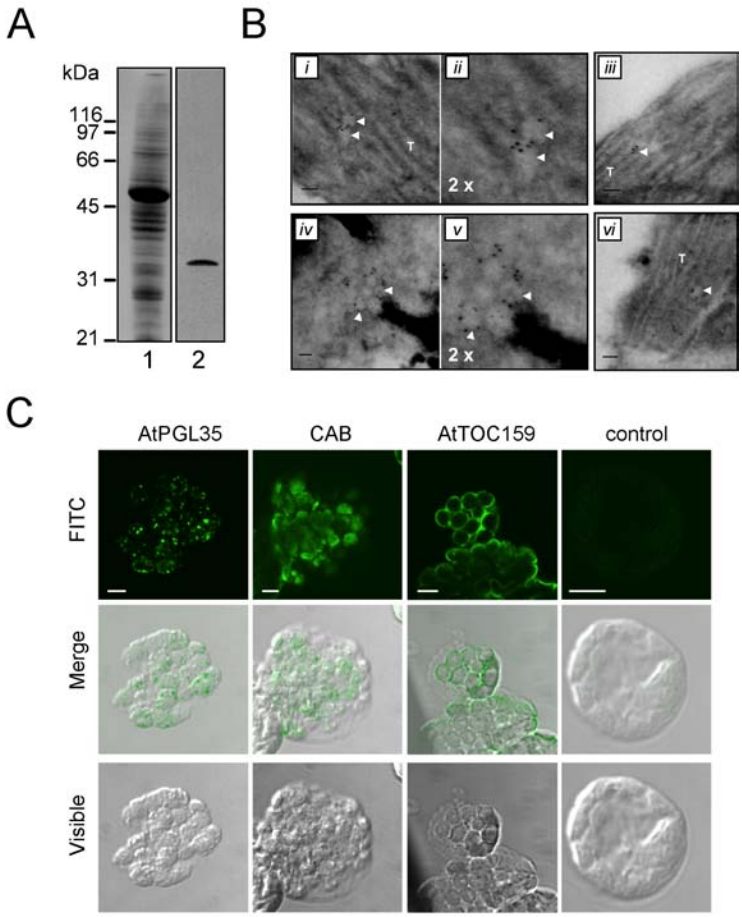

Figure 2.4: Sub-organellar localisation of AtPGL35. **A**, Detection of AtPGL35 in total protein extract prepared from Arabidopsis leaves. 25 μg proteins were resolved by SDS-PAGE, transferred to nitrocellulose membrane and stained with amidoblack (lane 1). AtPGL35 was detected by immunoblotting using a specific affinity purified antibody (lane 2). **B**, Gold immunolocalisation of AtPGL35 in mature leaves. Sections of Arabidopsis leaves were incubated with anti-PGL35 antibodies followed by secondary gold-conjugated antibodies and observed using transmission electron microscopy (*i* to *vi*). Panels *ii* and *v* are two fold enlargements from panels *i* and *iv*, respectively. Plastoglobules are highlighted with arrows; T, thylakoid membranes. Scale bars: 100 nm. **C**, Fluorescent immunolocalisation of AtPGL35 in protoplasts. Fixed protoplasts were probed with anti-AtPGL35, anti-AtTOC159 or anti-CAB antibodies, as indicated, or directly incubated with the fluorescein-labelled secondary antibody (control). The detection of the chromophore fluorescence (FITC) by confocal microscopy, bright-field microscopic images (visible) and merges from bright-field and fluorescent images (merge) are shown. Bar length: 5 μm.

chlorophyll florescence suggested labelling of chloroplast stroma. Expression of a GFP fusion to the transit peptide of RuBisCO small subunit (pSSU-GFP) in control experiments gave very similar GFP patterns. GFP and FDH-GFP (presequence of potato formate dehydrogenase-GFP) were used as cytosolic and mitochondrial markers, respectively. As expected, GFP signals and chlorophyll autofluorescence were clearly distinct in protoplasts transformed with these constructs.

To determine the targeting destination of full length AtPGL35, protoplasts were transformed with the full coding sequence of *AtPGL35* fused to GFP. Unlike the diffuse signals observed with the AtPGL35$_{1-74}$-GFP construct, globular fluorescent patterns were observed in chloroplasts. A dot-like pattern is consistent with plastoglobule localisation. Occasionally, a small fraction of the GFP-fusion protein was detected in the stroma or in the cytosol, suggesting incomplete chloroplastic import or assembly into plastoglobules. When compared with immunofluorescent results (Fig. 2.4C), the fluorescent signals in protoplasts overexpressing AtPGL35-GFP appeared larger and less numerous. At least three hypothesis could account for the formation of the large globular fluorescent structures in chloroplasts: i) Accumulation of AtPGL35-GFP may result in the formation of protein aggregates, ii) the GFP moiety of the fusion protein may lead to the formation of the structures, or iii) overexpression of AtPGL35 may cause enlargement of plastoglobules or formation of large plastoglobule clusters. Protein aggregation has been observed with other GFP fusion constructs expressed in protoplasts (data not shown). Consistently, irregular structures were observed, mostly in the cytosol. The regular, spherical structures in protoplasts expressing AtPGL35-GFP are therefore unlikely to represent protein aggregates. To distinguish between the two other hypothesis, other plastoglobulins were expressed as GFP fusion proteins in protoplasts. AtPGL34-GFP (Fig. 2.5), as well as AtPGL30.4-GFP (data not shown), accumulated in globular fluorescent structures inside chloroplasts. The fluorescent structures, apparently smaller and more numerous than those obtained with AtPGL35-GFP, were reminiscent of the immunofluorescent pattern obtained with anti-AtPGL35 antibodies. We therefore retained the hypothesis that overexpression of AtPGL35 may alter plastoglobule morphology.

To control the integrity of each GFP-fusion protein, transformed protoplasts were analysed by Western blotting using an anti-GFP serum. All GFP-fusion proteins had the expected mass. Detection of a double band in protoplasts expressing AtPGL35-GFP probably reflects presence of both precursor and mature forms of the protein and is consistent with occasional detection of cytosolic fluorescence.

AtPGL35 and AtPGL34 do not colocalise when expressed as fluorescent protein fusions

When different plastoglobulins (AtPGL35 and AtPG34) were expressed as GFP fusion proteins in Arabidopsis protoplasts, slightly different fluorescent patterns were observed, suggesting that the AtPGLs localised to different types of plas-

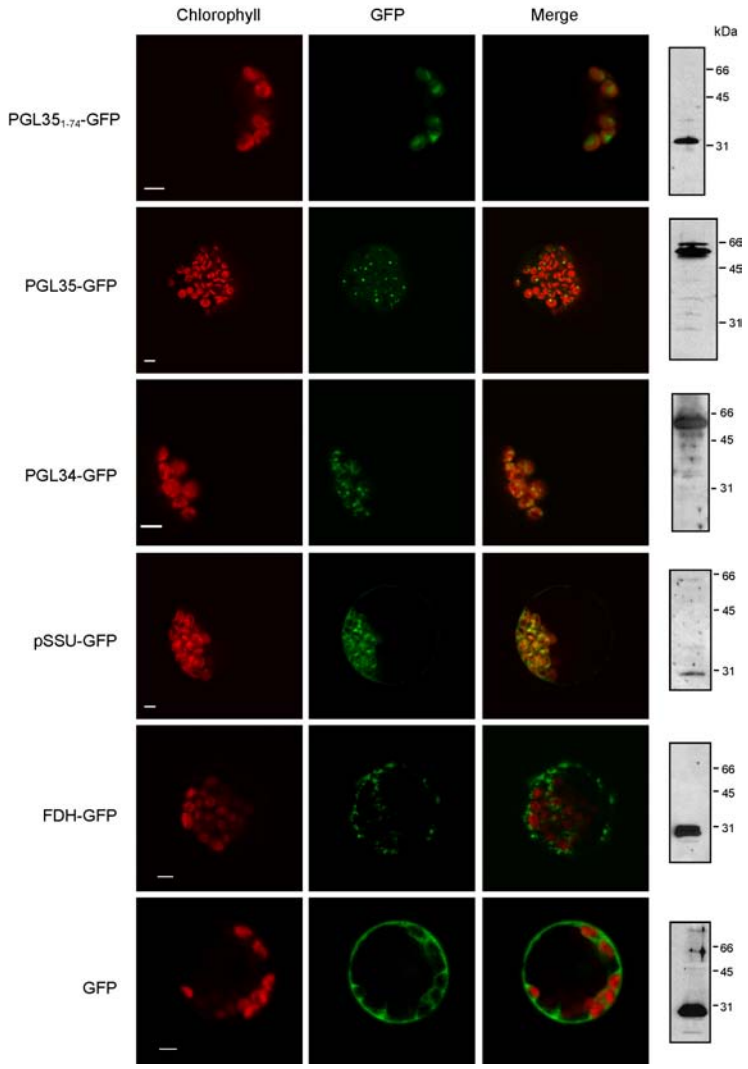

Figure 2.5: Transient expression of GFP-fusion proteins in Arabidopsis protoplasts. Protoplasts were transformed with plasmids encoding GFP fused to the N-terminal part of AtPGL35 (PGL35$_{1-74}$-GFP) or to full length AtPGL35 or AtPGL34 coding sequences (PGL35- or PGL34-GFP). GFP alone (GFP), mitochondrial potato formate dehydrogenase presequence (FDH-GFP) and stromal pea RuBisCO small subunit transit peptide (pSSU-GFP) were used as controls. Fusion proteins were visualised by confocal laser scanning microscopy 48h after transformation. Chlorophyll, GFP and merge indicate chlorophyll autofluorescence, GFP fluorescence, and the superposition of both fluorescent signals, respectively. Bar length: 5 μm. Panels on the right hand side show the detection of GFP fusion proteins in transformed protoplasts by immunoblotting, using anti-GFP antibodies.

toglobule or that overexpression of the AtPGLs have different effects on plastoglobule morphology. To address the possibility that AtPGL34 and AtPGL35 are targeted to different plastoglobule types, the two proteins were coexpressed as YFP and CFP fusions in protoplasts (Fig. 2.6). YFP and CFP are variants of GFP with excitation and emission spectra shifted toward yellow or blue, respectively, allowing simultaneous detection by confocal laser scanning microscopy. Fluorescent patterns obtained in cotransformed cells were similar to those observed in single transformation experiments. Structures labelled with CFP (AtPGL35) were in most cases also labelled with YFP (AtPGL34) but not reciprocally. This observation was confirmed by analysing pixel intensities in sections of the fluorescent images (Fig. 2.6B). In control experiments, protoplasts were cotransformed with constructs coding for AtPGL34-CFP and YFP. Fluorescent signals were observed in chloroplasts and in the cytosol and no cross-detection of YFP and CFP was detected. In contrast, a nearly exact overlap of the YFP and CFP channels was obtained in protoplasts cotransformed with AtPGL34-YFP and AtPGL34-CFP.

Fluorescent fusion proteins were detected by Western blotting in transformed protoplasts (Fig. 2.6C). Two bands corresponding in size to AtPGL35-CFP and AtPGL34-YFP were detected in the protein extract prepared from cotransformed protoplasts. Similar intensities of the two bands indicated similar expression levels of both proteins.

2.1.6 Using reverse genetics for the study of plastoglobulins

T-DNA insertional disruption of AtPGL35

To investigate the function of AtPGL35 *in vivo*, we searched the SALK database (Alonso *et al.*, 2003) for Arabidopsis mutant lines with T-DNA insertion in *AtPGL35* and identified 4 lines (024528, 026661, 040709, 130350). Insertion sites of the T-DNA left borders were determined by sequencing PCR products amplified with T-DNA and *AtPGL35*-specific primers. In lines 024528 and 026661, the insertion site was 7 bp upstream from the start codon. These lines were therefore not further analysed. In line 040709, the T-DNA was inserted in the first exon, 405 bp downstream from the start codon. Insertion in line 130350 was in the second intron, 52 bp downstream of the exon 2 / intron 2 boarder (Fig. 2.7C). For both 040709 and 130350 lines, plants homozygous for the T-DNA insertion were identified by PCR (Fig. 2.7A and B). These plants will further be designated as *pgl35-4* and *pgl35-5*, respectively. More detailed analysis of the T-DNA insertion in *pgl35-4* showed that T-DNA left boarders were present both at the 3' and 5' ends of the insertion, suggesting insertion of two T-DNA molecules at this loci. This hypothesis was confirmed by Southern analysis of *pgl35-4* genomic DNA (Fig. 2.8). After *Eco*RI restriction, two fragments migrating slightly below the 5 and 8 kb marker were detected. Assuming insertion of two T-DNA molecules as inverted repeats, sequence analysis predicts the formation of three fragments (4.66, 7.50 and 4.70 kb) detected by a left-boarder-specific

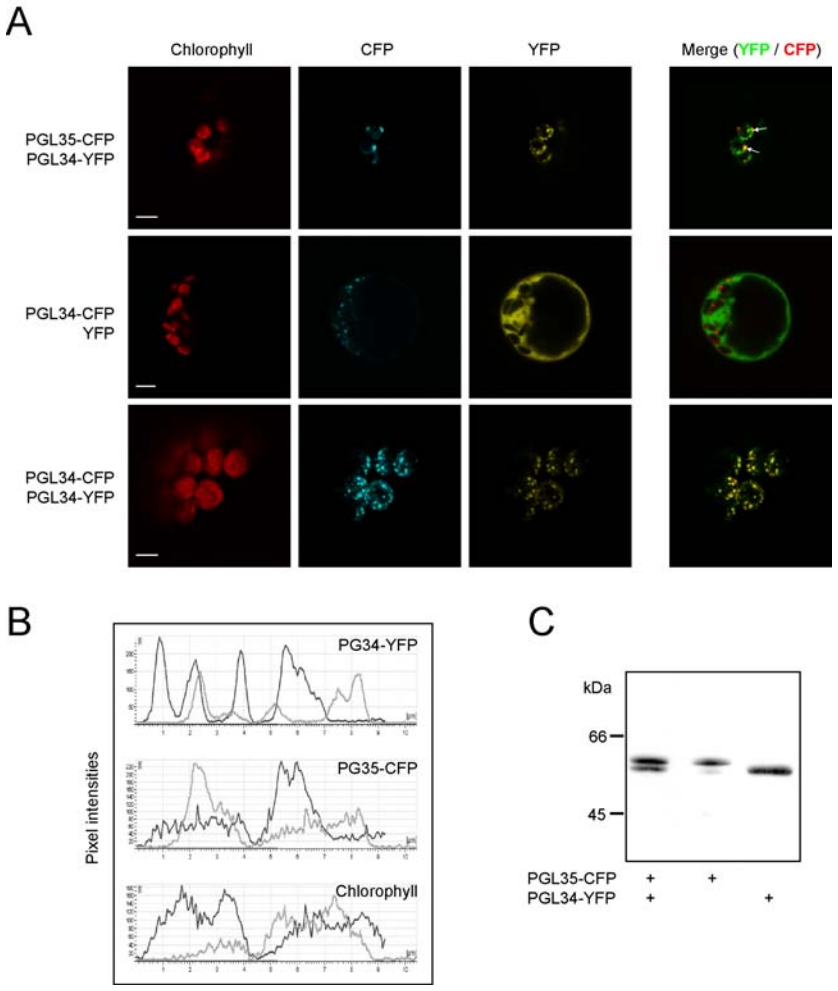

Figure 2.6: Colocalisation analysis of AtPGL35 and AtPGL34 in protoplasts. **A**, Protoplasts were cotransformed with AtPGL34-YFP and AtPGL35-CFP constructs. YFP and AtPGL34-CFP or AtPGL34-YFP and AtPGL34-CFP constructs were used in control experiments. CFP fluorescence (CFP) and YFP fluorescence (YFP) were monitored sequentially using distinct excitation wavelengths and detection windows. Chlorophyll: chlorophyll autofluorescence, merge: superposition of YFP and CFP signals (green and red pseudocolours, respectively). Bar length: 5 μm. **B**, Pixel intensities (black and grey traces) were measured across two narrow sections in confocal pictures from a protoplast cotransformed with AtPGL34-YFP and AtPGL35-CFP. Signals corresponding to AtPGL34-YFP, to AtPGL35-CFP and to chlorophyll autofluorescence are shown. **C**, Western blot analysis of protoplasts transformed with AtPGL35-CFP (PGL35-CFP), AtPGL34-YFP (PGL34-YFP) or with both constructs. The blot was probed with anti-GFP antibodies.

probe including an *Eco*RI site. For *Xba*I restriction, 2.37 and 5.34 kb fragments, including genomic sequence upstream and downstream from the insertion, are expected. Although only a smear, possibly due to incomplete digestion, was observed in the range of 5 kb with *pgl35-4* DNA after *Xba*I restriction, a band slightly below the 2.5 kb marker was detected, in agreement with the sequence analysis. No signal was detected with DNA from wild type plants, ruling out unspecific hybridisation. The data suggest presence of a single insertion locus in *pgl35-4*. 100% of the plants were resistant to phosphinothricin, indicating that seeds homozygous for the T-DNA insertion were received from the SALK collection.

Although the 5' end of the T-DNA insertion in *pgl35-5* could not be detected by PCR, a genomic fragment upstream from the T-DNA left boarder insertion site was amplified in *pgl35-5* homozygous plants (Fig. 2.7B, lane 5), indicating that no major chromosomal deletion took place at the *AtPGL35* locus in this line. In order to determine the number of T-DNA insertion loci in *pgl35-5* line, seeds from the parental plants (*pgl35-5.1* to *-5.4*) were germinated on phosphinothricin-containing media. The offspring of *pgl35-5.1* and *pgl35-5.3* plants showed a segregation (sensitive:resistant) close to 1:3 on selective media (Binomial test for plant 1 (24:90), p=0.19; for plant 2 (27:103), p=0.156), suggesting the presence of a single insertion locus in this line.

Absence of AtPGL35 does not lead to a visible or microscopic phenotype

To verify if *pgl35-4* and *pgl35-5* are real knock-out mutant lines for *AtPGL35*, mature leaves from homozygous mutant plants, as well as wild type leaves for control, were analysed by Western blotting (Fig. 2.9A). AtPGL35 was detected in wild type but neither in homozygous *pgl35-4* nor in homozygous *pgl35-5*, indicating that both lines have null alleles of *AtPGL35*. As shown in Fig. 2.9B and C, homozygous knock-out plants grown on soil did not exhibit a visible phenotype. Several Arabidopsis mutants with altered chloroplast morphology exhibit wild type phenotypes in standard growth condition (e.g. *arc* chloroplast replication mutants; Pyke, 1999). Therefore, to determine whether the morphology of plastoglobules or the ultrastructure of chloroplasts is affected in *AtPGL35* knock-out mutants, ultrathin sections were prepared from wild type and *pgl35-4* mature leaves. Membranes and plastoglobules were stained with osmium and sections were analysed by transmission electron microscopy (TEM). No difference was observed in chloroplasts from *pgl35-4* plants compared to wild type (Fig. 2.9D). Furthermore, a preliminary quantification did not reveal differences in plastoglobule sizes and numbers in the mutant (data not shown).

Down-regulation of AtPGL35 homologues using RNA-mediated gene silencing

The absence of macro- and microscopic phenotype in *AtPGL35* T-DNA insertional mutants implies that the protein is not essential for chloroplast function.

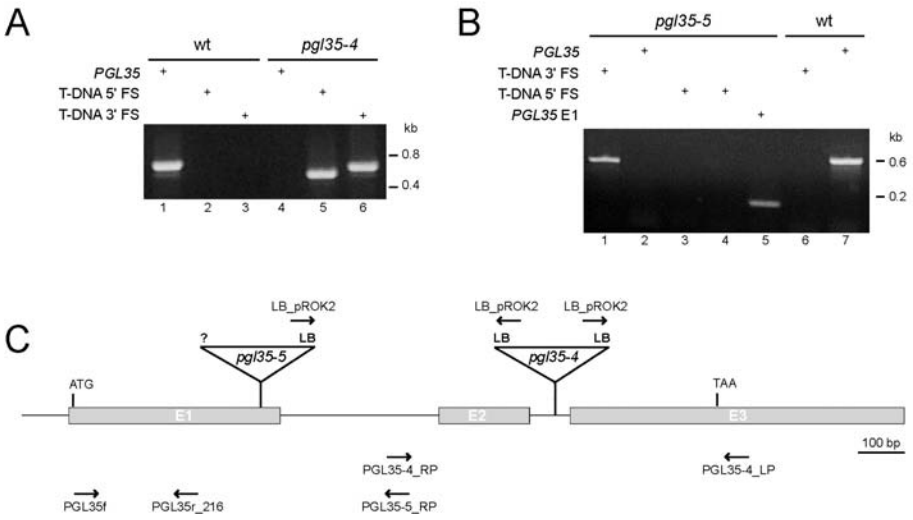

Figure 2.7: T-DNA insertion mutants in *AtPGL35*. **A**, PCR analysis of *pgl35-4* (SALK line 040709). DNA was extracted from wild type (wt) or homozygous *pgl35-4* plants. PCR reactions were designed to detect the wild type allele of *AtPGL35* (lanes 1 and 4) or the T-DNA 5' and 3' flanking sequences (FS, lanes 2 and 5 or 3 and 6, respectively). Primers used: PGL35-4_RP and PGL35-4_LP (1, 4); PGL35-4_RP and LB_pROK2 (2, 5); LB_pROK2 and PGL35-4_LP (3, 6). See methods part for primer sequences. **B**, PCR analysis of *pgl35-5* (SALK line 130350). DNA from wild type (wt) or homozygous *pgl35-5* plants was used for PCR analysis. Reactions were designed to detect the T-DNA 3' flanking sequence (lanes 1 and 6) or the presence of a wild type allele of *AtPGL35* (lanes 2 and 7). The T-DNA 5' flanking sequence (T-DNA 5' FS) could be amplified neither with primers specific for the left (line 3) nor the right (line 4) T-DNA boarder. In reaction 5, a genomic fragment in the exon 1 (E1) of *AtPGL35*, 189 bp upstream from the T-DNA insertion site, was amplified. Primers used: PGL35-5_RP and LB_pROK2 (1, 6); PGL35f and PGL35-5_RP (2, 7); PGL35f and LB_pROK2 (3); PGL35f and RB_pROK2 (4); PGL35f and PGL35r_216 (5). **C**, Mapping of T-DNA insertions in *pgl35-4* and *pgl35-5*. PCR product amplified using primers specific for *AtPGL35* and for the left boarder (LB) of the T-DNA insertion were used for DNA sequencing (*pgl35-4*: **A**, lane 5 and 6; *pgl35-5*: **B**, lane 1). The exon/intron structure of *AtPGL35* is supported by cDNA sequences (BT000148, BX828265, AY085330 and AY120766). Exons (E1, E2 and E3) and introns are indicated with grey boxes and lines, respectively. Start and stop codons are indicated. Positions of the primers used for PCR analysis are shown.

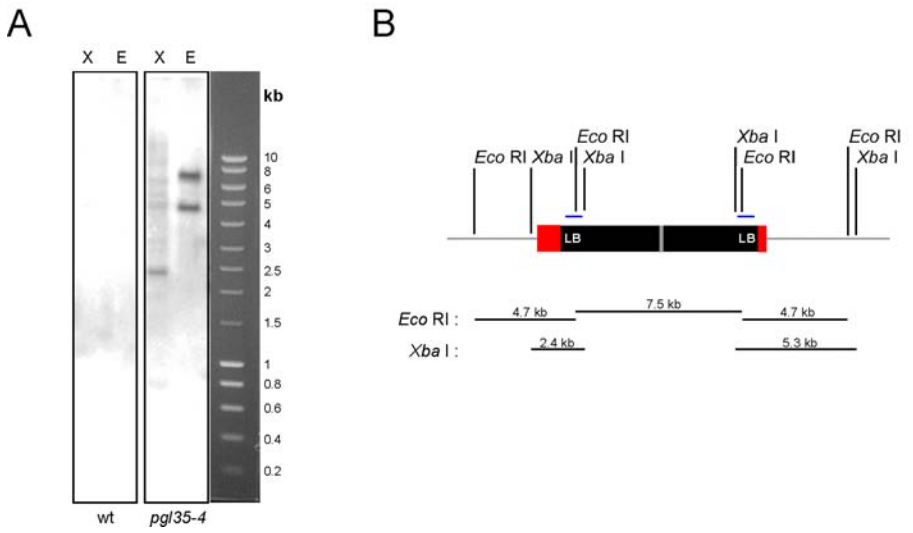

Figure 2.8: Southern blot analysis of line *pgl35-4*. **A**, DNA from wild type (wt) or *pgl35-4* plants was digested with *Xba*I (X) or *Eco*RI (E). Fragments containing the left boarder of the T-DNA insertion were detected with a specific probe as indicated in **B**. **B**, Model of the insertion consistent with sequencing and Southern blot results. Two T-DNA molecules (black) are inserted in *AtPGL35* (red) with their left boarders (LB) facing toward *AtPGL35* 3' and 5' ends. *Eco*RI and *Xba*I restriction fragments detected by a LB-specific probe (blue) are indicated.

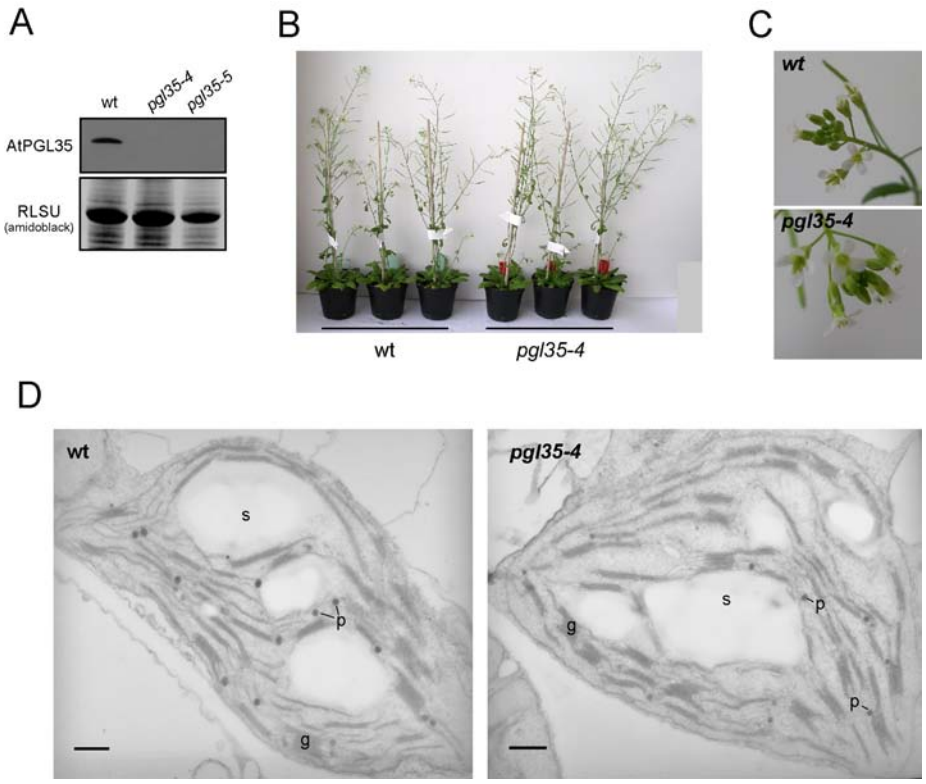

Figure 2.9: Absence of visible phenotype in plants lacking AtPGL35. **A**, Western analysis of lines *pgl35-4* and *pgl35-5*. Total proteins from wild type (wt), *pgl35-4* or *pgl35-5* leaves were resolved by SDS-PAGE, transferred to nitrocellulose membrane and stained with amidoblack. Similar intensities of the RuBisCO large sub-unit (RLSU) indicated equal loading amounts. AtPGL35 was detected by immunoblotting using a specific affinity purified antibody. **B**, Photographs from wild type and homozygous *pgl35-4* plants grown for 7 weeks on soil under long-day conditions. **C**, Details from inflorescences. **D**, Chloroplast ultrastructure in wilt type and *pgl35-4* leaves. Plants were grown on soil in short-days for one month and leaves were fixed in presence of osmium. Ultrathin sections were observed by transmission electron microscopy. s, starch granules; p, plastoglobules; g, thylakoid grana. Scale bars: 500 nm.

Since *AtPGL35* is a member of a multiple gene family, functional redundancy among plastoglobulins may account for the lack of apparent phenotype. Indeed, two close homologues of *AtPGL35* (*AtPGL33* and *AtPGL40*) are present in the Arabidopsis genome (see Fig. 2.1). Presence of numerous ESTs for *AtPGL33* and *-40* in the databases indicates that both genes are expressed. Furthermore, Northern and Western analysis from different organs showed that expression patterns from both homologues overlap with *AtPGL35* (Fig. 2.2B and D). AtPGL40 and/or AtPGL33 may therefore take over the function of AtPGL35 in the knock-out mutants. To investigate that possibility, and since T-DNA insertional mutants are not available yet for *AtPGL33* and *AtPGL40*, a gene silencing approach was chosen. When expressed in plants, constructs generating intron-containing self-complementary 'hairpin' RNA ($_{ihp}$RNA) efficiently trigger gene silencing (Smith *et al.*, 2000) In order to produce $_{ihp}$RNAs targeted against *AtPGL33* and *-40*, N-terminal fragments of the coding sequences (bp 2 to 350 or 2 to 450 of *AtPGL33* and *AtPGL40*, respectively) were cloned as inverted repeats in the pHANNIBAL vector (Wesley *et al.*, 2001) and sub-cloned in the pCHF5 binary vector (prof. C. Frankhauser), placing *AtPGL33* or *-40* inverted repeats under the control of the cauliflower mosaic virus (CaMV) 35S promoter and the RuBisCO small subunit (RSSU) terminator. Homozygous *pgl35-4* Arabidopsis plants were transformed with these constructs using the flower dip technique. Transformants were selected on phosphinothricin-containing media and are referred to as *pgl35-4*/$_{ihp}$*pgl33* or *-40*. Silencing efficiency in leaves was assessed by Western or RT-PCR analysis. As shown in Fig. 2.10B, abundance of AtPGL40 was strongly reduced in all transgenic lines tested. In eight *pgl35-4*/$_{ihp}$*pgl33* lines (out of 11 tested), no RT-PCR signal was obtained with *AtPGL33*-specific primers (Fig. 2.10C), indicating silencing of *AtPGL33*.

Although *pgl35-4*/$_{ihp}$*pgl33* (and *-40*) plants lacked or had strongly reduced levels of AtPGL35 and AtPGL33 (or -40), neither mutant seedlings grown on half MS media (data not shown) nor adult mutants grown on soil (Fig. 2.10D) exhibited an altered phenotype in standard growth conditions.

To generate triple mutants, *pgl35-4*/$_{ihp}$*pgl33* and *-40* T1 lines containing a single insertion locus were selected by analysing the segregation of their progeny on phosphinothricin (ppt). T2 plants from lines *pgl35-4*/$_{ihp}$*pgl40* 5, 6, 9 and 13 as well as *pgl35-4*/$_{ihp}$*pgl33* 5, 6, 14 and 15, which segregated 1:3 on selection media and showed reduced *AtPGL33* messenger or AtPGL40 protein levels, were germinated on phosphinothricin-containing media and used for reciprocal genetic crosses. In the first generation, plants should be homozygous with respect to the T-DNA insertion in *AtPGL35*. Upon self pollination and since parental plants were either homozygous or heterozygous for $_{ihp}$*pgl33* or *-40*, 4/9 lines are expected to be heterozygous for both $_{ihp}$*pgl33* or *-40* insertions, 4/9 for a single insertion and 1/9 should contain neither $_{ihp}$*pgl33* nor *-40* insertion. Presently, only T1 lines resulting from the crosses are available. Segregation analysis from the T2 will allow genotyping: T1 lines carrying both $_{ihp}$*pgl33* and *-40* insertions should segregate 3:1 (pptR:pptS). In contrast, T1 lines having only one or no insertion should segregate 1:1 or 0:1, respectively.

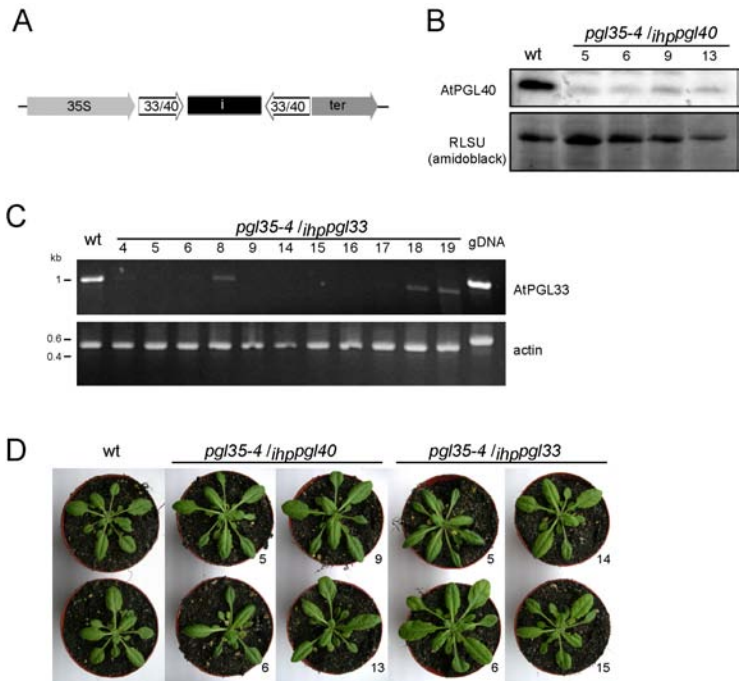

Figure 2.10: RNAi-mediated silencing of *AtPGL33* and *AtPGL40* in the *pgl35-4* knock-out background. **A**, intron-containing self-complementary 'hairpin' RNA ($_{ihp}$RNA) constructs for *AtPGL33 AtPGL40* gene silencing. N-terminal fragments of *AtPGL33* (33) or *AtPGL40* (40) coding sequences were cloned as inverted repeats in the pHANNIBAL vector. A cassette consisting of the repeats interrupted by an intron (i) from the pyruvate dehydrogenase kinase was inserted in the pCHF5 binary vector, placing the $_{ihp}$ sequence under the control of two repeats of the cauliflower mosaic virus 35S promoter (35S) and the terminator of the RSSU (ter). Transformation with the pCHF5 vector conferred resistance to kanamycin. **B**, Western analysis of *pgl35-4*/$_{ihp}$*pgl40* lines. Wild type (wt) plants were grown on half MS media and *pgl35-4*/$_{ihp}$*pgl40* (T2) plants (lines 5, 6, 9 and 13) were grown on kanamycin-containing media for 7 weeks. For each lines, five seedlings were used for protein extraction and Western analysis. AtPGL40 was detected using specific antibodies. The RuBisCO large sub-unit (RLSU) on the amidoblack stain of the membrane indicates equal loading amounts. **C**, Analysis of *pgl35-4*/$_{ihp}$*pgl33* lines (T2) by RT-PCR. Ten seedlings grown on selective media from each lines or wild type seedlings were used to prepare cDNAs. *AtPGL33* (AtPGL33) or *ACTIN* (actin) cDNAs were amplified by PCR using specific primers. gDNA, wild type genomic DNA. **D**, Photographs from adult wild type or *pgl35-4*/$_{ihp}$*pgl33* and *pgl35-4*/$_{ihp}$*pgl40* T2 plants. Line numbers are indicated.

2.2 Plastoglobules in oxidative stress response

2.2.1 High light stress leads to enlargement of plastoglobules in Arabidopsis leaves

Plants exposed to stressful environmental conditions need to respond to oxidative stress by scavenging reactive oxygen species (ROSs), notably in order to avoid oxidation of membrane lipids. Enlarged plastoglobules have been described in chloroplasts under abiotic stress conditions such as drought or hypersalinity (Eymery and Rey, 1999; Locy *et al.*, 1996), implicating them in stress tolerance.

To our knowledge, effects of environmental stresses on plastoglobule morphology have not been studied in plants from the Brassicaceae family. In order to determine whether plastoglobules are also directly or indirectly involved in oxidative stress response in Arabidopsis, adult plants were exposed during 48 hours to a strong white light with a photon flux density of 1200 μmol photons m^{-2} s^{-1}. Strong illumination is known to generate photooxidative stress in chloroplasts (Havaux *et al.*, 2005). After exposure to strong light, leaves had a strong purple colour, indicating accumulation of protective anthocyanins (Fig. 2.11D). To compare chloroplast ultrastructure in plants exposed to high light or let in standard conditions, ultrathin sections were prepared from rosette leaves and were observed by transmission electron microscopy (Fig. 2.11A and B). Plastoglobules in plastids from treated plants appeared larger and, interestingly, clusters of plastoglobules were frequently observed in treated samples. To obtain quantitative data, chloroplasts from the uppermost layer of adaxial mesophyll cells were randomly chosen at low TEM magnification. Plastoglobule sizes and abundance, as well as the number of plastoglobule clusters were then determined using the ImageJ freeware (http://rsb.info.nih.gov/ij/). As shown in Fig. 2.11C, plastoglobules were significantly larger in chloroplasts from plants exposed to high illumination. Plastoglobules were also slightly more abundant in stressed chloroplasts (1.46 vs. 1.03 plastoglobules μm^{-2} of chloroplast section). Clusters were defined as the presence of at least three plastoglobules separated by distances smaller than their radius. In ten plastids from treated plants, 6 plastoglobule clusters were observed. Clusters were not observed in plastids form control plants. Similar results were obtained after 8h of strong light treatment in an independent experiment (data not shown).

2.2.2 AtPGL transcripts accumulate under oxidative stress conditions

Upregulation of several PGLs has been correlated with various treatments generating reactive oxygen species (Gillet *et al.*, 1998; Monte *et al.*, 1999; Chen *et al.*, 1998; Pruvot *et al.*, 1996b; see Table 1.1). To assess whether the Arabidopsis plastoglobule marker protein AtPGL35 is upregulated in stress conditions, we first analysed public microarray datasets using the Genevestigator Digital Northern toolbox (Fig. 2.12). Both osmotic and salt stresses lead to accumu-

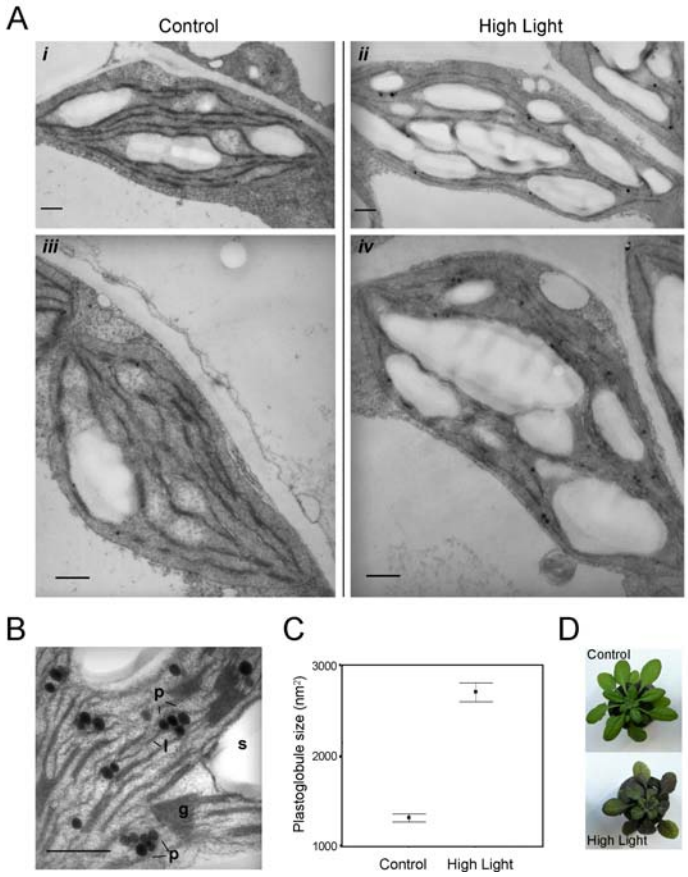

Figure 2.11: Effect of high light treatment on chloroplast ultrastructure. Four week-old Arabidopsis plants were exposed to continuous strong white light (1200 μmol photons m^{-2} s^{-1}, high light) for 48 hours. Control plants were let in short day conditions (8h light / 16h dark photoperiod). **A**, Young leaves from control plants (*i*, *iii*) or from plants exposed to strong illumination (*ii*, *iv*) were fixed and used to prepare ultrathin sections. Chloroplasts from the uppermost cell layer of the palisade parenchyma (adaxial side of leaves) were randomly chosen at low TEM magnification and pictures were subsequently taken at 3400 or 4600x magnification. Bar length: 500 nm. **B**, Detail showing plastoglobule clusters in a chloroplast exposed to strong illumination. p, plastoglobules; g, thylakoid granum; l, stroma lamellae; s, starch granule. Bar length: 500 nm. **C**, Surfaces of plastoglobules were measured in ten sections from control or stressed (high light) plants. Mean ± SE are shown; t-test: df = 279, t = -11.3, $p < 0.001$. **D**, Photographs from treated and control plants.

lation of *AtPGL35* transcripts (1.9 and 1.7 fold-increases after 24h treatment, respectively). Data from time course experiments showed that *AtPGL35* messengers accumulated already after 3 hours of osmotic stress treatment. Upregulation of *AtPGL35* in salt stress conditions was somewhat slower. Exogenous application of abscissic acid (ABA) also induced expression of *AtPGL35* after 3 hours (Fig. 2.12C).

2.2.3 Drought and photooxidative stress lead to accumulation of AtPGL35

Osmotic and salt stresses both lead to accumulation of reactive oxygen species in chloroplasts (Smirnoff, 1993; Hernandez *et al.*, 2001; Chinnusamy *et al.*, 2005). Induction of *AtPGL35* may therefore represent a general response to oxidative stress in chloroplasts rather than a specific response to salt or osmotic stress. If this is the case, other conditions leading to the formation of ROSs in chloroplasts should trigger the upregulation of *AtPGL35*. As shown in Fig. 2.13, drought and high light stresses caused accumulation of AtPGL35. Plants subjected to dehydration followed by 24h re-watering still contained higher levels of AtPGL35 than control pants, indicating stability of the protein. High light stress was accompanied by anthocyanin accumulation and most efficiently induced AtPGL35 (more than 10-fold).

2.2.4 AtPGL35 accumulates during ageing

Ageing is known to be a condition under which oxidative stress increases in chloroplasts (Munne-Bosch and Alegre, 2002). It is accompanied by raised levels of ROS and lipid radicals as well as of antioxidants such as tocopherols (Hollander-Czytko *et al.*, 2005). If oxidative stress leads to the upregulation of *AtPGL35* (as suggested by results in the previous section), the protein is expected to accumulate in older plants. To investigate that possibility, leaf material from 1 to 5 week-old plants was analysed by Northern and Western blot. (Fig. 2.14). Transcript levels were high in young seedlings (1 week-old), possibly reflecting light induction of the protein during germination (see Fig. 2.3). At week 4, when plants started bolting and showed accumulation of anthocyanins, *AtPGL35* mRNAs were again more abundant. Upregulation of *AtPGL35* transcription resulted in accumulation of the protein. Transcript abundance transiently decreased after week 1 but protein levels remained stable up to week 3, indicating stability of the protein.

During senescence, thylakoid membranes are degraded, plastoglobules enlarge and accumulate (Ghosh *et al.*, 2001). Involvement of AtPGL35 in this process was assessed using an artificial system for senescence induction, i.e. dark incubation of excised Arabidopsis leaves (Pruzinska *et al.*, 2003). After this treatment, levels of the RuBisCO large subunit and of CAB decreased (Fig. 2.14B). AtPGL35 was still detectable in senescing leaves but less abundant than in younger leaves, suggesting that the protein is not directly involved in plastoglobule formation during senescence. Other Arabidopsis PGLs may

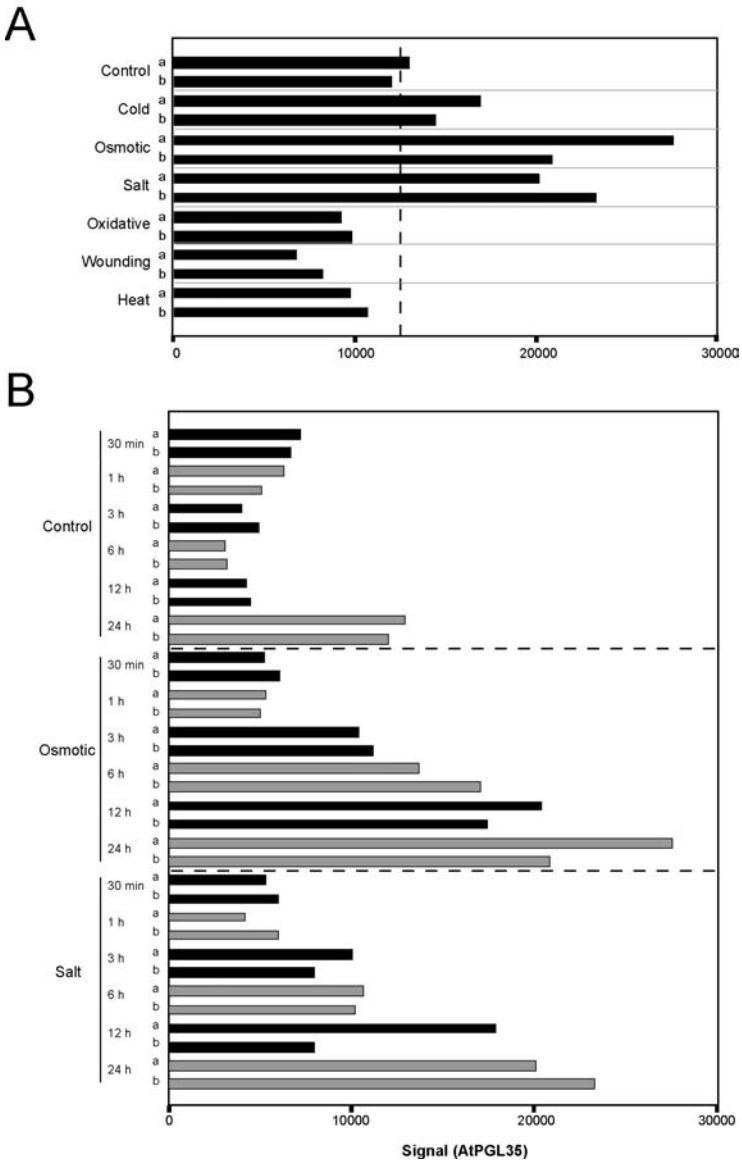

Figure 2.12: Digital Northern showing accumulation of *AtPGL35* transcripts under certain abiotic stress conditions and after ABA treatment (see caption on page 35).

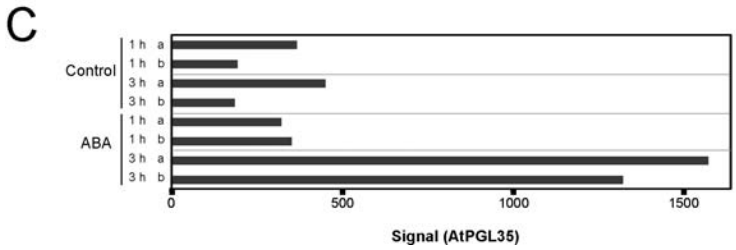

Figure 2.12: Digital Northern showing accumulation of *AtPGL35* transcripts under certain abiotic stress conditions and after ABA treatment (continued). **A**, Green parts from stressed or untreated (control) Arabidopsis plants (18 days-old) were used for microarray analysis. Treatments were the following: cold, 24h incubation at 4°C (Microarray Expression Set (ES) 1007966553); osmotic, 24h with 300 mM mannitol (ES 1007966835); salt, 24h with 150 mM NaCl (ES 1007966888); oxidative, 24h with 10 μM methyl viologen herbicide (ES 1007966941); wounding, wounding of leaves by punctuation and 24h incubation (ES 1007966439); heat, 3h of 38°C heat stress followed by 21h recovery at 25°C (ES 1007967124). Detailed description of the treatments is published on the TAIR website (http://www.arabidopsis.org). Control, untreated plants. **B**, Levels of *AtPGL35* transcripts in time course experiments. Plants used for microarray analysis were incubated with 300 mM mannitol (osmotic) or with 150 mM NaCl (salt) for 30 min, 1h, 3h, 6h, 12h or 24h. **C**, Response to abscisic acid (ABA, ES 1007964750). Arabidopsis seedlings (7 days-old) were treated with 10 μM ABA for 1 or 3 hours. **A**-**C**, Signals from replicate experiments (a, b) are shown.

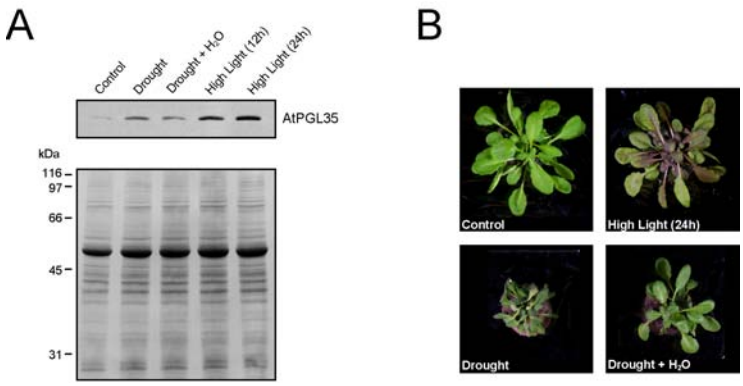

Figure 2.13: Accumulation of AtPGL35 in drought and high light conditions. Arabidopsis plants were grown on soil in short days for 4 weeks. Five plants stayed in short days and were used as control. Five plants were exposed to continuous strong white light (1200 μmol photons m^{-2} s^{-1}, high light) for 12 or 24 hours. Ten plants were withdrawn from watering during 4 days (drought). The drought treatment lead to a loss of fresh weight of about 50%. Half of the plants were re-watered for 24h (drought + H_2O). **A**, Western blot analysis. Total leaf protein extracts (25 μg) from control or treated plants were analysed by SDS-PAGE and immunoblotting using specific anti-AtPGL35 antibodies. **B**, Photographs showing control and treated plants.

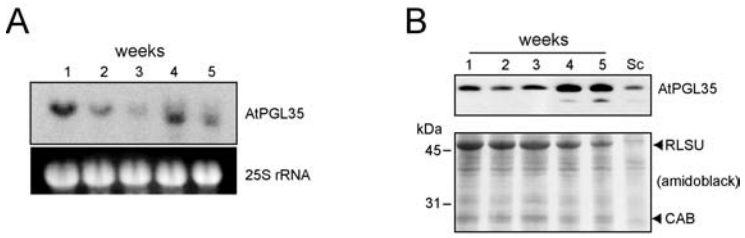

Figure 2.14: Time course of *AtPGL35* expression in Arabidopsis leaves. Cotyledons and rosette leaves from Arabidopsis plants growing on soil in long day conditions were collected 1 to 5 weeks after germination and used for Northern (**A**) or Western (**B**) analysis. **A**, RNA extracted from cotyledons or rosette leaves was used for acrylamide gel electrophoresis followed by Northern blotting. A specific [^{32}P]-labelled probe was used to detect *AtPGL35* transcripts. The 25S rRNA indicates equal loading amounts. **B**, Plants grown in the same conditions than in **A** were used for Western analysis. In addition, senescing material (Sc) was prepared by incubating for 8 days in the dark rosette leaves detached from 8 week-old plants. 25 μg of total proteins were separated by SDS-PAGE, blotted to nitrocellulose membrane and AtPGL35 was detected by immunoblotting. The amidoblack-stained membrane is shown. RLSU, large subunit of RuBisCO; CAB, chlorophyll a/b binding protein.

therefore be involved in this process. AtPGL34 notably, as suggested by expression profiling (see Fig. 2.2A), is a good candidate.

2.3 Plastoglobules and tocopherol metabolism

2.3.1 Tocopherol cyclase (AtVTE1) localises to plastoglobules

Plastoglobules from pea and tomato chloroplasts were shown to contain around a dozen different proteins. However, only members of the PAP/fibrillin family have been identified (Kessler *et al.*, 1999; Pozueta-Romero *et al.*, 1997). In an effort to unravel molecular functions of plastoglobules, the Arabidopsis plastoglobule proteome was analysed by tandem mass spectrometry (Dr. Bréhélin, University of Neuchâtel and Dr. Sacha Baginsky, ETH Zürich; Ytterberg *et al.*, 2006). Among proteins identified in the low density plastoglobule fraction were AtPGLs but also metabolic enzymes (See Table 4.2) including the tocopherol cyclase AtVTE1. The abundance of AtVTE1 and AtPGL33 peptides were comparable, suggesting relatively high abundance of AtVTE1.

To further investigate the subcellular localisation of AtVTE1, a construct encoding a C-terminal YFP fusion to AtVTE1 coding sequence (AtVTE1-YFP) was transformed in Arabidopsis protoplasts (Fig. 2.15A). Fluorescent signals

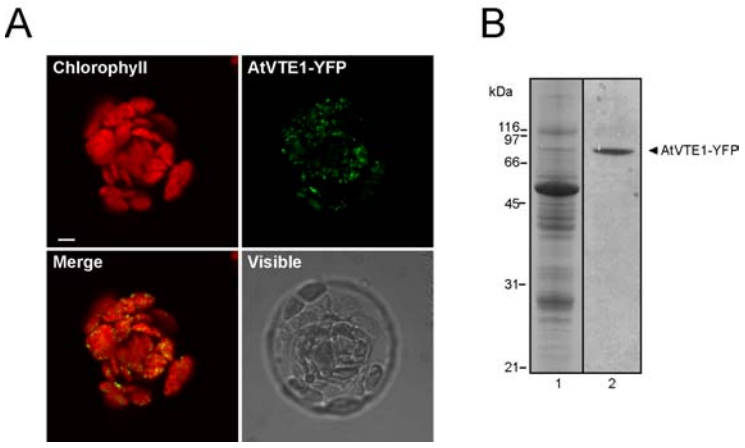

Figure 2.15: Transient expression of AtVTE1-YFP in protoplasts. **A**, Arabidopsis protoplasts expressing AtVTE1 as a C-terminal YFP fusion (AtVTE1-YFP) were analysed by confocal microscopy. Merge: superposition of chlorophyll autofluorescence (chlorophyll) and YFP signals. Visible: bright field image of the protoplast. Bar length: 5 μm. **B**, Western blot analysis of transformed protoplasts. Total proteins (25 μg) extracted from protoplasts transformed with the AtVTE1-YFP construct were used for SDS-PAGE followed by immunoblotting. Proteins were visualised by staining the membrane with amidoblack (lane 1). AtVTE1-YFP was detected using anti-GFP antibodies (lane 2).

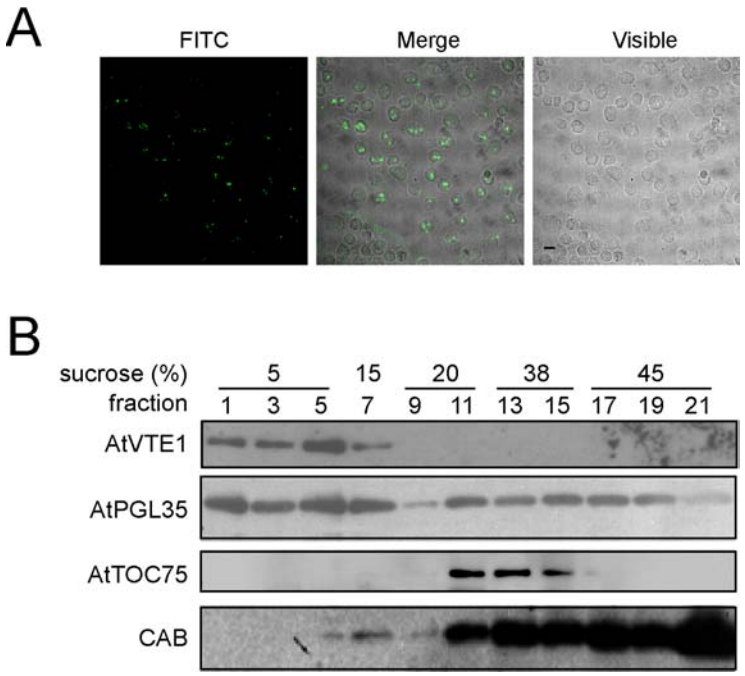

Figure 2.16: Localisation of AtVTE1 to plastoglobules. **A**, Fluorescent immunolocalisation of AtVTE1. Chloroplasts prepared from isolated protoplasts were fixed and probed with anti-AtVTE1 antibodies. Secondary FITC-coupled antibodies were used for visualisation. The detection of the chromophore fluorescence (FITC) by confocal microscopy, bright-field microscopic images (visible) and merges from bright-field and fluorescent images (merge) are shown. Bar length: 5 μm. **B**, Distribution of AtVTE1 in chloroplast fractions. Chloroplast membranes (derived from Arabidopsis plants expressing *AtPGL34g-YFP*) were separated by flotation on a discontinuous sucrose gradient as described in Fig. 2.24. The nitrocellulose membrane shown in Fig. 2.24B was probed with anti-AtVTE1 antibodies. Immunoblots identical to those on Fig. 2.24B showing the distribution of AtPGL35, AtTOC75 and CAB are presented.

were restricted to chloroplasts and dot-like patterns were observed, similar to the one obtained with AtPGL-GFP constructs. Integrity of the AtVTE1-YFP fusion protein was verified by Western blot analysis of transformed protoplasts. A single band migrating between the 97 and 66 kDa markers was detected with anti-GFP antibodies, in agreement with the predicted size of AtVTE1-YFP (44 kDa, AtVTE1 mature form fused to the 27 kDa eYFP, Fig. 2.15B).

To obtain additional evidence for the localisation of AtVTE1, fixed chloroplasts were incubated with anti-VTE1 antibodies. Primary antibodies where then decorated with FITC-conjugated secondary antibodies and fluorescein was detected by confocal laser microscopy (Fig. 2.16A). Fluorescent signals labelled globular structures overlapping with chloroplasts, consistent with plastoglobule localisation of VTE1.

In a third line of experiments, the distribution of AtVTE1 in chloroplast membrane fractions was analysed. Chloroplasts were homogenised and membranes were separated from soluble proteins by centrifugation at 100,000x g. The chloroplast membrane systems have different buoyant densities due to varying lipid to protein ratios. Thylakoid membranes include abundant photosynthetic proteins and have therefore a higher density (1.2 g/cm^3). In contrast, plastoglobules, which are mostly constituted of lipids, have a low budoyant density (0.9-1 g/cm^3). The density of envelope membrane is intermediate (1.1 g/cm^3). We took advantage of these properties to separate chloroplast membranes by flotation density gradient centrifugation. Fractions were collected from the gradient and analysed by Immunoblot (Fig. 2.16B). Antibodies against the CAB protein gave strong signals in fractions 11 to 21, indicating the presence of thylakoid membranes in the high density sucrose steps. Weaker CAB signals were present in fractions 5 to 9, most likely due to a minor presence of highly abundant thylakoid membranes in the low density fraction (5 and 15% sucrose steps). AtTOC75, a component of the chloroplast protein import machinery at the outer membrane, was detected in fractions 11 to 15. The sucrose density of these fractions (20-38%) is consistent with the presence of envelope membranes (Schnell and Blobel, 1993). In contrast to CAB and AtTOC75, AtPGL35 was enriched in fractions 1 to 7. The sucrose density of these fractions (5% and 15%) is consistent with isolation of plastoglobules (Kessler *et al.*, 1999; Greenwood *et al.*, 1963; Legget Bailey and Whyborn, 1963; Wu *et al.*, 1997). Notably, separate peaks of AtPGL35 in fractions 1 and 5-7 suggest the existence of plastoglobule populations of different densities, as previously reported (Legget Bailey and Whyborn, 1963). AtPGL35 was also detected in higher sucrose density fractions, as previously observed for pea PG1 (Kessler *et al.*, 1999). To analyse the distribution of AtVTE1 in chloroplast membranes, the fractions were probed with anti-VTE1 serum. AtVTE1 was detected in fractions 1-7 of the gradient and codistributed with AtPGL35 peak fractions.

To determine whether AtVTE1 colocalised with AtPGL35 (as suggested by the membrane fractionation experiment, the two proteins were coexpressed as YFP- and CFP-fusion proteins, respectively, in protoplasts (Fig. 2.17). AtPGL35-CFP as well as AtVTE1-YFP fluorescent signals were present in globular structures inside chloroplasts. Both the merge of the independent fluores-

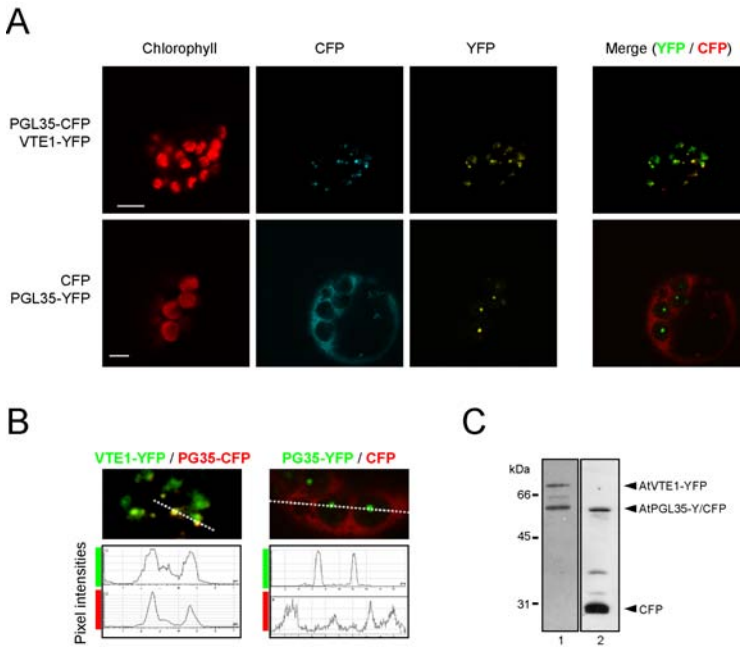

Figure 2.17: Colocalisation of AtPGL35 and AtVTE1 in Arabidopsis protoplasts. **A**, Protoplasts were cotransformed with AtVTE1-YFP and AtPGL35-CFP or with CFP and AtPGL35-YFP constructs. CFP fluorescence (CFP) and YFP fluorescence (YFP) were monitored by confocal microscopy. Chlorophyll, chlorophyll autofluorescence. Merge, superposition of YFP and CFP signals (green and red pseudocolours, respectively). Bar length: 5 μm. **B**, Pixel intensities in YFP and CFP channels were measured across sections indicated by dotted lines on the fluorescence images. **C**, Western blot analysis of protoplasts transformed with AtPGL35-CFP and AtVTE1-YFP (lane 1) or with AtPGL35-YFP and CFP (lane 2). The blot was probed with antibodies raised against GFP.

cence images and the pixel intensity analysis showed an overlap of the fluorescence, indicating colocalisation of AtPGL35 and AtVTE1 in plastoglobules.

Taken together, the data suggest that AtVTE1 is neither a component of the thylakoids nor of the inner envelope membrane but associated with plastoglobules.

2.3.2 γ-tocopherol methyl transferase (AtVTE4) localises at the chloroplast envelope

The tocopherol cyclase AtVTE1 catalyses the cyclisation of DMPQ precursors to δ- or γ-tocopherol which are methylated to lead β- or α-tocopherol. α and γ forms are the most abundant and their relative content varies in plant tissues.

Leaves mostly contain α-tocopherol (DellaPenna and Pogson, 2006). The final methylation step is catalysed by the γ-tocopherol methyl transferase (γ-TMT, AT1G64970), also named AtVTE4.

Since AtVTE1 was identified as a plastoglobule protein, we questioned whether AtVTE4 was also associated with plastoglobules. AtVTE4 has a predicted transit peptide (TargetP score = 0.95), indicating localisation in plastids. AtVTE4 was however not detected in the proteome of plastoglobules (see Table 4.2), indicating either a very low abundance of the protein or its localisation to an other chloroplast compartment. Furthermore, a γ-tocopherol methylase activity was detected in a chloroplast envelope preparations in earlier studies (Soll and Schultz, 1980; Soll *et al.*, 1985). To determine the localisation of AtVTE4, a GFP fusion to AtVTE4 coding sequence (AtVTE4-GFP) was transiently expressed in Arabidopsis leaves by particle bombardment. As shown in Fig. 2.18A, fluorescent rims around chloroplasts were detected in cells bombarded with the AtVTE4-GFP construct. Similar patterns were observed with a GFP fusion to the first transmembrane domain of AtTIC110 (AtTIC110$_{tm}$-GFP), used as a chloroplast envelope marker. In contrast, globular structures were observed in cells expressing the plastoglobule marker AtPGL35-GFP and fluorescent signals overlapped with chlorophyll autofluorescence in cells transformed with a GFP fusion to the RuBisCO small subunit transit peptide (pSSU-GFP). For several constructs, weak cytosolic fluorescence (similar to GFP patterns) was also observed, indicating incomplete import of fusion proteins into chloroplasts. The data suggest localisation of AtVTE4 to the chloroplast envelope. Similar results were obtained when AtVTE4-GFP was expressed in protoplasts (Fig. 2.18B). However, frequent aggregation of the fusion protein was observed in this system. A single peptide, migrating to the expected mass of AtVTE4-GFP (33 kDa of AtVTE4 mature form fused to the 27 kDa eGFP) was detected by immunoblot in transformed protoplasts (Fig. 2.18C).

2.4 Protein targeting to plastoglobules

2.4.1 Plastoglobulins lack strongly hydrophobic domains

The identification of proteins associated with plastoglobules implies that mechanisms ensuring protein targeting to plastoglobules must exist in plastids. However, nothing is known regarding these mechanisms and PGLs do not share conserved sequence motifs with other plant or animal lipid body proteins. Several types of proteins associated with lipid bodies have been described in prokaryotic and eukaryotic cells (reviewed in Murphy, 2001). Such proteins often contain hydrophobic domains protruding in the apolar lipid environment. Alternatively, motifs responsible for lipid association in apolipoproteins consist of amphiphatic α-helices and β sheets. In addition, other lipid body proteins such as adipophilin do not contain obvious lipid binding domains.

Hydrophobic domains of proteins can be visualised using the algorithm developed by Kyte and Doolittle (Kyte and Doolittle, 1982). None of the 13 Ara-

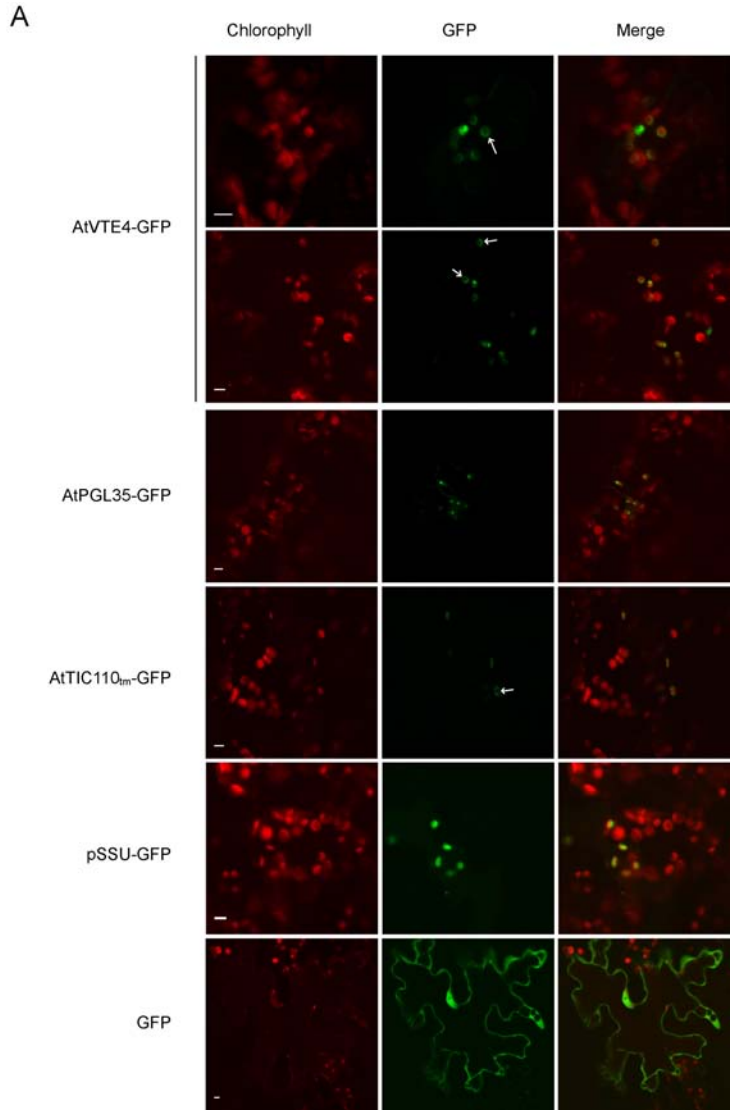

Figure 2.18: Localisation of γ-tocopherol methyl transferase AtVTE4 (see caption on page 44).

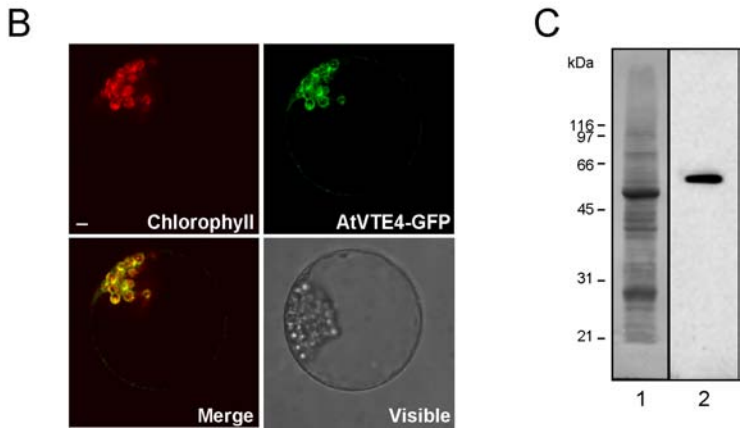

Figure 2.18: Localisation of γ-tocopherol methyl transferase AtVTE4 (continued). **A**, Transient expression of GFP-fusion proteins in leaves by particle bombardment. Rosette leaves from adult Arabidopsis plants were bombarded with gold particles coated with AtVTE4-GFP, AtPGL35-GFP, AtTIC110$_{tm}$-GFP, pSSU-GFP or GFP constructs. **B**, Protoplasts were transformed with AtVTE4-GFP construct. **A** and **B**, GFP fluorescence was visualised by confocal microscopy. Bar length: 5 μm. Merge, overlap of GFP and chlorophyll autofluorescence (chlorophyll); Visible, bright field picture. **C**, Western blot analysis of protoplasts transformed with AtVTE4-GFP. Proteins were visualised by staining the membrane with amidoblack (lane 1). AtVTE4-GFP was detected using anti-GFP antibodies (lane 2).

bidopsis PGLs contained strongly hydrophobic domains (above the 1.8 threshold using a window size of 19, see Fig. 2.19A). However, small stretches with higher hydropathy scores were observed in most AtPGL sequences. These stretches were found at different locations: shortly after the transit peptide, at the middle of the sequence or at the C-terminus. For comparison, hydropathy plots of an oleosin and of a caleosin, which associate with cytosolic oilbodies in oil-seeds, are shown (Fig. 2.19B).

2.4.2 Most of AtPGL34 sequence may be required for targeting the protein to plastoglobules

In the absence of data on the sequence requirement for plastoglobule targeting, we designed a series of C-terminal GFP fusion constructs that removed portions of AtPGL34 coding sequence (Fig. 2.20B). AtPGL34 was chosen for this study since the fluorescent patterns obtained with the AtPGL34-GFP construct were similar to those obtained in plastoglobule immunolocalisation experiments (see Fig. 2.4 and 2.5). Three domains with higher hydrophobic scores can be visualised in the Kyte and Doolittle hydropathy plot of AtPGL34. These domains comprise residues 80-94 (H1), 142-161(H2) and 273-282 (H3). Furthermore, we reasoned that if a domain responsible for targeting or anchoring PGLs to plastoglobules exists, it may be conserved among the different Arabidopsis PGLs. As revealed by sequence alignments (see Fig. 2.1), AtPGLs share conserved domains near the N- and C-termini of the proteins. In AtPGL34, the N-terminal domain comprises residues 103 to 138 but the conserved C-terminal domain is lacking. Both homology and hydropathic criteria were therefore taken into account for the choice of the deletion constructs. The shortest construct ($AtPGL34_{1-56}$-GFP) only comprised 3 residues in addition to the predicted transit peptide and was designed as a stromal control. The second construct, comprising the amino acids 1-133 ($AtPGL34_{1-133}$-GFP), contained the H1 domain as well as the conserved motif. The construct $AtPGL34_{1-170}$-GFP included in addition the H2 motif. The fourth construct ($AtPGL34_{1-290}$-GFP) comprised H1, H2 and H3 motifs, as well as the conserved region. An additional N-terminal deletion construct ($AtPGL34_{1-56..134-308}$-GFP), lacking residues 57-133, only contained H2 and H3 motifs.

As shown in Fig. 2.20B, $AtPGL34_{1-56}$-GFP and $AtPGL34_{1-133}$-GFP gave diffuse signals broadly overlapping with the autofluorescence from the chlorophyll. In several chloroplasts however, peak GFP and chlorophyll fluorescence did not overlap, suggesting that both fusion proteins localised in the stroma. In contrast, when $AtPGL34_{1-290}$-GFP construct was expressed in protoplasts, the fusion protein localised to small punctuated structures, similarly to the full length protein. A distinct pattern was observed with $AtPGL34_{1-170}$- and $AtPGL34_{1-56..134-308}$-GFP constructs. Fewer and larger fluorescent spots were observed in chloroplasts, suggesting mistargeting or protein aggregation.

Mistargeting (or aggregation) of AtPGL34 deletion constructs imply that the corresponding fusion proteins do not colocalise with full-length AtPGL34. We therefore cotransformed protoplasts with AtPGL34-CFP and AtPGL34 deletion

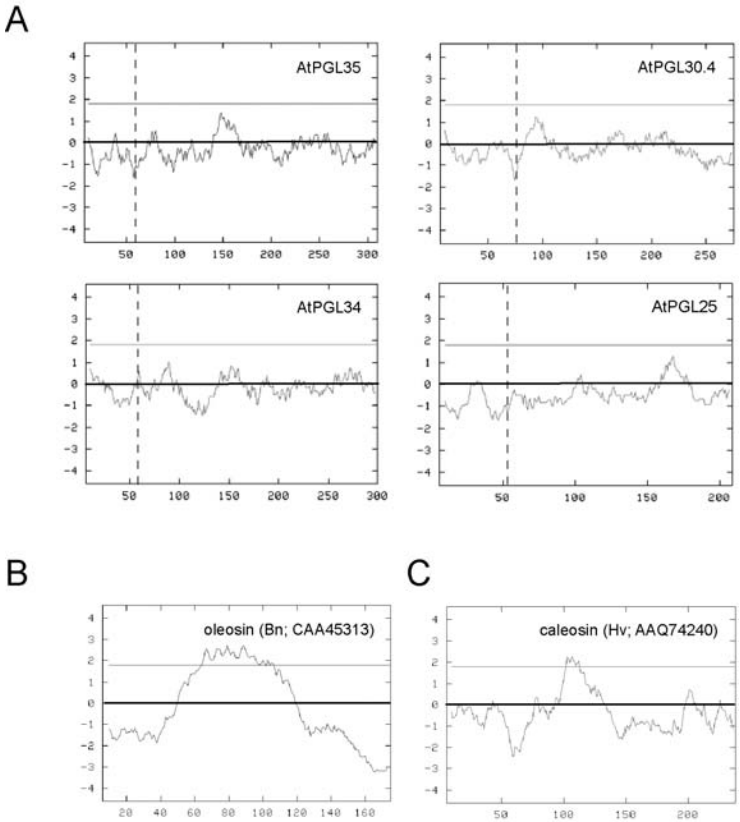

Figure 2.19: Hydropathic character of plant oilbody proteins. Kyte and Doolittle hydropathy plots of AtPGLs (**A**), of a rapeseed oleosin (**B**) and of a caleosin from barley (**C**) are represented. Positive values are attributed to hydrophobic residues. A window size of 19 amino acids was used. Peaks with scores greater that 1.8 (pale horizontal lines) identify putative transmembrane regions. Dotted lines indicate predicted cleavage sites of transit peptides. Bn, *Brassica napus*; Hv, *Hordeum vulgare*; GeneBank accession numbers are indicated.

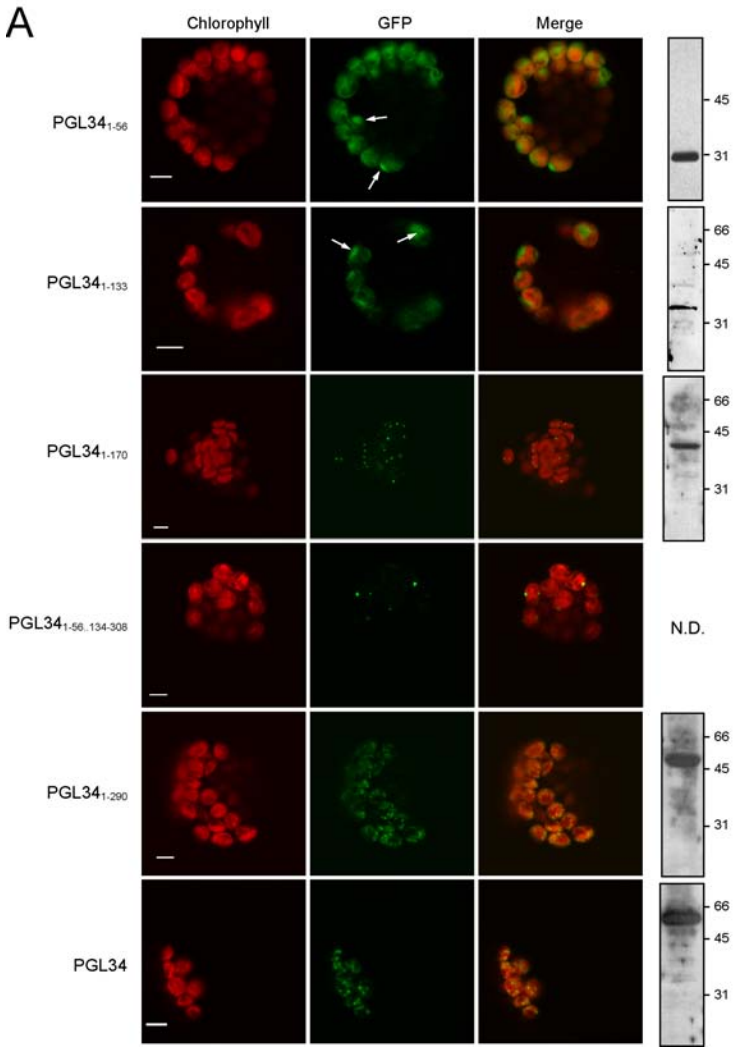

Figure 2.20: Transient expression of GFP fused to AtPGL34 fragments (see caption on page 48).

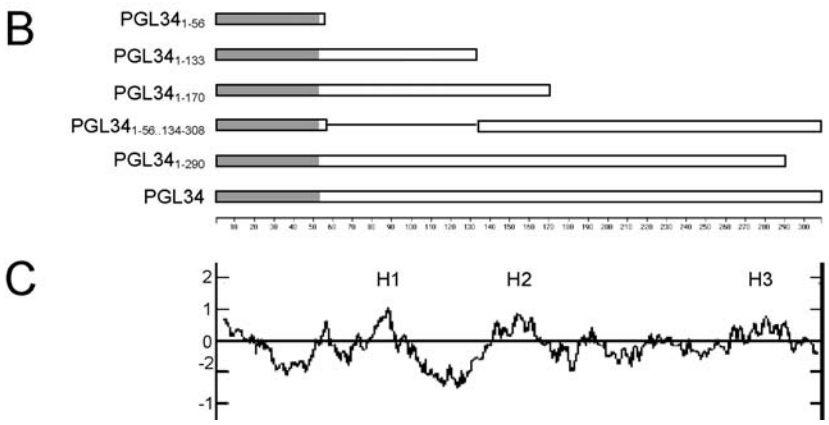

Figure 2.20: Transient expression of GFP fused to AtPGL34 fragments (continued). **A**, Arabidopsis protoplasts were transformed with fragments of, or with full length AtPGL34 coding sequence fused to GFP, as indicated. GFP signals (GFP) were detected by confocal microscopy. Arrows indicate strong GFP signals overlapping with weak chlorophyll autofluorescence signals (chlorophyll). Merge: overlap of chlorophyll and GFP signals. Scale bars: 5 μm. The panels on the right hand side show the detection of GFP fusion proteins in transformed protoplasts by immunoblotting, using anti-GFP antibodies. N.D., not detected. **B**, Schematic representation of the constructs. The transit peptide of AtPGL34 (PGL34) is in grey. **C**, Kyte and Doolittle hydropathy plot of AtPGL34. Domains with higher hydropathy scores (H1-H3) are indicated.

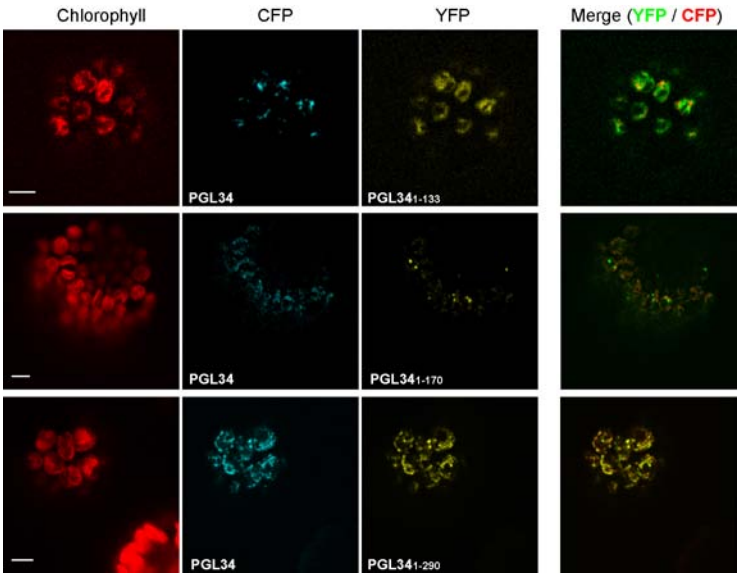

Figure 2.21: Cotransformation of Arabidopsis protoplasts with full length and truncated AtPGL34. Protoplasts coexpressing AtPGL34-CFP and AtPGL34$_{1-133}$-YFP, AtPGL34$_{1-170}$-YFP or AtPGL34$_{1-290}$-YFP were analysed by confocal microscopy. Colours are as in Fig. 2.17. Bar length, 5 μm.

constructs fused to YFP (Fig. 2.21). As revealed in merged fluorescent images, CFP and YFP signals did not overlap in protoplasts expressing AtPGL34 and AtPGL34$_{1-133}$. In contrast, AtPGL34-CFP and AtPGL34$_{1-290}$-YFP colocalised, indicating that the short C-terminal hydrophilic part of the protein is dispensable for targeting. The strong punctuate signals observed in protoplasts expressing AtPGL34$_{1-170}$ were not labelled with AtPGL34-CFP, confirming mistargeting and/or aggregation of the truncated protein.

2.4.3 Transgenic Arabidopsis plants expressing *AtPGL34-YFP*

Based on fluorescence patterns, we have deduced that full length AtPGL34 fused to GFP localised to plastoglobules. Moreover, the preliminary results obtained with AtPGL34-GFP deletion constructs suggested that most of AtPGL34 sequence is required for correct targeting. In order to substantiate our hypothesis that chimaera plastoglobulin fusion proteins can be directed to plastoglobules, wild-type plants were stably transformed with the coding sequence of YFP fused to *AtPGL34*. Regulatory elements are often found in introns and in 3' UTRs. Moreover, we observed that transgene expression driven by the strong CaMV 35S promoter often leads to gene silencing. We therefore used the genomic sequence of *AtPGL34* (Fig. 2.22A).

Ten primary transformants were identified on selection media and homozygous T3 lines containing a single insertion locus were identified by segregation analysis (data not shown). When illuminated with UV light and observed under the binocular microscope, plants from different lines exhibited various levels of YFP fluorescence. Representative examples are shown in Fig. 2.22B. To demonstrate the presence of AtPGL34$_g$-YFP in the transgenic plants, protein extracts prepared from wild type or transgenic seedlings were analysed by Western blot (Fig. 2.22D). No signal was detected in the wild type, indicating specificity of the anti-GFP antibody. In the transgenic lines, a peptide with an apparent mass of 55 kDa, the predicted mass of PGL34-YFP (28.3, processed PGL34 and 26.9, YFP), was decorated with anti-GFP antibodies. A second band, migrating slightly higher and possibly representing partially cleaved precursor, was also recognised. Signal intensities from different lines correlated with the fluorescence levels observed in the leaves. Differences in expression levels probably reflected positional effects of the T-DNA insertions (Goodrich and Tweedie, 2002). Plants from the line 5.2, which showed strongest expression of AtPGL34$_g$-YFP, were further analysed. Although weaker than in leaves, YFP fluorescence was also detected in roots (Fig. 2.22C). This observation is in accordance with DNA microarray results (see Fig. 2.2A) showing the presence of *AtPGL34* transcripts in most plant organs including roots.

More detailed pictures of AtPGL34$_g$-YFP signals were obtained by confocal microscopy analysis of leaves and roots (Fig. 2.23). In both organs, punctuated signals were observed. In leaves, the signals were detected in epidermal as well as in mesophyll cells. YFP patterns were indeed similar to those observed in protoplasts transiently expressing *AtPGL34-YFP*. In roots, strongest signals were observed in the vasculature and in nascent secondary roots.

2.4.4 AtPGL34g-YFP associates with low-density particles *in vivo*

The fluorescent patterns observed in plants expressing *AtPGL34$_g$-YFP* and in protoplasts transformed with AtPGL34-GFP construct suggested association of the fusion proteins with plastoglobules. To verify this hypothesis, chloroplast membranes from transgenic *AtPGL34$_g$-YFP* plants were used for gradient flotation centrifugation (Fig. 2.24). Proteins extracted from the different sucrose gradient fractions were used for SDS-PAGE, transferred to a nitrocellulose membrane and stained with amidoblack. In lanes corresponding to the low-density fractions 1-7 (5 and 15% sucrose steps), a dominant band was observed between the 66 and 45 kDa markers, at the expected size of AtPGL34$_g$-YFP (55 kDa). After immunoblotting with anti-GFP antibodies, strong signals overlapping with the visible bands were detected, confirming the identity of the 55 kDa peptide. AtPGL34$_g$-YFP codistributed with AtPGL35 in the gradient fractions and peak AtPGL34$_g$-YFP signals were clearly distinct from peak AtTOC75 and CAB signals. Moreover, analysis by confocal microscopy revealed that the low density fractions 1 and 7 (5 and 15% sucrose steps, respectively) contained numerous globular fluorescent structures. These data strongly suggest association

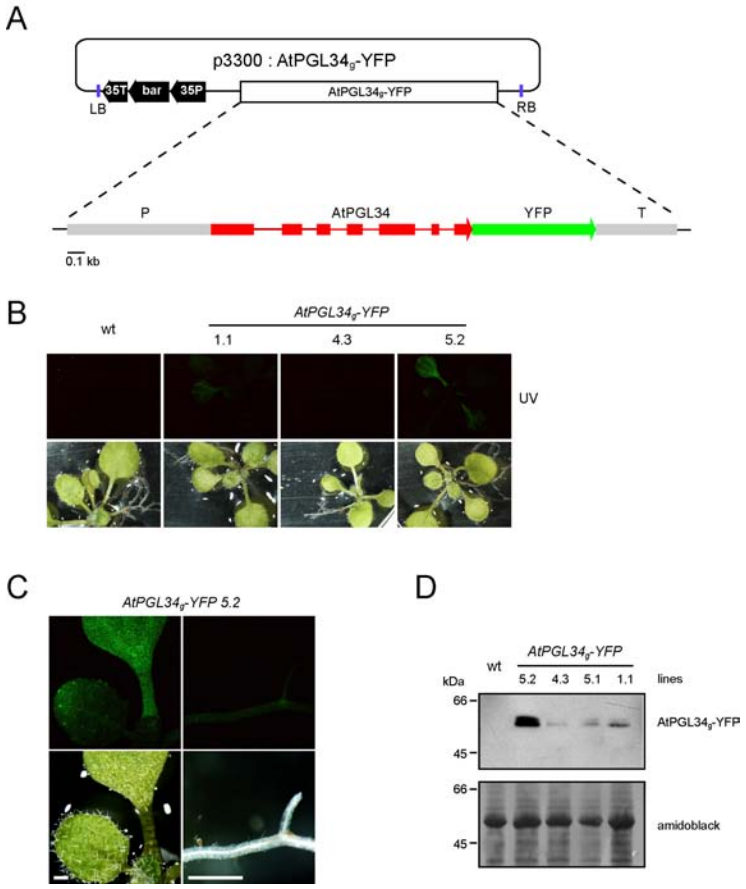

Figure 2.22: Transgenic plants expressing *YFP* fused to *AtPGL34* genomic sequence. **A**, Scheme of the construct used for plant transformation. The genomic sequence of *AtPGL34*, comprising the 5' upstream region (P), *AtPGL34* exons and introns, as well as the 3' downstream region (T), was fused to the yellow fluorescent protein (YFP) and inserted in the p3300 binary vector. The vector contained the bar gene (phosphinotricin acetyl transferase) under the control of the CaMV 35S promoter (35P) and the CaMV 3'UTR (35T, polyA signal) for selection. LB and RB, T-DNA left and right boarders. **B**, Detection of AtPGL34$_g$-YFP with UV light. Wild type (wt) and *AtPGL34$_g$-YFP* plants from different T3 lines (1.1, 4.3 and 5.2) were observed with a binocular equipped with a UV lamp Fluorescent signals (UV) are shown in green. **C**, Enlargements from **B** showing YFP signals in leaves and roots from a transgenic plant (line 5.2). Scale bars: 0.5 mm. **D**, Western blot analysis of rosette leaves from wild-type and *AtPGL34$_g$-YFP* plants. AtPGL34$_g$-YFP was detected using anti-GFP antibodies. Protein staining (amidoblack) indicates similar loading amounts.

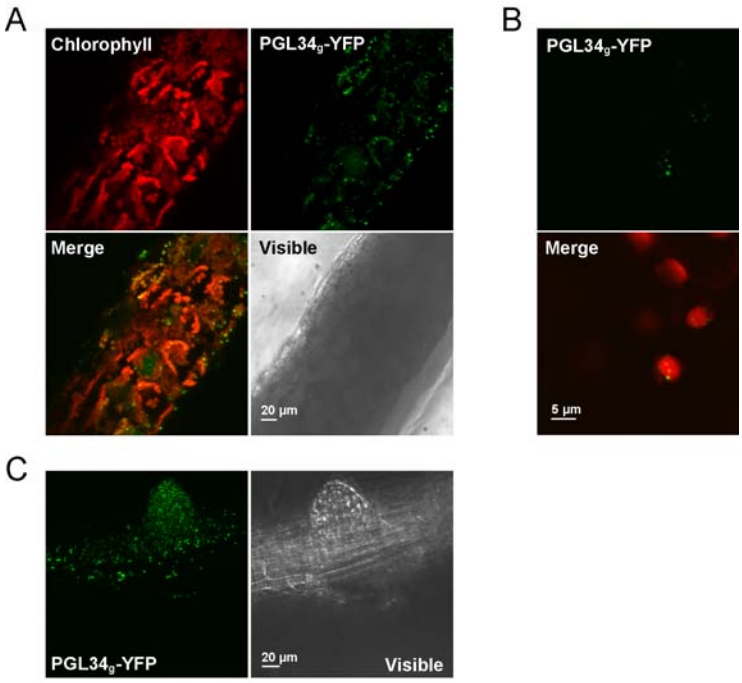

Figure 2.23: Analysis of *AtPGL34$_g$-YFP* plants by confocal microscopy. A leaf section (**A**, **B**) and a root (**C**) from an adult transgenic plant (line 5.2) were observed with a confocal microscope. **A** and **C**, Z-projections from optical sections are shown. **B**, Higher magnification showing chloroplasts from a mesophyll cell. Visible, bright-field microscopic images; Merge, superimposing of chlorophyll autofluorescence (chlorophyll) and YFP fluorescence (AtPGL34$_g$-YFP).

of AtPGL34$_g$-YFP with plastoglobule lipid bodies.

The fluorescent structures observed in fraction 1 appeared somewhat larger than those in fraction 7. Using the ImageJ software, mean areas (± SE) of fluorescent spots were determined to be 0.121 ± 0.006 μm^2 in fraction 1 and 0.072 ± 0.003 μm^2 in fraction 7. The difference in particle size suggest the existence of plastoglobule populations of different densities, as previously reported (Legget Bailey and Whyborn, 1963).

2.4.5 Yield estimation of recombinant protein

Strong immunoblotting signals suggested that substantial levels of recombinant proteins were synthesised, at least in line 5.2. The amount of AtPGL34$_g$-YFP in crude plant extracts was estimated by comparing immunoblot signals with serial dilutions of purified GFP produced in Escherichia coli (Fig. 2.25). AtPGL34$_g$-YFP was calculated to account for approximately 0.2% of total leaf protein.

2.4.6 Phenotype of *AtPGL34$_g$-YFP*-expressing plants

Plant from different lines expressing *AtPGL34$_g$-YFP* at various levels were indistinguishable from wild-type when grown in short or long-day conditions. The germination rate of transgenic seeds (line 5.2) was equal to wild type (Pearson Chi-Square test, n=358, p=0.33). Fluorescence measurements revealed similar maximum photosystem II quantum efficiencies (Fv/Fm) in transgenic vs. wild type leaves (Fig. 2.26B), ruling out major inhibitory effects of plastoglobule targeting on photosynthesis. Moreover, rosettes from wt and *AtPGL34$_g$-YFP* adult plants had similar fresh weigh (Fig. 2.26C).

The data indicate that plant growth and development were not affected by the accumulation of AtPGL34$_g$-YFP in plastoglobules. Together with the simple purification procedure of plastid lipid bodies, they demonstrate an excellent potential for protein accumulation in plastoglobules.

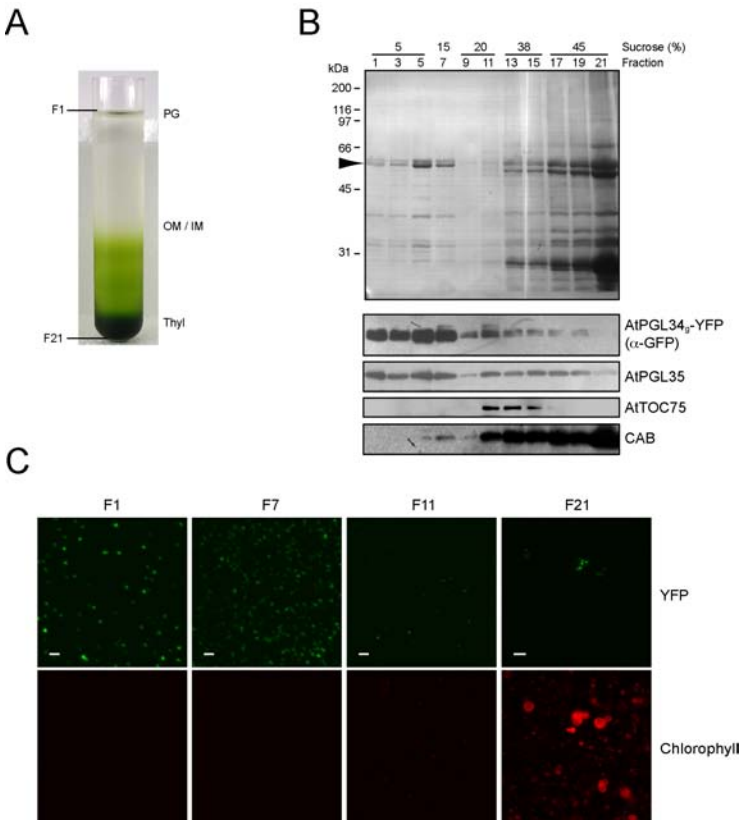

Figure 2.24: Analysis of *AtPGL34$_g$-YFP* plants by gradient flotation centrifugation. **A**, Total membranes from a crude chloroplast preparation were separated by flotation centrifugation on a discontinuous sucrose gradient PG, plastoglobules; OM/IM, outer and inner envelope membranes; Thyl, thylakoid membranes. Fractions 1 and 21 (F1 and F21) are indicated. **B**, SDS-PAGE analysis of fractions from the sucrose gradient. After ultracentrifugation, fractions of 0.5 ml were collected from the top of the gradient. Proteins contained in 400 μl of fractions 1 to 7, 200 μl of fractions 9 to 15, 100 μl of fractions 17 and 19 or 50 μl of fraction 21 were separated by SDS-PAGE, transferred to a nitrocellulose membranes and stained with amidoblack. The nitrocellulose membrane was then probed with antibodies against GFP, AtPGL35, AtTOC75 and CAB, as indicated. **C**, Analysis by confocal microscopy of the representative fractions 1, 7, 11 and 21 (F1-21, corresponding to 5, 15, 20 and 45% sucrose steps, respectively). YFP fluorescent signals (YFP) and chlorophyll autofluorescence (chlorophyll) are shown. Scale bars: 1 μm (F1-11) or 5 μm (F21).

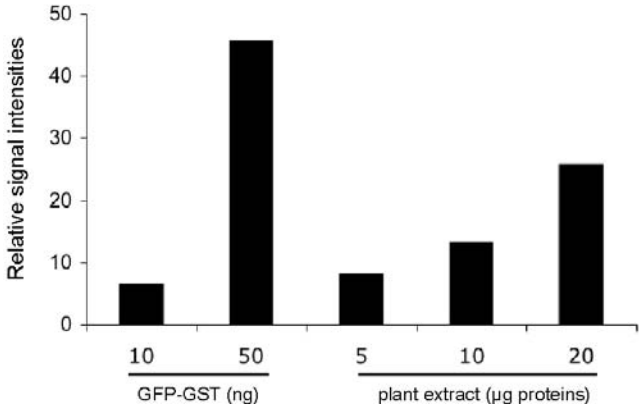

Figure 2.25: Yield estimation of AtPGL34$_g$-YFP recombinant protein. Different amounts of total protein extracts from line 5.2 were subjected to SDS-PAGE in parallel with different amounts of recombinant GST-GFP, as indicated. Signals were quantified using a CCD camera and the Quantity One software.

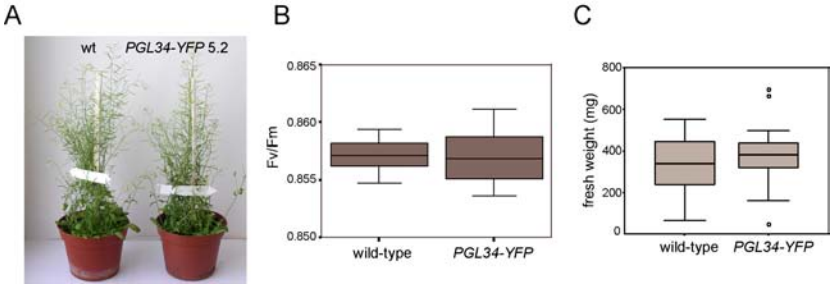

Figure 2.26: Phenotype of *AtPGL34$_g$-YFP* plants. **A**, Photographs from wild-type or *AtPGL34$_g$-YFP* plants (line 5.2) grown for 8 weeks in 16/8 hour light/dark conditions. **B**, Maximum photosystem II quantum efficiencies (Fv/Fm). T-test: t=0.17, p=0.67, n=14. **C**, Fresh weight of rosette leaves five weeks after germination. T-test: t=-1.22, p=0.23. At least 19 plants were measured. Normal distribution of the data (**B** and **C**) was verified using the Kolmogorov-Smirnov test ($p > 0.1$).

Chapter 3

Discussion

3.1 Towards understanding the functions of plastoglobulins

3.1.1 Arabidopsis plastoglobulins associate with plastoglobules

Proteins of the PAP/fibrillin family (bell pepper fibrillin and pea PG1) were previously shown to localise to the periphery of plastoglobules or of related chromoplast fibrils (Deruère *et al.*, 1994; Pozueta-Romero *et al.*, 1997; Kessler *et al.*, 1999). However, CDSP34 and C40.4 potato plastoglobulins were localised mainly in the stroma and thylakoids (Monte *et al.*, 1999; Eymery and Rey, 1999; Rey *et al.*, 2000), suggesting that proteins from the PAP/fibrillin family may associate with thylakoid membranes in addition to plastid lipid bodies. Here, the localisation of AtPGL35 and AtPGL34, two Arabibidopsis PGLs was studied. Using immunogold labelling on leaf sections and immunofluorescence on fixed protoplasts, AtPGL35 was localised in chloroplast plastoglobules (Fig. 2.4). Moreover, GFP-fusions to AtPGL34 and -35 were apparently targeted to plastoglobules *in vivo* (Fig. 2.5). Association of AtPGL34-YFP with low-density particles was further confirmed by flotation centrifugation (Fig. 2.24).

AtPGL35, as well as AtPGL30.4, -33, -40 and -25/29 have previously been shown to behave as peripheral components of thylakoid membranes by TX-114 extraction (Friso *et al.*, 2004). In a separate study, AtPGL35, -40, -33, -30.4, -45 and -25 were identified in the 8 M urea extract of chloroplast membranes, also suggesting a peripheral membrane association (Kleffmann *et al.*, 2004). With the exception of AtPGL45, all these proteins were identified in the proteome of plastoglobules (Ytterberg *et al.*, 2006; Vidi *et al.*, 2006). It is therefore likely that PAP/fibrillins extracted by TX-114 or 8 M urea were present in plastoglobules attached to thylakoids (Lichtenthaler, 1969; Kessler *et al.*, 1999; Austin *et al.*, 2006) and therefore identified as thylakoid proteins.

Because specific labelling of plastoglobules was observed in tobacco, Ara-

bidopsis and spinach chloroplasts using antibodies raised against PG1 (Austin *et al.*, 2006), it seems unlikely that plastoglobulin localisation differs in plant species. Although it can not be excluded that some PGLs associate with thylakoids rather than plastoglobules, the localisation of CDSP34 and C40.4 might need to be re-evaluated.

3.1.2 Distinct plastoglobule populations or molecular functions of plastoglobulins?

In protoplasts coexpressing *AtPGL34* and *AtPGL35* coding sequences fused to GFP variants, the corresponding signals were largely separated (Fig. 2.6). Instead, AtPGL35 colocalised with AtVTE1 and with the fructose-bisphosphate aldolase 2 isoform (not shown).

Different populations of plastoglobules might therefore exist, as suggested in previous studies (Legget Bailey and Whyborn, 1963; Kessler *et al.*, 1999). Certain subsets of proteins , e.g. enzymes, might be restricted to given plastoglobule types. To verify this hypothesis, it will be interesting to selectively immuno-purify plastoglobules using antibodies directed against different PGLs or plastoglobule-associated enzymes.

Plastoglobulins may also have different molecular functions. Several lines of evidence indicate that levels of AtPGL35 are linked with plastoglobule abundance: i) High expression of *AtPGL35* in petals correlates with the accumulation of lipid bodies in leukoplasts (Pyke and Page, 1998). ii) Upregulation of *AtPGL35* in stress conditions parallels the increase in plastoglobule volume (Eymery and Rey, 1999). iii) Overexpression of *AtPGL35* as a GFP fusion lead to the formation of large globular structures, probably corresponding to swollen globules or to plastoglobule clusters (Austin *et al.*, 2006). In contrast to AtPGL35, AtPGL34-GFP localised to smaller structures. AtPGL34 may therefore be targeted to pre-existing plastoglobules. Consistent with this hypothesis, the large structures containing AtPGL35-CFP were also labelled with AtPGL34-YFP but smaller structures containing AtPGL34-YFP did not contain AtPGL35-CFP (Fig. 2.6).

3.1.3 Plastoglobulin expression patterns highlight ubiquity of plastoglobules

Expression data showed that plastoglobulins are expressed in most (if not all) organs (Fig. 2.2A). However, expression levels of most AtPGLs were highest in green tissues and messengers of at least five AtPGLs accumulated after exposure to light (Fig. 2.3A), in agreement with a function for plastoglobules in chloroplast metabolism.

During germination or de-etiolation, prolamellar bodies are rapidly converted into thylakoids. The number of plastoglobules was reported to decrease during this process (Lichtenthaler, 1968). It has therefore been proposed that lipids stored in plastoglobules are utilised for the synthesis of thylakoids. According to this model, one might expect the decrease of plastoglobule abundance

to be accompanied by a drop of PGL levels. However, all AtPGLs were expressed in cotyledons and, related to total protein contents, AtPGL35 and -30.4 e.g. were clearly more abundant in light-grown than in dark-grown seedlings (Fig. 2.3C). Moreover, only a single Arabidopsis PGL homologue (AtPGL45) was identified in a low density fraction derived from rice etioplasts (Ytterberg *et al.*, 2006).

These observations may nevertheless be reconciled with the 'lipid reservoir' hypothesis: i) Germination is accompanied by *de novo* lipid synthesis (Davies *et al.*, 1980). Newly synthesised lipids may therefore move through plastoglobules and balance the disappearance of the pre-existing plastoglobules. ii) The number and volume of chloroplasts strongly increase during greening (Possingham and Saurer, 1969). It may be more appropriate to correlate PGL levels to the volume of plastids in dark or light-grown seedlings. Further work is necessary to define the role of plastoglobules in thylakoid genesis. It would notably be interesting to compare plastoglobule lipid composition in etiolated and de-etiolated plants. Transgenic plants expressing AtPGL-YFP fusion proteins under the control of the endogenous promoter may also provide useful tools to follow plastoglobule dynamics during greening. An alternative hypothesis is that plastoglobules do not represent a storage compartment for thylakoid structural lipids (galactolipids) or precursors thereof (notably di- and triacylglycerols) in proplastids and etioplasts. They may rather store antioxidants to protect developing membranes. Tocopherol contents were indeed shown to increase during germination (Munne-Bosch and Alegre, 2002).

During leaf senescence, enlargement and accumulation of plastoglobules has been observed together with disappearance of thylakoid membranes (e.g. Tuquet and Newman, 1980; Ghosh *et al.*, 2001). Moreover, carotenoid esters and free fatty acids are enriched in plastoglobules derived from gerontoplasts (in comparison to chloroplasts), indicating that lipids from degenerating thylakoid membranes accumulate in plastoglobules (Tevini and Steinmüller, 1985). As expected, several AtPGLs are expressed in senescing leaves (Fig. 2.2A). Interestingly, highest levels of *AtPGL24* transcript were present in senescing material, indicating that the protein may be implicated in this process.

AtPGLs were also expressed in non-green tissues such as pollen, petals and, to a lesser extent, roots. Intracellular lipid bodies are present in vegetative cells of pollen grains (Piffanelli *et al.*, 1998) and serve as a source of energy and structural lipids for pollen germination. Similarly to seed oleosomes, the oilbodies are thought to derive mostly from the endoplasmic reticulum and oleosins were detected amongst pollen proteins (Kim *et al.*, 2002). In contrast to most other organs, only five AtPGL genes (out of 11 for which probesets were available) were expressed in pollen. *AtPGL31*, however, showed highest relative expression in these cells. The protein may therefore be associated with certain pollen lipid bodies and/or participate in their formation.

In floral buds, young petals are green and contain chloroplasts. During the development of the petal lamina, plastids loose their chlorophyll and differentiate into leukoplasts, resulting in a white petal blade (Pyke and Page, 1998). Large and numerous plastoglobules are characteristic of leukoplasts. It is there-

fore not surprising that plastoglobulin transcripts were detected in this organ (Fig. 2.2A). High *AtPGL35* mRNA and protein levels were notably detected in flowers (Fig. 2.2B,D).

Root cells contain amyloplasts and proplastids, the latter containing numerous plastoglobules (Yu and Li, 2001). In Western blot experiments, lowest AtPGL40, -35 and -30.4 levels were detected in roots. (Fig. 2.2D). The data are consistent with gene expression profiling studies (Fig. 2.2A), where the root to leaf signal ratio was 0.16 for *AtPGL35*. This ratio was 0.4 for *AtPGL34* and the YFP signals detected in roots from $AtPGL34_g$-*YFP* plants was only about half of that observed in leaves (Fig. 2.22). *AtPGL34* messengers did not accumulate after exposure to light (Fig. 2.3), consistent with expression in green and in non-photosynthetic tissues. Fluorescent globular structures observed in roots from reporter plants were particularly dense in emerging lateral roots (Fig. 2.23), possibly due to the presence of numerous proplastids in these zones (Whatley, 1983).

The fact that AtPGLs are differentially expressed in plant organs (leaves, petals, siliques, roots), which contain different plastid types (chloroplasts, leukoplasts, elaioplasts or proplastids), suggest that the proteins may have different molecular functions (e.g. plastoglobule generation, stabilisation, fusion) and/or that they may associate with different types of lipids. The observation that PAP1, -2 and -3 plastoglobulins in *Brassica rapa* are associated with specific tissues (Kim *et al.*, 2001) support this idea.

3.1.4 Stress leads to the upregulation of *AtPGL35*

Under various environmental conditions resulting in oxidative stress, plastoglobules enlarge or accumulate in clusters (see above). In parallel, a number of studies have shown that proteins from the PAP/fibrillin family are upregulated by abiotic stress (see Table 1.1). Consistent with these observations, Arabidopsis *PGL35* (and *-33*) transcripts were shown to accumulate in stress conditions (Fig. 2.12, Laizet *et al.*, 2004) and AtPGL35 accumulated after drought or high light treatments, as well as during ageing (Fig. 2.13 and 2.14). In contrast to AtPGL35, AtPGL40 and -30.4 were not significantly induced by drought and photooxidative stress (data not shown). Moreover, transcription profiling revealed that plastoglobulin transcripts other than from *AtPGL35* did not accumulate in stress conditions or after ABA treatment (data not shown). The data therefore suggest that AtPGL35 (and maybe AtPGL33) are the only AtPGLs responsive to environmental stresses. In a recent report, Yang et al. (2006) showed that tolerance of photosystems to photooxidative damage positively correlates with AtPGL35 protein levels. Moreover, overexpression of fibrillin in potato plants increased plastoglobule number and drought stress tolerance (Rey *et al.*, 2000). In Arabidopsis, high illumination treatment was accompanied by increased plastoglobule size and formation of plastoglobule clusters. It is tempting to propose that these morphological changes were caused by increased levels of AtPGL35/33.

3.1.5 Functions of plastoglobulins are partially redundant

Arabidopsis knock-out plants for *AtPGL35* (*pgl35*; Fig. 2.9) or for other AtPGLs (Dr. C. Bréhélin, personal communication), did not show growth defects nor any visible phenotype under standard growth conditions. Moreover, chloroplast ultrastructure in *pgl35* plants was not different from wild-type (Fig. 2.9D).

Single knock-out mutants from multiple copy genes often lack visible phenotype (Bouche and Bouchez, 2001). The presence of highly homologous genes among the Arabidopsis plastoglobulin family (Fig. 2.1) and the observation that three AtPGL genes may be issued from recent gene duplication suggest function redundancy, especially between highly similar proteins.

In particular, AtPGL35 and -33 probably represent functional homologues. The proteins are 76% identical and the distribution of *AtPGL35* and *AtPGL33* messengers in the different organs was very similar (Fig. 2.2B). The simultaneous reduction of AtPGL35 and -33 (or AtPGL35, -33 and -40) in the *pgl35/$_{ihp}$pgl33* (or *pgl35/$_{ihp}$pgl33/-40*) plants may provide insight into the functions of PGLs. Further investigation will focus on photooxidative stress tolerance of the mutants, as well as on their chloroplast and leukoplast ultrastrucutres.

3.2 Plastoglobules as synthesis and storage sites for tocopherols

3.2.1 Localisation of the tocopherol cyclase to plastoglobules

The pathway leading to tocopherols has been elucidated using radio-labelling studies and, more recently, using molecular genetic tools (see Hofius and Sonnewald, 2003; DellaPenna, 2005; DellaPenna and Pogson, 2006 for review). Homogentisic acid (HGA) and phytyldiphosphate (phytyl-PP) serve as precursors for tocopherol biosynthesis. (Fig. 3.1A). HGA derives from the shikimate pathway and is synthesised from tyrosine via Tyr transaminase and 4-hydroxyphenylpyruvate dioxygenase (HPPD/PDS1; Garcia *et al.*, 1999; Norris *et al.*, 1998). This reaction is the only step in tocopherol biosynthesis occurring outside chloroplasts, in the cytosol. HGA is then prenylated to 2-methyl-6-phytyl-1,4-benzoquinone (MPQ) by addition of a phytyl molecule through the action of HGA phytyltransferase (HPT1/VTE2; Savidge *et al.*, 2002; Collakova and DellaPenna, 2001, 2003). In labelling experiments, Soll *et al.* (1985) showed the presence of HPT activity in inner chloroplast membranes purified from spinach leaves. While it is generally accepted that phytyl-PP originates directly from geranylgeranyldiphosphate (GGDP; Hofius and Sonnewald, 2003; Keller *et al.*, 1998), it has also been proposed that tocopherol phytyl tails might derive from chlorophyll (Lichtenthaler, 1968). Indeed, Valentin and colleagues (2006) have recently shown that reduced tocopherol content in the *vte5* mutant is caused by defective phytol kinase activity, suggesting that phytyl-PP may

be synthesised from chlorophyll breakdown products. Part of the MPQ pool is subsequently methylated to 2,3-dimethyl-6-phytyl-1,4-benzoquinone (DMPQ) by 2-methyl-6-phytyl-1,4-benzoquinone methyltransferase (APG1/E37/VTE3; Motohashi *et al.*, 2003; Cheng *et al.*, 2003; Van Eenennaam *et al.*, 2003), which is highly similar to the 37 kDa polypeptide from spinach inner chloroplast membrane (Block *et al.*, 1983). The corresponding methyl transferase activity was detected in chloroplast inner membrane fractions (Soll *et al.*, 1980; Soll and Schultz, 1980; Soll *et al.*, 1985).

Cyclisation and methylation of MPQ and DMPQ leads to the formation of the four major tocopherol forms (α-, β-, γ- and δ-tocopherol) that differ only in position and number of methyl groups on the aromatic ring. In Arabidopsis, ring closure is catalysed by VTE1 (Porfirova *et al.*, 2002). AtVTE1 is an orthologue of the maize sucrose export deficient 1 protein (SXD1; Provencher *et al.*, 2001). Although SXD1 was originally implicated in transferring chloroplast signals relevant to the carbohydrate status to the nucleus (Provencher *et al.*, 2001), the protein was shown to have tocopherol cyclase activity and thus to be a functional orthologue of Arabidopsis VTE1 (Sattler *et al.*, 2003). Cyclisation of DMPQ in γ-tocopherol was reported to occur in total chloroplast membrane fractions (Camara *et al.*, 1982). The tocopherol cyclase activity, however, was at the detection limit when chloroplast envelope membranes were used for the assay (Soll and Schultz, 1980; Soll *et al.*, 1985), suggesting that the cyclase reaction takes place in another chloroplast compartment. In labelling experiments using membrane fractions from bell pepper chromoplasts (Arango and Heise, 1998), ^{14}C-radiolabelled DMPQ accumulated in the lightest sucrose fraction. In contrast, ^{14}C-α-tocopherol was predominantly detected in the fraction corresponding to inner membranes. Although the authors claimed to have localised tocopherol biosynthesis at the inner membrane of chromoplasts, their data rather suggest that DMPQ (transiently) accumulates in an other compartment.

We present Western blotting of membrane fractions, immunofluorescent localisation of AtVTE1 in fixed chloroplasts as well as transient expression of AtVTE1-YFP fusion protein (Fig. 2.15 and 2.16) as evidence for the plastoglobule localization of AtVTE1. The codistribution of AtVTE1 with AtPGL35 in the membrane fractionation experiment (Fig. 2.16B) and microscopic colocalization of corresponding YFP and CFP-fusion proteins (Fig. 2.17) suggest that plastoglobules are the unique site of AtVTE1. The observation that DMPQ accumulates in plastoglobules prepared from *vte1* plants (Dr. P. Dörmann, personal communication) further indicates that AtVTE1 activity is located in plastoglobules. Plastoglobule localisation of VTE1 is consistent with the hydrophobic character of the protein (Stocker *et al.*, 1996) and with the absence of predicted transmembrane domain.

In chloroplasts, most γ-tocopherol molecules are further methylated to lead to the most abundant α-tocopherol form. This reaction is catalysed by γ-tocopherol methyl transferase (γ-TMT/AtVTE4; Bergmüller *et al.*, 2003), the enzymatic activity of which was measured in chloroplast envelope preparations (Soll and Schultz, 1980; Soll *et al.*, 1985). Localisation of AtVTE4 to the chloro-

plast envelope was confirmed by transiently expressing the protein as a GFP fusion in leaf epidermal cells (Fig. 2.18).

3.2.2 A model for tocopherol biosynthesis

Based on the data, we propose a working model for tocopherol biosynthesis in chloroplasts (Fig. 3.1B). Distinct localisations of tocopherol biosynthetic enzymes imply transport of precursors inside chloroplasts: i) Trafficking DMPQ to plastoglobules for ring cyclisation and ii) re-distribution of α-tocopherol from the chloroplast inner membrane to the other plastid compartments. Although a direct transport of DMPQ from the envelope to plastoglobules is proposed, it cannot be excluded that DMPQ is first directed to thylakoid membranes and subsequently accumulates in plastoglobules.

How tocopherols and tocopherol precursors are transported inside chloroplasts is not known and plastidic lipid transport in general is still poorly understood. Lipids may laterally diffuse from the envelope to thylakoids at contact sites (Siegenthaler, 1998). Such contacts have been observed in Chlamydomonas during greening (Hoober *et al.*, 1990) but are usually not observed in developed chloroplasts. Plastoglobules have been proposed to function as transporters (Kessler *et al.*, 1999). However, association of plastoglobules with envelope membranes in mature chloroplasts has not been reported (Austin *et al.*, 2006). In ultrastructural studies, vesicles originating from the envelope membranes were observed (e.g. Westphal *et al.*, 2001; Morre *et al.*, 1991) and a vesicular transport of lipids inside chloroplasts was proposed (see Benning *et al.*, 2006 for review). Such vesicles are absent in *vipp1*, a pale green Arabidopsis mutant with a constitutively high chlorophyll fluorescence and distorted and reduced thylakoid membranes (Kroll *et al.*, 2001). It may be interesting to measure prenylquinone contents in *vipp1* plastoglobules. If tocopherols and their precursors are transported by vesicles, DMPQ is expected to accumulate in the envelope membrane of *vipp1* plants. The albino *vipp1* phenotype is consistent with altered lipid trafficking. However, several albino mutants unrelated to vesicular transport (e.g. *ppi2*, defective in plastid protein import [Bauer *et al.*, 2000]; *var1-1*, knock-out for a chloroplastic FtsH protease [Sakamoto *et al.*, 2002] or *cla1*, impaired in methyl-erythritol-phosphate synthesis [Estevez *et al.*, 2000; Mandel *et al.*, 1996]), have a chloroplast ultrastructure similar to *vipp1*, obviously due to pleiotropic effect of the mutations. Moreover, envelope-derived vesicles were not observed with cryo-electron microscopy techniques (Dr. J. R. Austin, personal communication). The exact nature of the vesicles is therefore still a matter of active research.

Certain lipids including tocopherols might also be translocated by transporter proteins. However, tocopherol binding proteins have not been identified in plants yet. In human liver cells, α-tocopherol is transported by α-TTP, a protein from the SEC14-like family. Human TAP (tocopherol associated protein), an other member of the SEC14-like protein family, has also been shown to bind to α-tocopherol (Zimmer *et al.*, 2000). Database searches revealed that 24 Arabidopsis proteins are similar to TAP (BLAST e-values comprised between

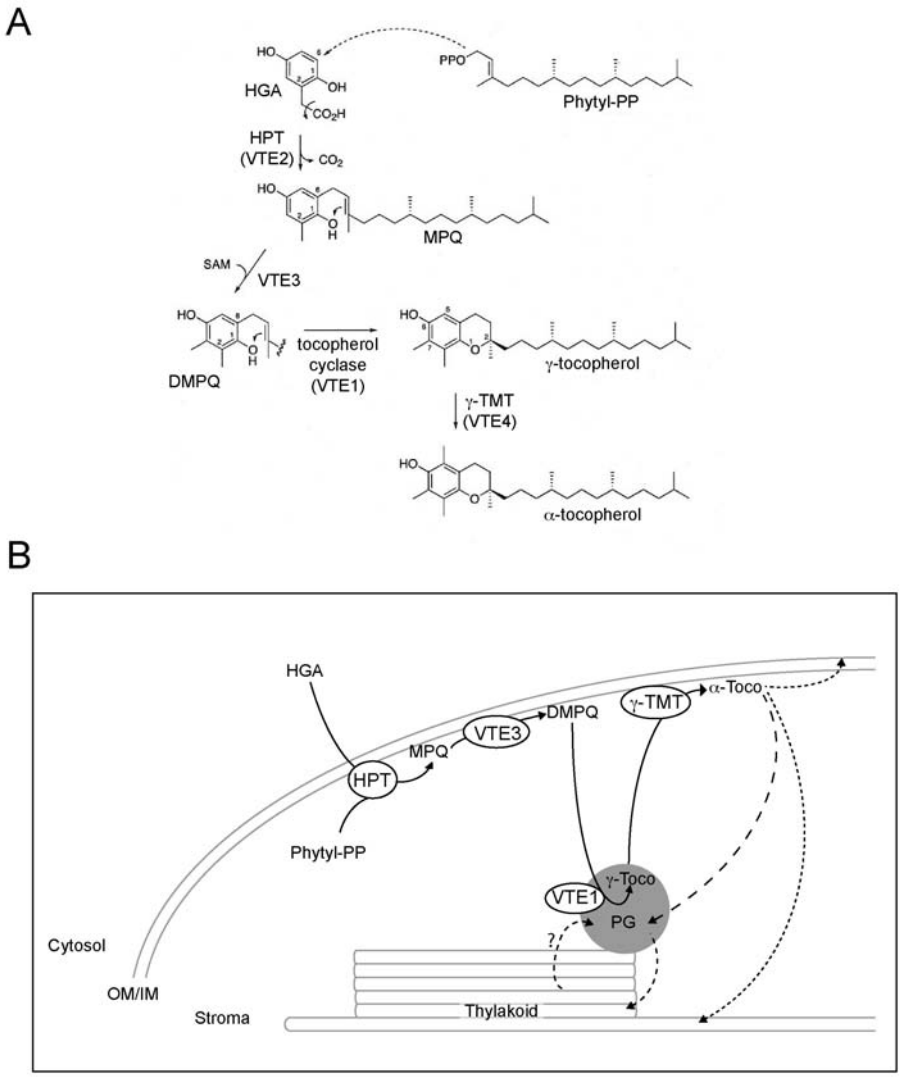

Figure 3.1: Tocopherol synthesis in chloroplasts. **A**, The biosynthetic pathway of α-tocopherol (adapted from Schneider, 2005). **B**, Spatial model for tocopherol biosynthesis. HGA, Homogentisate; Phytyl-PP, phytyl-diphosphate; MPQ, 2-methyl-6-phytyl-1,4-benzoquinone; DMPQ, 2,3-dimethyl-6-phytyl-1,4-benzoquinone; Toco, tocopherol; OM/IM, outer and inner chloroplast membranes; PG, plastoglobule; HPT, HGA phytyltransferase; VTE3, MPQ methyltransferase; VTE1, tocopherol cyclase; γ-TMT, γ-tocopherol methyl transferase.

10^{-25} and 10^{-5}) and that 3 sequences are similar to α-TTP (protein BLAST e-values $< 10^{-5}$). Arabidopsis SEC14-like proteins are therefore good candidate tocopherol transporters.

Proteins from the PAP/fibrillin family have been proposed to directly interact with carotenoids in chromoplast fibrils (Vishnevetsky *et al.*, 1999) but experimental evidence are lacking. The possible function of PGLs as lipid transporters, in addition to their structural function has not been investigated. It might therefore be interesting to test whether PGLs can bind to tocopherols (or to other plastoglobule lipids).

3.2.3 VTE1 provides a molecular link between plastoglobules and oxidative stress response

Stressful conditions often lead to an increase in leaf tocopherol contents (Munne-Bosch and Alegre, 2002). Tocopherol synthesis, for example, is upregulated after exposure to high light intensities (Collakova and DellaPenna, 2003; Kanwischer *et al.*, 2005) and messenger levels of *AtVTE1*, notably, strongly increase after the treatment (Kanwischer *et al.*, 2005). In parallel, plastoglobules increase in size and number under conditions resulting in oxidative stress (Bondada and Syvertsen, 2003; Rey *et al.*, 2000; Eymery and Rey, 1999, Fig 2.11). Changes in plastoglobule morphology probably reflect increased needs for antioxidants under stress conditions: Swelling of plastoglobules may indeed allow accumulation of tocopherols (and possibly other antioxidants such as zeaxanthin) and enzymes such as the tocopherol cyclase.

3.2.4 Why do tocopherols accumulate in plastoglobules?

Tocopherols were shown to protect thylakoid lipid membranes and PSII from photooxidative damage (Havaux *et al.*, 2005); a site of action of tocopherols is therefore the thylakoids. Plastoglobules and thylakoid membranes were recently shown to form a continuum (Austin *et al.*, 2006). Therefore, tocopherols probably diffuse between these two compartments.

In addition to tocopherols, plastoglobules were reported to contain phylloquinone (vitamin K, "A1") and high amounts of plastoquinone (PQH_2) (Legget Bailey and Whyborn, 1963; Lichtenthaler and Sprey, 1966; Lichtenthaler and Peveling, 1967). Both quinones are involved in the electron transport chain in thylakoid membranes. Like tocopherols, quinones probably extensively diffuse in the thylakoid-plastoglobule lipid continuum. Plastoglobules may therefore represent a storage compartment for reduced PQH_2 pools. Furthermore, presence of tocopherols in plastoglobules may protect this pool from oxidative damage. Similarly, tocopherols accumulating in chromoplasts plastoglobules and fibrils (Lichtenthaler, 1969) probably protect accumulated carotenoids from oxidation.

3.2.5 Recycling of oxidised tocopherols

Reduction of lipid peroxyl radicals by tocopherol leads to the formation of tocopheroxyl radicals. In animal systems, tocopherol can be restored by reduction of tocopheroxyl radical with ascorbate or ubiquinol (Schneider, 2005). In plants, however, the corresponding reactions have not been reported. Tocopherols also react with ROS such as hydroperoxyl radicals ($HOO^{\cdot}$), leading tocopherol quinones. Tocopherol quinones may be recycled to tocopherols or degraded (DellaPenna and Pogson, 2006). No evidence favouring either mechanism has been reported yet.

Plastoglobules emerge as a potential site for recycling tocopherols (Fig. 3.1B). It will be interesting to address whether unknown proteins identified in the plastoglobule proteome may carry out (part of) the reactions necessary for tocopherol recycling.

3.3 Signalling mechanisms involving plastoglobules

Abscissic acid (ABA) is known to mediate many aspects of adaptation to abiotic stresses (Shinozaki and Yamaguchi-Shinozaki, 2000). As revealed by transcription profiling, ABA treatment lead to an accumulation of *AtPGL35* and/or *-33* transcripts (Fig. 2.12). In an earlier study, ABA was also shown to induce the expression of *CDSP34*, a potato gene highly similar to *FIBRILLIN* and *AtPGL35* (Gillet *et al.*, 1998). The authors further showed that transcripts from the tomato *CDSP34* ortholog also accumulated after both ABA or dehydration treatments in wild type plants and in *flacca* tomato mutants (impaired in ABA biosynthesis). In contrast, accumulation of tomato CDSP34 did not occur in the *flacca* background unless exogenous ABA was supplied, indicating that an ABA-dependant post-transcriptional mechanism controls the expression of *LeCDSP34*. In a recent report, Yang *et al.* (2006) demonstrated accumulation of AtPGL35 after exogenous application of ABA. Moreover, using yeast-two-hybrid and pull-down assays, the authors could show a direct interaction between the transit peptide of AtPGL35 and ABI1 (a key player of ABA signalling), further implicating ABA in the post-transcriptional regulation of *AtPGL35* expression. Interestingly, AtVTE1 transcripts also accumulated after 3h treatment with 10μM ABA (3.3 fold, Genevestigator, [Zimmermann *et al.*, 2004]). These observations suggest that ABA mediates the accumulation of tocopherols both by up-regulating their synthesis and by increasing the volume of plastoglobules - their storage compartment.

The first, rate-limiting step of ABA biosynthesis is the cleavage of 9-cis-epoxycarotenoids (Schwartz *et al.*, 2003). Interestingly, a 9-cis-epoxycarotenoid (NCE) dioxygenase isoform (AtCCD4, At4g19170) was identified in the plastoglobule proteome (Ytterberg *et al.*, 2006; Vidi *et al.*, 2006). To address the possible involvement of AtCCD4 in abscisic acid biosynthesis, future work will address whether the protein possesses a NCE cleavage activity. Arabidopsis

ccd4 null mutants may also prove useful tools with regard to its role in ABA synthesis. Plastoglobules serve as storage compartments for quinones and tocopherols in chloroplasts. They might therefore represent 'sensors' of the redox status of plastids. Taking this into consideration, the possible localisation of (part of) ABA biosynthesis in plastoglobules may be rationalised.

In addition to a role as antioxidants, tocopherols have been shown to possess non-antioxidant functions in animal systems (Rimbach *et al.*, 2002; Azzi *et al.*, 2002, 2004). Protein phosphatase 2A, e.g., was shown to be activated specifically by α-tocopherol. Moreover, γ-tocopherol has a negative effect on cyclo-oxygenase activity, resulting in decreased levels of prostaglandin E_2.

Tocopherols may also have non-antioxidant functions in plants. Disruption of tocopherol cyclase activity in the maize *sucrose export defective 1* (*sxd1*) mutant (Provencher *et al.*, 2001), or down-regulation of the potato ortholog gene by RNAi (Hofius *et al.*, 2004) caused callose deposition in plasmodesmata and accumulation of soluble sugars, consistent with functions of tocopherols beyond photooxidative protection. Tocopherols have indeed been proposed to regulate jasmonic acid (JA) synthesis by modulating the accumulation of JA lipid hydroperoxide precursors (Munne-Bosch and Alegre, 2002; Munne-Bosch, 2005).

Conversely, JA was shown to regulate tocopherol levels in Arabidopsis by inducing the expression of HPPD (Falk *et al.*, 2002) as well as of a tyrosine aminotransferases, catalysing the formation of p-hydroxyphenylpyruvate (from which HGA derives) from L-tyrosine (Lopukhina *et al.*, 2001; Sandorf and Hollander-Czytko, 2002). Moreover, addition of JA to Arabidopsis cell cultures increased α-tocopherol contents (Gala *et al.*, 2005). Thus, tocopherol levels may indirectly regulate the amount of JA in the leaves and vice versa. The allene oxide synthase (AOS), involved in the biosynthesis of JA precursor OPDA, was identified in the plastoglobule proteome (Ytterberg *et al.*, 2006; Vidi *et al.*, 2006). As for ABA biosynthesis, plastoglobules in addition to containing lipid precursors may act as redox sensors for JA biosynthesis.

Rather than being mere storage compartments, we propose that plastoglobules are metabolically active and that they also participate in a signalling network involving ABA and JA.

3.4 Plastoglobules as a potential protein destination for molecular farming

3.4.1 Targeting YFP to plastoglobules: a proof-of-concept

Proteins are massively used in medicine as diagnostic reagents, drugs or vaccines. Moreover, the rapid discovery of new pharmaceutical proteins leads to an increased demand for production of recombinant proteins (Joshi and Lopez, 2005). To date, production of recombinant proteins rely on microbial fermentation or on insect and mammalian cell cultures. These systems allow highly controlled manufacturing procedures essential for product quality. However,

they have disadvantages in term of cost and scalability. Pathogen contamination of animal cell cultures also represent an important safety issue.

Plants are now being recognised as an alternative system for the production of recombinant proteins. Plant expression systems allow large scale production of recombinant proteins with accurate folding and assembly of protein complexes (Ma *et al.*, 2003; Fischer *et al.*, 2004; Ma *et al.*, 2005a,b). Importantly, plant systems offer the possibility of lowering production costs by a factor of 10 to 100 compared to traditional systems (Menkhaus *et al.*, 2004; Joshi and Lopez, 2005). Chloroplasts have proven a useful cellular compartment for protein accumulation owing to their large size and number. Moreover, transplastomic plants (produced by introducing DNA into the chloroplast genome) enable high yields in recombinant proteins due to a high transgene copy number and limited epigenetic phenomena. Contamination of wild and crop species by pollen flow is also largely circumvented by organellar transformation (Bock, 2001). Important issues for industrial production of plant-derived recombinant proteins are extraction and purification (Giddings *et al.*, 2000). Standard protocols include homogenisation of plant biomass followed by chromatographic methods. However, high abundance of secondary compounds, especially in tobacco, is problematic for chromatographic procedures. therefore, developing a cost-effective preliminary (or alternative) purification step is required (Menkhaus *et al.*, 2004).

Due to their low density, plastoglobules can readily be purified by flotation centrifugation (Picher *et al.*, 1993; Kessler *et al.*, 1999). Plant cells contain roughly 29'000 different proteins and chloroplast are constituted of more than 2'000 different proteins (Cline, 2000). Targeting recombinant proteins to plastoglobules, the proteome of which only consists of about 20 core components (see Table 4.2), followed by plastoglobule purification may therefore represent an effective purification step. We examined the possibility of targeting a recombinant model protein (YFP) to plastoglobules and to recover it in purified plastoglobule fractions. For that purpose, transgenic plants expressing YFP as a C-terminal fusion to AtPGL34 were generated (Fig. 2.22) and chloroplast membranes derived from these plants were fractionated by density gradient flotation centrifugation. AtPGL34-YFP was detected in the low-density fractions by Western blot and fluorescence imaging (Fig. 2.24), indicating targeting to plastoglobules.

3.4.2 Preliminary experiments failed to identify a targeting determinant for plastoglobules

Although plastoglobulins associate with lipid bodies, their overall amino acid composition is not hydrophobic (Grand average of hydropathicity (GRAVY) index = -0.268 for AtPGL35). A somewhat hydrophobic central domain in fibrillin, also present in AtPGL35 and -33, has been proposed to penetrate in the hydrophobic core of fibrils or plastoglobules, anchoring the proteins like drawing pins (Vishnevetsky *et al.*, 1999; Austin *et al.*, 2006). Oleosins, which associate with cytosolic oilbodies in oil-seeds and in tapetum cells, have been shown to have such a topology. Oleosins are constituted of a 72-residue central

hydrophobic stretch surrounded by an N-terminal hydrophilic domain and a C-terminal domain forming an amphiphatic α-helix (Hsieh and Huang, 2004). It should be noted that the 16-residue hydrophobic stretch in fibrillin/AtPGL35/-33 (W I L A/V Y T S F V/S G L F P L L A/S) is much smaller than the one in oleosins and is interrupted by polar residues. Moreover, AtPGL30, -30.4 and -34 which were identified as plastoglobule-associated proteins in two independent studies (Ytterberg *et al.*, 2006; Vidi *et al.*, 2006) lack a similar central domain. Therefore, association of PGLs with plastoglobules may rather rely on interactions with surface lipids, as proposed by Kim *et al.* (2001). Several AtPGLs (AtPGL40, -35, -33, -25, -30.4, -29 and -24) contain a C-terminal RGD adhesion recognition motif, which has been implicated in cell adhesion (D'Souza *et al.*, 1991) This motif is also present in other PGLs including the turnip PAP1, -2 and -3, pea PG1, fibrillin and cucumber ChrC (Kim *et al.*, 2001; Kessler *et al.*, 1999; Deruère *et al.*, 1994; Vishnevetsky *et al.*, 1996). The implication of this motif in PGL function and targeting is however unknown.

Several proteins are known to associate with oilbodies in animal systems. Hydrophobic domains of human caveolin-1 are essential for targeting the protein to ER-derived lipid droplets (Ostermeyer *et al.*, 2004). In contrast, several other proteins associated with oil bodies including ADRP do not contain long hydrophobic domains. Discontinuous segments from ADRP are required for targeting to lipid bodies (Targett-Adams *et al.*, 2003).

The Arabidopsis PGL34 plastoglobulin typically lacks a large hydrophobic domain (Fig. 2.19). Fusing truncated *AtPGL34* sequences to GFP revealed that most of the protein sequence was necessary for obtaining GFP patterns similar to full length AtPGL34-GFP (Fig. 2.20). Only the AtPGL34_{1-290} deletion construct, which lacked a 18-residue hydrophilic C-terminal stretch, colocalised with full length AtPGL34 (Fig. 2.21). In the perspective of using plastoglobules as a destination for recombinant proteins, full length PGLs should therefore be used as vectors. In order to allow an additional purification step, expression constructs could include a protease recognition site followed by an affinity tag between the PGL and the transgene sequences.

Protein targeting to plastoglobules obviously implicates structural features of PGLs but may also require interactions with regulatory proteins. Such proteins may be of low abundance and may not have been detected in the proteome analysis. A possible way to identify factors involved in plastoglobule protein targeting would be to mutagenise plants expressing $AtPGl34_g$-*YFP* and to screen for altered YFP patterns (e.g. loss of punctuate signals, large fluorescent structures).

3.4.3 Viability of transgenic plants

Our data suggests that the viability of plants expressing the AtPGL34-YFP fusion protein was not affected. i) Germination rate of transgenic plants was identical to wild-type. ii) Fresh weight and iii) quantum efficiency, indicative of the status of the photosynthetical apparatus, were similar to wild type in standard conditions. Targeting recombinant proteins to plastoglobules may avoid

deleterious effects on photosynthesis light reactions as well as on metabolic processes occurring in the stroma. Moreover, overexpression of the plastoglobulin fibrillin in tobacco plants has previously been shown to enhance drought stress tolerance (Rey *et al.*, 2000).

3.4.4 Engineering fruit or leaf crops instead of *A. thaliana*

Although Arabidopsis was used for a proof-of-concept, it is obviously not a system of choice for producing recombinant proteins on an industrial scale. Leaf crops having a high biomass yield such as spinach, potato or tobacco should be envisaged. Contamination of food supply with transgenic plant products as well as transgene flow to wild relatives or traditional corps represent major concerns for molecular farming. In this respect, tobacco would have the advantages of not being a food crop and of being amenable to chloroplastic transformation. Legumes such as soybean or alfalfa are also interesting alternatives because they require little fertilisation.

Plastoglobulin genes are highly conserved throughout the plant kingdom. Homologues of AtPGL35 and AtPGL34 were notably found in the tobacco genome (http://www.tobaccogenome.org/index.html). It is therefore likely that homologues of AtPGLs could be successfully used as targeting vectors in many plant species.

Several studies (cited in the introduction) have established that plastoglobules drastically increase in size and number during chloroplast breakdown in senescing tissues. It is tempting to propose to place PGL fusion proteins under the control of senescence-inducible promoters or to drive transgene expression in senescing material with inducible promoters. Alternatively, chromoplasts of ripening fruits, which massively accumulate plastoglobules or related fibrils (Vishnevetsky *et al.*, 1999), may also be envisaged as a destination for PGL fusion proteins.

Many questions however are still open. i) Transplastomic plants expressing PGL fusion proteins may potentially produce very high amounts of recombinant proteins. However it will be necessary to test whether proteins synthesised inside chloroplasts can associate with plastoglobules. Effects of very large amounts of PGL fusion proteins on plant viability will also have to be determined. ii) In the study presented here, YFP was used as model protein. It will be interesting to test whether proteins having other properties (stability, solubility) can also be targeted to plastoglobules with a PGL fusion system. iii) Shelf live of the starting material is an important aspect for large-scale production and freezing or drying leaf material prior to extraction procedures may be required. The integrity of PGL fusion proteins after desiccation and the amenability of dried material for plastoglobule purification will therefore have to be determined.

Answering these questions will require further research and will be essential to address the potential of plastoglobule targeting systems for molecular farming.

Chapter 4

Materials and Methods

4.1 Materials

4.1.1 Biological material

Arabidopsis

Wild type (wt) Arabidopsis plant always refers to *Arabidopsis thaliana* (L.) Heynh. var. Columbia 2. T-DNA insertion lines from the SALK collection were obtained from the Nottingham Arabidopsis Stock Centre (NASC, http://arabidopsis.info).

Micro-organisms

Escherichia coli DH5-α were from Invitrogen and *E. coli* BL21(DE3) cells were from Novagen. *Agrobacterium tumefaciens*, strain C58 were kindly provided by Dr. Roger Kuhn (Institute of Plant Sciences, ETH Zurich, Switzerland).

4.1.2 Oligonucleotides

Oligonucleotides were synthesized at Microsynth GmbH.

4.1.3 cDNA clones

cDNA clones were obtained from the Arabidopsis Biological Resource Centre (ABRC, http://www.biosci.ohio-state.edu/~plantbio/Facilities/abrc/abrchome.htm).

4.1.4 Plasmids

pET21d and pCAMBIA3300 were obtained from Novagen and CAMBIA, respectively. pHANNIBAL is described in Wesley *et al.* 2001 and was obtained from CSIRO Plant Industry. pCHF5 was kindly provided by Dr. C.

Frankhauser (Center for Integrative Genomics, University of Lausanne, Switzerland). pCHF5 is a pCAMBIA3300 derivative with the cauliflower mosaic virus (CaMV) 35S promoter and the RuBisCO small subunit terminator flanking the multiple cloning site. pCL60 (described in Bauer *et al.*, 2000) is a pBluescript SK-(Stratagene) derivative with a CaMV 35S promoter and a nopaline synthase (nos) terminator cassette containing the coding sequence for enhanced green fluorescent protein (GFP; Becton Dickinson Biosciences Clontech). An *Nco*I site containing the start codon of GFP is available to insert cDNA fragments to be expressed as C-terminal GFP fusion proteins. pCL61 and pCL62 were kindly provided by Dr. Andreas Hiltbrunner (Institute for Biology, Albert-Ludwigs University Freiburg, Germany). They are derivatives from pCL60 with CFP or YFP replacing GFP, respectively. pCL60-AtVTE4 was obtained from Dr. P. Dörmann (Max-Planck-Institute of Molecular Plant Physiology, Golm, Germany). pCL61-AtVTE1 was obtained from Dr. C. Bréhélin (University of Neuchâtel, Switzerland). pCL60-AtTIC110$_{tm}$, containing a GFP fusion to the transmembrane domain of AtTIC110, was obtained from Dr. M. Alvarez-Huerta (University of Utrecht, The Netherlands). pCL60-pSSU, containing the transit peptide sequence of the small subunit of pea RuBisCO fused to GFP, was obtained from Dr. A. Hiltbrunner. The FDH-GFP construct was a gift from Dr. I. Small (University of Paris-Sud, France) and is described in Ambard-Bretteville *et al.* (2003).

4.1.5 Chemicals

Unless stated otherwise, the chemicals were purchased from Fluka Chemie GmbH.

4.1.6 Antibodies

Antibodies specific to AtTOC159 or AtTOC75 have been described (Bauer *et al.*, 2000; Hiltbrunner *et al.*, 2001). Sera against AtPGL40 and AtPGL30.4 were kindly provided by Dr. C. Bréhélin. Serum raised against GFP was a gift from Dr. E. Schäfer (Institute for Biology, Albert-Ludwigs University Freiburg, Germany). Antibodies specific to the chlorophyll a/b binding protein (CAB) were kindly provided by Dr. K. Apel (Institute of Plant Sciences, ETH Zurich, Switzerland). Serum against the large subunit of RuBisCO (RLSU) was kindly provided by Dr. S. Crafts-Brandner (US department of Agriculture, Phoenix, USA). Serum against AtVTE1 was a gift from Dr. P. Dörmann. Anti-AtPGL35 antibodies are described below.

4.2 Methods

4.2.1 Physiological methods

Growing *A. thaliana* on Murashige and Skoog medium

Seeds were surface sterilised in chlorine vapour as described by S. Clough and A. Bent (http://plantpath.wisc.edu/~afb/vapster.html). Germination was synchronised by exposing the seeds 2 days at 4°C in the dark. For preparation of protoplasts, plants were grown on 0.8% (w/v) Phyto Agar (Durchefa) containing 0.5x Murashige and Skoog medium (MS; Duchefa) under long-day conditions [16 h light (120 μmol m^{-2} s^{-1}), 8 h dark; 21°C)]. Selection of phosphinothricin-resistant plants was done on half MS medium supplemented with 0.8% (w/v) sucrose and 30 μg/ml phosphinothricin (BASTA; Duchefa).

Segregation analysis on phosphinothricin

For segregation analysis, seeds were germinated in petri dishes on Whatman paper moistened with 0.5x MS and 30 μg/ml phosphinothricin. Plates were incubated in long-day conditions for one week before counting sensitive and resistant plants.

Growing *A. thaliana* on soil

Seeds were set on sandy soil (Top Dressing, Ricoter). Germination was synchronised as above. Plants were grown under short- (8 h light, 16 h dark) or long-day (16 h light, 8 h dark) conditions.

Oxidative stress by high light treatment

For high light treatments, plants grown in short days were incubated in a Percival growth chamber (CLF Plant Climatics) with continuous high light (1200 μmol m^{-2} s^{-1}). Incubation times are indicated in the Result section.

4.2.2 Methods for molecular cloning

Standard protocols were used for cloning (Sambrook and Russell, 2001). DNA fragments were amplified using a proof-reading DNA polymerase (*pfu*, Promega) and oligonucleotides including appropriate restriction sites. EST-clones, pre-existing plasmid-constructs or genomic DNA extracted from Arabidopsis plants were used as templates for PCR. PCR products and plasmids were digested (restriction enzymes from New England Biolabs or Promega) and purified from agarose gels using the QIAquick kit (Quiagen). Vectors were dephosphorylated using shrimp alkaline phosphatase (Roche) according to the manufacturer's recommendations. T4 DNA ligase (New England Biolabs) was used to ligate vectors and inserts as described (Sambrook and Russell, 2001). Ligation reactions were subsequently transformed by heat shock into competent *E. coli* DH5-α cells (Sambrook and Russell, 2001). Competent *E. coli* cells were prepared as

described (Inoue *et al.*, 1990). Selection was done on LB medium [25g/l LB Broth Miller (Becton Dickinson Diagnostic Systems), 1.2% (w/v) Agar Bacteriological Grade (ICN Biomedicals)] supplemented with appropriate antibiotics. Clones were selected by PCR and restriction digestion and DNA sequences were verified by sequencing (Microsynth GmbH or Synergene Biotech GmbH).

4.2.3 Plasmid isolation and purification

For small-scale plasmid isolation, the GenElute Plasmid Miniprep Kit (Sigma) was used according to the suppliers instructions. The PureYield^{TM} Plasmid Midiprep System (Promega) was used for plasmid isolation from 100 ml culture volume.

4.2.4 Transient transformation of *A. thaliana* protoplasts

DNA constructs for transient expression in protoplasts

Complete coding sequences, excluding the stop codon, were amplified from *AtPGL35* and *AtPGL34* cDNA clones (U16632 and U15686 respectively) by PCR using 5' and 3' primers including *Nco*I sites. *AtPGL34*: 5'-cat gcc ATG GCA TTG ATC CAA CAT GG-3' / 5'-cat gcc atg gcA CTG TTG TAT TCA AGA TTC TCT ACA AC-3'; AtPGL35: 5'-cat gcc ATG GCG ACG GTA CCA TTG-3' / 5'-cat gcc atg gcA GGG TTT AAG AGA GAG CTT CCT TC-3'. The PCR products were ligated in the *Nco*I site of either pCL60, pCL61 or pCL62, resulting in C-terminal GFP, YFP or CFP fusions under the control of the CaMV 35S promoter and the nos terminator.

Partial *AtPGL34* N-terminal sequences were amplified from pCL60-AtPGL34 using the 5' primer 5'-gct cta gaA TGG CAT TGA TCC AAC ATG G-3' containing a *Xba*I site and 3' primers containing *Nco*I sites: 5'-cat gcc atg gcA ACC ATA GCT CTG CAT ATC ATT C-3' ($AtPGL34_{1-56}$), 5'-cat gcc atg gcA CTC CAT CTA CCT TCA AGA TAA GG-3' ($AtPGL34_{1-133}$), 5'-cat gcc atg gcA TCT TTA ATG AAT ATT TCC A-3' ($AtPGL34_{1-170}$), 5'-cat gcc atg gcT TCC ACC CTC GTT AGA AC-3' ($AtPGL34_{1-290}$). The PCR products were ligated into the *Xba*I and *Nco*I sites of pCL61 or pCL60. To obtain pCL60-$AtPGL34_{1-56..134-308}$, a cDNA fragment coding for the C-terminal part of *AtPGL34* was amplified from pCL60-AtPGL34 using 5'-cat gcc atg gcc TTT GAG TGG TTT GGA GTC AAC-3' and 5'-cat gcc atg gcA CTG TTG TAT TCA AGA TTC TCT ACA AC-3' primers. The DNA fragment was digested with *Nco*I and ligated in the *Nco*I site of pCL60-$AtPGL34_{1-56}$.

Protoplast transformation

Transient transformation of protoplasts was done using the polyethylene glycol method as described (Jin *et al.*, 2001), but reducing cellulase and macerozyme (Serva) concentrations to 1% and 0.25% (w/v) respectively.

Confocal laser scanning microscopy

Fluorescence in transformed protoplasts was monitored 48 to 80 h after transformation by confocal laser scanning microscopy. The FITC (488 nm) laser line from a LEICA TCS 4D microscope (LEICA Microsystems) was used to detect GFP. For double fluorescent experiments, CFP and YFP were detected sequentially using 458 and 514 nm laser lines, as well as 460-510 nm and 520-588 nm detection windows, from a LEICA SP2 AOBS microscope. Chlorophyll autofluorescence was monitored using either 594 nm or TRITC (568 nm) excitation wavelengths.

4.2.5 Transient transformation of *A. thaliana* leaves by particle bombardment

Gold particles (BioRad Laboratories, 1.0 μm and Aldrich, 1.5-3 μm) were sterilised in ethanol and resuspended in water to a final concentration of 60 μg/μl. 50 μl aliquots consisting of a 1:1 mixture of microcarrier from BioRad and Aldrich were prepared. Plasmid DNA (5 μg) was precipitated on the gold carrier by adding 50 μl 2.5 M $CaCl_2$ and 20 μl 0.1 M spermidine free base under continuous vortexing. After washing with ethanol, DNA-coated gold particles were suspended in ethanol, spread on 4 macrocarrier discs (BioRad Laboratories) and used for bombardment. Leaves from mature *A. thaliana* plants grown on soil for 4 to 7 weeks were placed upside-down on 0.5x MS medium and bombarded with a PDS-1000/He BIOLISTIC® Particle Delivery System (BioRad Laboratories) operating at 1100 PSI He pressure, according to the manufacturer's recommendations.

24 to 48 h after transformation, leaves were stuck on glass slides with lanolin and GFP fluorescence in transformed cells was monitored by confocal laser scanning microscopy (see section 4.2.4) using water immersion objectives.

4.2.6 Stable transformation of Arabidopsis

'Hairpin RNA' constructs for gene silencing

N-terminal fragments of *AtPGL33* and *AtPGL40* cDNAs were amplified by PCR from pCL60-AtPGL33 and pCL60-AtPGL40 (Dr. Bréhélin, University of Neuchâtel, Switzerland) using 5' primers including *Xho*I and *Xba*I sites (5'-ccc tcg agt cta gaT GGC GAC GGT ACA ATT GTC-3' and 5'-ccc tcg agt cta gaT GGC TAC GCT CTT CAC CGT C-3', respectively) and 3' primers containing *Hind*III and *Eco*RI sites (5'-gga att caa gct tTG TGT GAT TAG ATC TCC GAT TTC-3' and 5'-gga att caa gct tAG TCG GGT CAG ACA CCG C-3', respectively). *AtPGL33* and *AtPGL40* cDNA fragments were then digested with either *Xho*I and *Eco*RI or *Hind*III and *Xba*I and ligated in the corresponding sites of pHANNIBAL, resulting in intron-containing hairpin (ihp) constructs. These 'hairpin' cassettes were excised from the pHANNIBAL vectror by *Xba*I restriction digest and ligated in the *Xba*I site of pCHF5 binary vector, yielding pCHF5-AtPGL33$_{ihp}$ and pCHF5-AtPGL40$_{ihp}$.

Genomic AtPGL34-YFP construct

AtPGL34-YFP genomic construct comprises the 5' upstream region (up to the adjacent gene), *AtPGL34* genomic sequence (introns and exons, without Stop codon) in frame with *YFP* and the 3' downstream region (terminator, down to the adjacent gene). The primers: 5'-ccg cgg ccg cAA ACA GGT TCT CTT GTT ACT CTG ATT C-3' (includes *Not*I) and 5'-ggg cgg ccg cag atC TCG GTC TCT CAA AGG ATG TG-3' (includes *Bgl*II and *Not*I) were used to amplify *AtPGL34* terminator. *AtPGL34*, as well as 0.85 kb 5' upstream region, were amplified by PCR using the primer set: 5'-cat gcc atg gag atC TTC GGT GAG GAA CAA GAC TT-3' (includes *Nco*I and *Bgl*II) / 5'-cat gcc atg gcA CTG TTG TAT TCA AGA TTC TCT ACA AC-3' (includes *Nco*I). The DNA fragment corresponding to *AtPGL34* terminator was digested with *Not*I and ligated in the *Not*I site of pCL61, yielding pCL61-AtPGL34$_{ter}$. The DNA fragment comprising the 5' upstream region and *AtPGL34* was digested with *Nco*I and ligated in the *Nco*I site of pCL61-AtPGL34$_{ter}$, yielding pCL61-AtPGL34$_{g}$. *AtPGL34$_{g}$-YFP* was then excised from pCL61 by restriction digest with *Kpn*I. Fragments were blunted using T4 DNA polymerase (New England Biolabs) and ligated in the *Sma*I site of pCAMBIA3300, yielding pCAMBIA3300-AtPGL34$_{g}$-YFP.

Transformation of *Agrobacterium tumefaciens* by electroporation

A. tumafaciens, strain C58 were grown in liquid YEB media [0.5% (w/v)Bacto-Trypton, 0.5% (w/v) Bacto-Pepton, 0.1% (w/v) yeast-extract (all from Difco), 2 mM $MgCl_2$] until an optical density (546nm) of 0.8 was achieved. Cells were pelleted (10 min, 4°C, 2'000g) and washed with a 10% glycerol solution. 50 ng plasmid DNA were used for electroporation in a MicroPulser (BioRad Laboratories) device, according to the manufacturer's instructions. Transformants were selected on YEB media supplemented with 1.2% (w/v) agar (bacteriological grade, ICN Biomedicals) and appropriate antibiotics.

Arabidopsis transformation

A. thaliana plants were transformed using the floral dip method as described (Bechthold *et al.*, 1993; Clough and Bent, 1998). Transformants were selected on plates containing phosphinothricin (see section 4.2.1 on page 73).

4.2.7 Diagnostic PCR on plants

Rapid DNA extraction

DNA was prepared from leaf material using the simple DNA preparation method described on the University of Wisconsin Biotechnology Center Web site: http://www.biotech.wisc.edu. Leaf tissue corresponding to 0.5 cm^2 was ground in 0.2 M Tris/HCl pH 9, 0.4 M LiCl, 25 mM EDTA, 1% (w/v) SDS. The homogenate was cleared by centrifugation (5 min, 16'000x g, 4°C), supplemented

with an equal volume of isopropanol and centrifuged again (45 min, 16'000x g, RT). The supernatant was discarded and the DNA pellet was washed with 80% (v/v) ethanol. Finally, DNA was dried and resuspended in 50 μl TE (10 mM Tris/HCl pH 8, 1 mM EDTA).

PCR analysis

PCR reactions contained 2 μl DNA solution, 0.5 U GoTaq DNA polymerase (Promaga), as well as 0.2 mM dNTPs (Eurobio) in a total volume of 25 μl. The primer sets 35-4_RP: 5'-CTG TGT GTA GTT ATG AGC CTT CG-3' / 35-4_LP: 5'-CAC TAG TAA ACA TAG ACA GAT GGG-3' and 35-5_RP: 5'-CGA AGG CTC ATA ACT ACA CAC AG-3' / 35-5_LP: 5'-CAT GCC ATG GCG ACG GTA CCA TTG-3' were used to detect wild type *AtPGL35* in *pgl35-4* and *pgl35-5* lines, respectively. T-DNA insertions were detected using the LBpROK2 primer: 5'-TGG ACT CTT GTT CCA AAC TG-3' in combination with 35-4_RP and 35-5_RP. The PCR program was as follows: 2 min, 94°C, 40x (30 s, 94°C; 30 s, 50°C; 1 min, 72°C). PCR reactions were analysed by agarose gel electrophoresis according to standard protocols (Sambrook and Russell, 2001).

4.2.8 Fluorescence imaging in transgenic plants

YFP fluorescence was detected using a Nikon SMZ 1000 binocular equipped with a GFP long pass (GFP-L) filter. For higher resolution imaging, roots or leaf sections were analysed by confocal microscopy using GFP settings as described in section 4.2.4.

4.2.9 Southern and Northern analysis

DNA extraction from *A. thaliana* leaves

Genomic DNA was extracted using the CTAB method (Murray and Thompson, 1980). Arabidopsis leaves were ground to fine powder in liquid nitrogen and incubated 1h in extraction buffer [2% (w/v) cetyltrimethylammonium bromide (CTAB), 1.4 M NaCl, 20 mM EDTA, 100 mM Tris/HCl pH 8, 0.2% (v/v) β-mercaptoethanol; heated at 60°C]. Proteins were extracted with an equal volume of $CHCl_3$: isoamyl alcohol (24 : 1) and debris were cleared by centrifugation (10 min, 20°C, 500x g). DNA was precipitated with isopropanol, pelleted (10 min, 20°C, 7'500x g) and rinsed in washing buffer [70% (v/v) ethanol, 10 mM ammonium acetate]. DNA pellets were lyophilised and dissolved in water. After a second precipitation with isopropanol, DNA was resuspended in water and used for digestion.

Restriction digest and Southern transfer

DNA (30 μg) was digested for 4 h in a total volume of 25 μl with 30u *Xba*I or *Eco*RI (New England Biolabs) and separated on agarose gel as described

(Sambrook and Russell, 2001). The DNA was then transferred to Porablot-NY plus nylon membrane (Macherey-Nagel) by capillary transfer as described (Sambrook and Russell, 2001). Finally, the membrane was baked 2 h at 80°C to immobilise DNA.

RNA extraction

Plant material was ground in liquid nitrogen, homogenized in extraction buffer [0.5 M Tris/HCl pH 8.2, 0.25 M EDTA, 5% (w/v) SDS] and extracted with phenol : chloroform : isoamylalcool (25 : 24 : 1). After centrifugation (10 min, 12'000x g, 20°C), the aqueous phase was extracted with chloroform : isoamylalcool (24 : 1) and mixed with equal volume of 6 M lithium chloride. RNA was precipitated for 15 h at 0°C and pelleted (15 min, 12'000x g, 4°C). The pellet was rinsed twice with 3 M sodium acetate pH 5.2, once with 70% (v/v) ethanol, air-dried and resuspended in water treated with diethyl pyrocarbonate (DEPC).

Northern transfer

Total RNA (10 μg) was separated on a formaldehyde agarose gel and transferred to Porablot-NY plus nylon membrane (Macherey-Nagel) by capillary transfer as described (Sambrook and Russell, 2001). RNA was immobilised on the membrane by UV crosslinking.

Synthesis of radio-labelled probes

Probes were synthesised using the The Prime-It ®II Random Primer Labelling Kit (Stratagene) in presence of 0.2 μM [α^{32}P]dCTP (3 Ci/μmol, Amersham Biosciences, cat. n° AA0005) as described by the supplier. To remove unincorporated nucleotides,the labelling reaction was passed over a MicroSpin^{TM} S-300 HR column (Amersham Biosciences) equilibrated with STE buffer (10 mM Tris/HCl pH 8, 0.1M NaCl, 1 mM EDTA). Templates for *AtPGL33* and *AtPGL35* - specific probes were amplified from pCL60-AtPGL33 (Dr. Bréhélin, University of Neuchâtel, Switzerland) and pCL60-AtPGL35 (see section 4.2.4 on page 74) using the primer sets (5'-CAA CAT GCC ATG GCG ACG GTA CAA TTG-3', 5'-GAC CAT GCC ATG GGA TTC AAG AGA GGG-3') and (5'-CAT GCC ATG GCG ACG GTA CCA TTG-3', 5'-CAT GCC ATG GCA GGG TTT AAG AGA GAG CTT CCT TC-3'), respectively. The template for the synthesis of a probe specific to the left border of *pgl35-4* T-DNA insertion was obtained by PCR amplification from *pgl35-4* genomic DNA, using the primers 5'-CTT CAC CGC CTG GCC CTG AG-3' and 5'-CCC CGA TCG TTC AAA CAT TTG GC-3'.

Hybridisation of radioactive probes

Hybridisation of radioactive probes to Southern and Northern blot membranes and subsequent washing steps were done as described (Sambrook and Russell,

2001). Radioactive signals were detected by exposing the membranes to X-ray films (Kodak BioMax).

4.2.10 RT-PCR

Before reverse transcription, total RNA (see section 4.2.9 on page 78) was treated with DNase RQ1 (Promega) according to the supplier's recommendations. The DNase was then heat-inactivated and first strand synthesis was performed as described (Gubler and Hoffman, 1983). Briefly, oligo(dT)15-mers (Promega) were added to 5 μg DNase-treated RNA. Secondary RNA structures were denatured by incubating for 10 min at 70°C and reverse transcription was performed in the presence of 0.6 mM dNTPs and 200u moloney murine leukemia virus Reverse Transcriptase (Promega) according to the supplier's recommendations. All steps were carried out in the presence of RNasin RNase inhibitors (Promega). cDNAs were directly used for PCR reactions. The primer sets 5'-CAA CAT GCC ATG GCG ACG GTA CAA TTG-3' / 5'-GAC CAT GCC ATG GGA TTC AAG AGA GGG-3' and 5'-GTT AGC AAC TGG GAT GAT ATG G-3' / 5'-CAG CAC CAA TCG TGA TGA CTT GCC C-3' were used to amplify AtPGL33 and ACTIN2 cDNAs, respectively.

4.2.11 Purification of plastoglobules from *A. thaliana*

Crude chloroplast preparation

Leaves from Arabidopsis plants grown on soil for 4 weeks were harvested and immersed 30 min in tap water in the dark at at 4°C. All subsequent steps were also carried out at 4°C. Leaf material was homogenized in HB buffer (450 mM sorbitol, 20 mM Tricine/KOH pH 8.4, 10 mM EDTA, 10 mM $NaHCO_3$, 1 mM $MnCl_2$) with a Waring blender and filtered through cheese cloth and miracloth. Chloroplasts were sedimented (2 min 700x g), washed with TrE (50 mM Tricine/HCl pH 7.5, 2 mM EDTA) and hypertonically lysed 10 min in TrE + 0.6 M sucrose. Chlorophyll concentration was determined using the method of Arnon (Arnon, 1949) and was adjusted to 2 mg/ml. To prevent proteolytic degradation, 0.5% (v/v) protease inhibitor cocktail for plant cell extracts (Sigma P9599) was added to the lysate. The lysate was frozen at −80°C, thawed on ice and used for chloroplast membrane fractionation.

Plastoglobule purification

Lysed chloroplasts were diluted 3 times with TrE buffer and homogenised with a Potter homogeniser. Total membranes, corresponding to 10 mg of chlorophyll, were sedimented at 100'000x g and resuspended in 3 mL 45% sucrose in TrE buffer using a Potter homogeniser. Membranes were overlaid with a discontinuous sucrose gradient consisting of 2 ml 38% sucrose, 2 ml 20% sucrose, 1.4 ml 15% sucrose and 2.7 ml 5% sucrose in TrE buffer and centrifuged for 17 h at 100'000x g and 4°C (SW41Ti rotor, Beckman). 0.5 ml fractions were collected

starting from the top of the gradient and used for confocal microscopy analysis or Western blotting.

4.2.12 Preparation of anti-AtPGL35 antibody

The coding sequence of *AtPGL35* was sub-cloned from pCL60-AtPGL35 (see section 4.2.4 on page 74) in pET21d-H6. pET21d-H6 was obtained by digesting pET21d (Novagen) with *Nco*I and *Eco*RI and inserting a hexahistidinyl (His_6) tag in frame with the *Nco*I site using the primers 5'-CAT GGG TCA CCA TCA CCA TCA CCA TTA ACT GCA GG-3' and 5'-AAT TCC TGC AGT TAA TGG TGA TGG TGA TGG TGA CC-3'. The full length His_6-tagged precursor protein was expressed in *E. coli* BL21 (DE3) (Novagen) and purified under denaturing conditions by Ni-NTA affinity chromatography (Qiagen), according to the manufacturers recommendations. Eight aliquots of purified AtPGL35 (100 μg recombinant protein in [10 mM NaH_2PO_4, 10 mM Tris/HCL pH 8.0, 0.8 M urea, 10% glycerol]) were used to produce rabbit polyclonal antibodies (Eurogentec).

Antibodies were affinity purified using recombinant AtPGL35 coupled to Affi-Gel10 (Bio-Rad Laboratories).

In order to purify anti-AtPGL35 antibodies, recombinant AtPGL35 proteins were coupled to Affi-gel10 (Bio-Rad Laboratories) according to the supplier's instructions. Serum from the immunised rabbit was incubated with the Affi-Gel slurry for 2 h on a rolling shaker at 4°C. Affi-Gel beads were washed extensively with PBS (140 mM NaCl, 2.7 mM KCl, 10 mM Na_2HPO_4, 1.8 mM KH_2PO_4 pH 7.4). Bound antibodies were eluted with 0.2 M glycine (pH 2.2). Tris/HCl pH 9.0 was added to affinity-purified antibodies to adjust the pH to 7.

4.2.13 Protein extraction and Western blot analysis

Total proteins were isolated from Arabidopsis leaves, roots, stems, floral buds, flowers, siliques or seeds according to Rensink *et al.* et al. (1998). To avoid proteolytic degradation, 0.5% (v/v) protease inhibitor cocktail for plant cell extracts (Sigma P9599) was added to the extraction buffer. Proteins were concentrated by chloroform - methanol precipitation (Wessel and Flügge, 1984) and resuspended in sample buffer [50 mM Tris/HCl pH 6.8, 0.1 M DTT, 2% (w/v) SDS, 0.1% (w/v) bromophenol blue, 10% (v/v) glycerol].

Protoplasts transiently expressing GFP, CFP and YFP fusion proteins were centrifuged 1 min at 100x g. Total proteins were extracted and concentrated as above.

Proteins were separated by SDS-PAGE and blotted onto Protran® nitrocellulose membrane (Schleicher & Schuell) using the Mini-PROTEAN System (Bio-Rad Laboratories). Western blot membranes were stained with Amido Black (= Naphthol Blue Black) as described (Sambrook and Russell, 2001) and scanned. To block unspecific binding of antibodies, membranes were incubated in blocking buffer [PBS (150 mM NaCl, 7.5 mM Na_2HPO_4, 1.5 mM NaH_2PO_4), TBS

Table 4.1: Antibody dilutions for immunoblotting and immunofluorescence. Incubation buffers and approximate incubation times for immunoblotting are indicated. See the text for buffer compositions. Mp, skim milk powder; o/n, over night.

Antibody	**Dilution (v/v)**	**Buffer**	**Inc. time**
α-AtPGL35	(1/3000)	TBS-T 5% Mp	1h
α-AtPGL40	(1/3000)	TBS-T 5% Mp	1h
α-AtPGL30.4	(1/3000)	TBS-T 5% Mp	1h
α-CAB	(1/10000) or (1/50000)	TBS-T 5% Mp	1-3h
α-AtTOC75	(1/3000)	PBS 3% Mp	1h
α-AtVTE1	(1/2000)	PBS 2% Mp	2-6h
α-GFP	(1/1000)	PBS 5% Mp	1h-o/n

(25 mM Tris/HCl pH 7.4, 140 mM NaCl, 2.7 mM KCl) or TBS-tween (TBS-T; TBS, 0.05% (v/v) Tween® 20) containing 5% (w/v) skim milk powder] Membranes were then incubated for 60 min or longer with adequate antibody dilutions in blocking buffer. (see Table 4.1) and washed extensively with PBS, TBS or TBS-T buffer. To reveal primary antibodies, membranes were incubated 30 min with a 3'000x dilution of horseradish peroxidase-coupled goat anti-rabbit IgG (Bio-Rad Laboratories) in blocking buffer. After washing with PBS/TBS/TBS-T buffer, signals were detected by enhanced chemiluminescence. The membranes were incubated 1 min in [0.1 M Tris/HCl pH 8.5, 1.25 mM 3-aminophthalhydrazide (= luminol), 0.2 mM p-coumaric acid, 0.009% (v/v) H_2O_2] and exposed to high performance chemiluminescence films (Amersham Biosciences). Alternatively, luminescence was monitored and quantified using a ChemiDock system and the QuantityOne software (both from BioRad).

4.2.14 Immunolocalization in protoplasts

Immunolocalization in isolated protoplasts was performed as described by Matsui *et al.* et al. (1995) with the following modifications. Polysine slides (BDH Laboratories) were used. Protoplasts were fixed with 4% (v/v) formaldehyde in W5 buffer [154 mM NaCl, 125 mM $CaCl_2$, 5 mM KCl, 5 mM glucose, 1.5 mM MES pH 5.6] and permeabilized with 0.5% (v/v) NP-40 in W5. Primary antibodies were diluted 1:50 (v/v, anti-CAB serum) and to 15 ng/μl (anti-AtTOC159 and anti-AtPGL35). Slides were mounted in SlowFade solution (Molecular Probes) and fluorescence of the fluorescein-coupled secondary antibody (Pierce) was monitored by confocal scanning microscopy using the FITC (488 nm) laser line from a LEICA TCS 4D microscope.

4.2.15 Electron microscopy and immunocytochemistry

Ultrastructural analysis of chloroplasts

Leaves from adult *A. thaliana* plants were fixed over night at 4°C in 50 mM sodium cacodylate containing 2.5% (w/v) glutaraldehyde, post-fixed with 1%

(w/v) osmium tetroxide for 2 h at 20°C, dehydrated in ethanol and acetone series and included in Spurr epoxy resin (Polyscience). Ultrathin sections of 90 nm were prepared using an Ultracut-E microtome (Reichert-Jung), mounted on copper grids and contrasted with uranyl acetate and Reynolds lead solution (Reynolds, 1963). Sections were observed with a Philips CM100 electron microscope operating at 60 kV. Plastoglobule size was quantified using the ImageJ software (http://rsb.info.nih.gov/ij/).

Immunogold-electron microscopy

Adult Arabidopsis leaves were fixed over night in 50 mM sodium cacodylate containing 4% (w/v) paraformaldehyde and 2% (w/v) glutaraldehyde at 4°C. After dehydration in ethanol, samples were embedded in LR-White resin (London Resin Company LTD). Ultrathin sections were prepared as above and were mounted on nickel grids. Sections were pre-treated with 0.5 M ammonium chloride for 1h, washed with TBT buffer [20 mM Tris/HCl pH 8.5; 150 mM NaCl; 20 mM sodium azide; 0.1% (w/v) bovine serum albumin; 0.1% (v/v) Tween20] supplied with 1% (v/v) goat serum (GS, Sigma G9023), and incubated for 30 min on TBT supplied with 10% (v/v) GS. Incubation with affinity purified anti-AtPGL35 was performed over-night at 4°C. Antibodies were diluted 10 times in TBT + 1% GS buffer. Sections were incubated without anti-AtPGL35 in control experiments. After washings with TBT + 1% GS, primary antibodies were revealed by incubation on a 1:30 (v/v) dilution of gold-conjugated anti-rabbit IgG (Sigma G7402, in TBT + 1% GS). Sections were rinsed with distilled water, contrasted with 1% (w/v) tannic acid, saturated uranyl acetate and Reynolds lead solution and observed with a Philips CM100 electron microscope.

4.2.16 Fluorometry

Maximum quantum efficiency of photosystem II (Fv/Fm) was measured using a Handy Plant Efficiency Analyser chlorophyll fluorometer (Hansatech Instruments). Leaves were dark-adapted 20 min prior to measurements.

4.2.17 Bioinformatics

DNA microarray data were retrieved from public database and analysed using the Geenevestigaror toolbox (Zimmermann *et al.* et al. 2004; https://www.genevestigator.ethz.ch/at/). Kyte and Doolittle hydropathy plots (Kyte and Doolittle, 1982) were calculated at http://occawlonline.pearsoned.com/bookbind/pubbooks/bc_mcampbell_genomics_1/medialib/activities/kd/kyte-doolittle.htm or using the Protean software from DNA* (http://www.dnastar.com/). ESTs from plastoglobulin genes were retrieved from The Arabidopsis Resource (http://-www.arabidopsis.org/). The ClustalW software (http://www.ch.embnet.org-/software/ClustalW.html) was used to generate multiple sequence alignments as well as dendrograms. Alignments were edited using the BOXSHADE software (http://www.ch.embnet.org/software/BOX_form.html). The phyloden-

dron program (http://iubio.bio.indiana.edu/treeapp/treeprint-form.html) was used to draw phylogenetic trees.

Appendix: The Arabidopsis plastoglobule proteome

Table 4.2. Proteins identified by tandem mass spectrometry in Arabidopsis low-density chloroplast membrane fraction. Proteins were divided in four groups: PAP/fibrillins, chloroplast metabolic proteins, unclassified proteins and thylakoid components. Prediction of subcellular localisation using the TargetP software are shown. Pept. nb., total number of peptides identified in replicate preparations; P, plastid; M, mitochondria. From Vidi *et al.*, (2006).

AGI code	Name, annotation or domain	**Pept. nb.**	**TargetP**
PAP/fibrillins			
At3g26070	AtPGL25, plastid-lipid associated protein PAP	4	P
At2g42130	AtPGL30	5	P
At3g23400	AtPGL30.4, plastid-lipid associated protein PAP	134	P
At4g22240	AtPGL33, plastid-lipid associated protein PAP	66	P
At3g58010	AtPGL34	33	P
At4g04020	AtPGL35, plastid-lipid associated protein PAP	160	P
At2g35490	AtPGL40, plastid-lipid associated protein PAP	103	P
Chloroplast metabolism protein			
At2g21330	AtFBA1, fructose-bisphosphate aldolase	120	P
At4g38970	AtFBA2, fructose-bisphosphate aldolase	93	P
At2g01140	AtFBA3, fructose-bisphosphate aldolase	5	P
At5g42650	AtAOS, allene oxide synthase	63	P
At4g19170	AtCCD4, 9-cis-epoxycarotenoid dioxygenase	45	P
At4g32770	AtVTE1, tocopherol cyclase	50	P

Unclassified proteins			
At5g08740	Unknown, NADH dehydrogenase-like protein	33	P
At5g05200	Unknown, ABC1 motif/ putative kinase	19	M
At1g79600	Expressed protein, ABC1 family protein, chaperonin	2	P
At1g54570	Expressed protein, esterase; lipase; thioesterase	24	P
At3g26840	Expressed protein, esterase; lipase; thioesterase	14	P
At1g78140	Hypothetical protein, menaquinone biosynthesis, methyltransferase-related	3	M
At2g41040	Expressed protein, methyltransferase-related	2	P
At1g32220	Unknown, 3-beta hydroxysteroid dehydrogenase/isomerase	25	P
At2g34460	Unknown, flavine reductase, steroid biosynthesis	32	P
At4g13200	Expressed protein	28	P
At3g10130	Unknown, SOUL heme-binding family protein, weak similarity to heme-binding protein	15	P
At1g06690	Unknown, aldo-keto reductase, ANC transporters family signature	4	P
At3g26060	Peroxiredoxin Q	6	P
At1g52590	Expressed protein,	2	P
Thylakoid components			
At5g66570	PSII-O, photosystem II oxygen-evolving complex	6	P
At3g50820	PSII-O, photosystem II oxygen-evolving complex	3	P
At5g01530	Lhcb4, putative chlorophyll a/b-binding protein	2	P
At1g29910	Lhca2, chlorophyll a/b-binding protein	12	P
At4g10340	Lhcb5, chlorophyll a/b-binding protein - like	3	P
At1g61520	Lhca2, PSI type III chlorophyll a/b-binding protein	3	P
At3g54890	Chlorophyll a/b-binding protein	3	P
At2g05070	Putative chlorophyll a/b binding protein	2	P

at4g12800	PSI-L, probable photosystem I chain XI precursor	2	P
At4g28750	PSI-E, putative photosystem I reaction center subunit IV	2	P
At1g31330	PSI-F, photosystem I reaction center subunit III	7	P
At4g09650	AtpD, ATPase delta subunit	5	P
At4g02770	PSI-D, putative photosystem I reaction center subunit II	2	P
AtCg00480	AtpB, ATP synthase CF1 beta chain	10	-
AtCg00350	PsaA, PSI P700 apoprotein A1	3	-
AtCg00280	PsbC, PSII CP43 subunit of the photosystem II reaction center.	4	-

Bibliography

Alonso, J. M., Stepanova, A. N., Leisse, T. J., Kim, C. J., Chen, H., Shinn, P., Stevenson, D. K., Zimmerman, J., Barajas, P., Cheuk, R., Gadrinab, C., Heller, C., Jeske, A., Koesema, E., Meyers, C. C., Parker, H., Prednis, L., Ansari, Y., Choy, N., Deen, H., Geralt, M., Hazari, N., Hom, E., Karnes, M., Mulholland, C., Ndubaku, R., Schmidt, I., Guzman, P., Aguilar-Henonin, L., Schmid, M., Weigel, D., Carter, D. E., Marchand, T., Risseeuw, E., Brogden, D., Zeko, A., Crosby, W. L., Berry, C. C., and Ecker, J. R. (2003). Genome-wide insertional mutagenesis of *Arabidopsis thaliana*. *Science*, **301**(5633), 653–7.

Ambard-Bretteville, F., Small, I., Grandjean, O., and Colas des Francs-Small, C. (2003). Discrete mutations in the presequence of potato formate dehydrogenase inhibit the *in vivo* targeting of GFP fusions into mitochondria. *Biochem Biophys Res Commun*, **311**(4), 966–71.

Amrani, A. E., Couee, I., Carde, J. P., Gaudillere, J. P., and Raymond, P. (1994). Modifications of etioplasts in cotyledons during prolonged dark growth of sugar beet seedlings (identification of etiolation-related plastidial aminopeptidase activities). *Plant Physiol*, **106**(4), 1555–1565.

Arango, Y. and Heise, K. P. (1998). Tocopherol synthesis from homogentisate in capsicum anuum l. (yellow pepper) chromoplast membranes: evidence for tocopherol cyclase. *Biochem J*, **336**, 531–3.

Arnon, D. (1949). Copper enzymes in isolated chloroplasts. Phenoloxidase in *Beta vulgaris*. *Plant Physiol*, **24**, 1–15.

Austin, J. R., Frost, E., Vidi, P. A., Kessler, F., and Staehelin, L. A. (2006). Plastoglobules are lipoprotein sub-compartments of the chloroplast that are permanently coupled to thylakoid membranes and contain biosynthetic enzymes. *Plant Cell*, **18**, 1693–1703.

Azzi, A., Ricciarelli, R., and Zingg, J. M. (2002). Non-antioxidant molecular functions of α-tocopherol (vitamin E). *FEBS Lett*, **519**(1-3), 8–10.

Azzi, A., Gysin, R., Kempna, P., Munteanu, A., Negis, Y., Villacorta, L., Visarius, T., and Zingg, J. M. (2004). vitamin E mediates cell signaling and regulation of gene expression. *Ann N Y Acad Sci*, **1031**, 86–95.

Bailey, S., Thompson, E., Nixon, P. J., Horton, P., Mullineaux, C. W., Robinson, C., and Mann, N. H. (2002). A critical role for the VAR2 FtsH homologue of *Arabidopsis thaliana* in the photosystem II repair cycle *in vivo*. *J Biol Chem*, **277**(3), 2006–11.

Bauer, J., Chen, K., Hiltbunner, A., Wehrli, E., Eugster, M., Schnell, D., and Kessler, F. (2000). The major protein import receptor of plastids is essential for chloroplast biogenesis. *Nature*, **403**(6766), 203–7.

Bauer, J., Hiltbrunner, A., and Kessler, F. (2001). Molecular biology of chloroplast biogenesis: gene expression, protein import and intraorganellar sorting. *Cell Mol Life Sci*, **58**(3), 420–33.

Bechthold, N., Ellis, J., and Pelletier, G. (1993). *in planta* Agrobacterium-mediated gene transfer by infiltration of A*rabidopsis thaliana* plants. *CR Acad Sci Ser III Sci Vie*, **316**, 1194–1199.

Benning, C., Xu, C., and Awai, K. (2006). Non-vesicular and vesicular lipid trafficking involving plastids. *Curr Opin Plant Biol*, **9**(3), 241–7.

Bergmüller, E., Porfirova, S., and Dörmann, P. (2003). Characterization of an Arabidopsis mutant deficient in gammaα-tocopherol methyltransferase. *Plant Mol Biol*, **52**(6), 1181–90.

Block, M. A., Dorne, A. J., Joyard, J., and Douce, R. (1983). Preparation and characterization of membrane fractions enriched in outer and inner envelope membranes from spinach chloroplasts. ii. biochemical characterization. *J Biol Chem*, **258**(21), 13281–6.

Bock, R. (2001). Transgenic plastids in basic research and plant biotechnology. *J Mol Biol*, **312**(3), 425–38.

Bondada, B. R. and Syvertsen, J. P. (2003). Leaf chlorophyll, net gas exchange and chloroplast ultrastructure in citrus leaves of different nitrogen status. *Tree Physiol*, **23**(8), 553–9.

Bouche, N. and Bouchez, D. (2001). Arabidopsis gene knockout: phenotypes wanted. *Curr Opin Plant Biol*, **4**(2), 111–7.

Camara, B., Bardat, F., Seye, A., D'Harlingue, A., and Moneger, R. (1982). Terpenoid metabolism in plastids: Localization of α-tocopherol synthesis in capsicum chromoplasts. *Plant Physiol*, **70**(5), 1562–1563.

Chen, H.-C., Klein, A., Xiang, M., Backhaus, R. A., and Kuntz, M. (1998). Drought- and wound-induced expression in leaves of a gene encoding a chromoplast carotenoid-associated protein. *Plant J*, **14**(3), 317–326.

Cheng, Z., Sattler, S., Maeda, H., Sakuragi, Y., Bryant, D. A., and DellaPenna, D. (2003). Highly divergent methyltransferases catalyze a conserved reaction in tocopherol and plastoquinone synthesis in cyanobacteria and photosynthetic eukaryotes. *Plant Cell*, **15**(10), 2343–56.

Chinnusamy, V., Jagendorf, A., and Zhu, J. K. (2005). Understanding and improving salt tolerance in plants. *Crop Sci*, **45**, 437–448.

Cline, K. (2000). Gateway to the chloroplast. *Nature*, **403**(6766), 148–9.

Clough, S. J. and Bent, A. F. (1998). Floral dip: a simplified method for Agrobacterium-mediated transformation of A*rabidopsis thaliana*. *Plant J*, **16**(6), 735–43.

Cobbett, C. S., May, M. J., Howden, R., and Rolls, B. (1998). The glutathione-deficient, cadmium-sensitive mutant, *cad2-1*, of A*rabidopsis thaliana* is deficient in γ-glutamylcysteine synthetase. *Plant J*, **16**(1), 73–8.

Collakova, E. and DellaPenna, D. (2001). Isolation and functional analysis of homogentisate phytyltransferase from *Synechocystis sp.* pcc 6803 and Arabidopsis. *Plant Physiol*, **127**(3), 1113–24.

Collakova, E. and DellaPenna, D. (2003). The role of homogentisate phytyltransferase and other tocopherol pathway enzymes in the regulation of tocopherol synthesis during abiotic stress. *Plant Physiol*, **133**(2), 930–40.

Conklin, P. L., Williams, E. H., and Last, R. L. (1996). Environmental stress sensitivity of an ascorbic acid-deficient Arabidopsis mutant. *Proc Natl Acad Sci U S A*, **93**(18), 9970–4.

Davies, A. O., James, A. T., Jeffcoat, R., and L., H. J. (1980). *Changes in lipid composition and synthesis and in chloroplast structure observed in greening barley leaves*, volume 6 of *Developments in plant biology*, chapter Lipid metabolism in chloroplasts and leaves, pages 85–90. Elsevier North-Holland Biomedical Press.

DellaPenna, D. (2005). A decade of progress in understanding vitamin E synthesis in plants. *J Plant Physiol*, **162**(7), 729–37.

DellaPenna, D. and Pogson, B. (2006). Vitamin synthesis in plants: Tocopherols and carotenoids. *Annu Rev Plant Biol*, **57**, 711–738.

Deruère, J., Römer, S., d'Harlingue, A., Backhaus, R. A., Kuntz, M., and Camara, B. (1994). Fibril assembly and carotenoid overaccumulation in chromoplasts: a model for supramolecular lipoprotein structures. *Plant Cell*, **6**(1), 119–33.

D'Souza, S. E., Ginsberg, M. H., and Plow, E. F. (1991). Arginyl-glycyl-aspartic acid (RGD): a cell adhesion motif. *Trends Biochem Sci*, **16**(7), 246–50.

Duret, S., Bonaly, J., Bariaud, A., Vannereau, A., and Mestre, J. C. (1986). Cadmium-induced ultrastructural changes in Euglena cells. *Environ Res*, **39**(1), 96–103.

Ebel, B., Rosenkranz, J., Schiffgens, A., and Lutz, C. (1990). Cytological observations on spruce needles after prolonged treatment with ozone and acid mist. *Environ Pollut*, **64**(3-4), 323–35.

Estevez, J. M., Cantero, A., Romero, C., Kawaide, H., Jimenez, L. F., Kuzuyama, T., Seto, H., Kamiya, Y., and Leon, P. (2000). Analysis of the expression of *cla1*, a gene that encodes the 1-deoxyxylulose 5-phosphate synthase of the 2-c-methyl-d-erythritol-4-phosphate pathway in Arabidopsis. *Plant Physiol*, **124**(1), 95–104.

Eymery, F. and Rey, P. (1999). Immunocytolocalization of CDSP 32 and CDSP 34, two chloroplastic drought-induced stress proteins in *Solanum tuberosum* plants. *Plant Physiol Biochem*, **37**(4), 305–312.

Falk, J., Kraub, N., Dahnhardt, D., and Krupinska, K. (2002). The senescence associated gene of barley encoding 4-hydroxyphenylpyruvate dioxygenase is expressed during oxidative stress. *J Plant Physiol*, **159**(11), 1245–1253.

Fischer, R., Stoger, E., Schillberg, S., Christou, P., and Twyman, R. M. (2004). Plant-based production of biopharmaceuticals. *Curr Opin Plant Biol*, **7**(2), 152–8.

Foyer, C. H. and Noctor, G. (2005). Redox homeostasis and antioxidant signaling: a metabolic interface between stress perception and physiological responses. *Plant Cell*, **17**(7), 1866–75.

Friso, G., Giacomelli, L., Ytterberg, A. J., Peltier, J. B., Rudella, A., Sun, Q., and Wijk, K. J. (2004). In-depth analysis of the thylakoid membrane proteome of A*rabidopsis thaliana* chloroplasts: new proteins, new functions, and a plastid proteome database. *Plant Cell*, **16**(2), 478–99.

Fukushima, M., Enjoji, M., Kohjima, M., Sugimoto, R., Ohta, S., Kotoh, K., Kuniyoshi, M., Kobayashi, K., Imamura, M., Inoguchi, T., Nakamuta, M., and Nawata, H. (2005). Adipose differentiation related protein induces lipid accumulation and lipid droplet formation in hepatic stellate cells. *In Vitro Cell Dev Biol Anim*, **41**(10), 321–4.

Gala, R., Mita, G., and Caretto, S. (2005). Improving α-tocopherol production in plant cell cultures. *J Plant Physiol*, **162**(7), 782–4.

Garcia, I., Rodgers, M., Pepin, R., Hsieh, T. F., and Matringe, M. (1999). Characterization and subcellular compartmentation of recombinant 4-hydroxyphenylpyruvate dioxygenase from Arabidopsis in transgenic tobacco. *Plant Physiol*, **119**(4), 1507–16.

Ghosh, S., Mahoney, S. R., Penterman, J. N., Peirson, D., and Dumbroff, E. B. (2001). Ultrastructural and biochemical changes in chloroplasts during *Brassica napus* senescence. *Plant Physiol Biochem*, **39**, 777–784.

Giacomelli, L., Rudella, A., and van Wijk, K. J. (2006). High light response of the thylakoid proteome in A*rabidopsis thaliana* wild type and the ascorbate deficient mutant vtc2-2; a comparative proteomics study. *Plant Physiol*, **14**(2), 685–701.

Giddings, G., Allison, G., Brooks, D., and Carter, A. (2000). Transgenic plants as factories for biopharmaceuticals. *Nat Biotech*, **18**(11), 1151–1155.

Gillet, B., Beyly, A., Peltier, G., and Rey, P. (1998). Molecular characterization of CDSP 34, a chloroplastic protein induced by water deficit in *Solanum tuberosum* L. plants, and regulation of CDSP 34 expression by ABA and high illumination. *Plant J*, **16**(2), 257–62.

Goodrich, J. and Tweedie, S. (2002). Remembrance of things past: chromatin remodeling in plant development. *Annu Rev Cell Dev Biol*, **18**, 707–46.

Greenwood, A. D., Leech, R. M., and Williams, J. P. (1963). The osmiophilic globules of chloroplasts. I. Osmiophilic globules as a normal component of chloroplasts and their isolation and composition in *Vicia faba* L. *Biochim Biophys Acta*, **78**, 148–162.

Gubler, U. and Hoffman, B. J. (1983). A simple and very efficient method for generating cDNA libraries. *Gene*, **25**, 263–269.

Guiamet, J. J., Pichersky, E., and Nooden, L. D. (1999). Mass exodus from senescing soybean chloroplasts. *Plant Cell Physiol.*, **40**(9), 986–992.

Hadjeb, N., Gounaris, I., and Price, C. A. (1988). Chromoplast-specific proteins in capsicum annuum. *Plant Physiol*, **88**, 42–45.

Havaux, M., Eymery, F., Porfirova, S., Rey, P., and Dörmann, P. (2005). vitamin E protects against photoinhibition and photooxidative stress in A*rabidopsis thaliana*. *Plant Cell*, **17**(12), 3451–69.

Hennig, L., Stoddart, W. M., Dieterle, M., Whitelam, G. C., and Schafer, E. (2002). Phytochrome E controls light-induced germination of Arabidopsis. *Plant Physiol*, **128**(1), 194–200.

Hernandez, J. A., Ferrer, M. A., Jimenez, A., Barcelo, A. R., and Sevilla, F. (2001). Antioxidant systems and O^{2-}/H_2O_2 production in the apoplast of pea leaves. Its relation with salt-induced necrotic lesions in minor veins. *Plant Physiol*, **127**(3), 817–31.

Hiltbrunner, A., Bauer, J., Vidi, P. A., Infanger, S., Weibel, P., Hohwy, M., and Kessler, F. (2001). Targeting of an abundant cytosolic form of the protein import receptor atToc159 to the outer chloroplast membrane. *J Cell Biol*, **154**(2), 309–16.

Hofius, D. and Sonnewald, U. (2003). vitamin E biosynthesis: biochemistry meets cell biology. *Trends Plant Sci*, **8**(1), 6–8.

Hofius, D., Hajirezaei, M. R., Geiger, M., Tschiersch, H., Melzer, M., and Sonnewald, U. (2004). RNAi-mediated tocopherol deficiency impairs photoassimilate export in transgenic potato plants. *Plant Physiol*, **135**(3), 1256–68.

Hollander-Czytko, H., Grabowski, J., Sandorf, I., Weckermann, K., and Weiler, E. W. (2005). Tocopherol content and activities of tyrosine aminotransferase and cystine lyase in Arabidopsis under stress conditions. *J Plant Physiol*, **162**, 767–770.

Hoober, J. K., Maloney, M. A., Asbury, L. R., and Marks, D. B. (1990). Accumulation of chlorophyll a/b-binding polypeptides in C*hlamydomonas reinhardtii* y-1 in the light or dark at 38 °C: Evidence for proteolytic control. *Plant Physiol*, **92**(2), 419–426.

Hope, R. G., Murphy, D. J., and McLauchlan, J. (2002). The domains required to direct core proteins of hepatitis C virus and GB virus-B to lipid droplets share common features with plant oleosin proteins. *J Biol Chem*, **277**(6), 4261–70.

Hou, A., Liu, K., Catawatcharakul, N., Tang, X., Nguyen, V., Keller, W., Tsang, E., and Cui, Y. (2005). Two naturally occurring deletion mutants of 12s seed storage proteins in *Arabidopsis thaliana*. *Planta*, **222**(3), 512.

Howden, R., Andersen, C. R., Goldsbrough, P. B., and Cobbett, C. S. (1995). A cadmium-sensitive, glutathione-deficient mutant of A*rabidopsis thaliana*. *Plant Physiol*, **107**(4), 1067–73.

Hsieh, K. and Huang, A. H. (2004). Endoplasmic reticulum, oleosins, and oils in seeds and tapetum cells. *Plant Physiol*, **136**(3), 3427–34.

Imamura, M., Inoguchi, T., Ikuyama, S., Taniguchi, S., Kobayashi, K., Nakashima, N., and Nawata, H. (2002). ADRP stimulates lipid accumulation and lipid droplet formation in murine fibroblasts. *Am J Physiol Endocrinol Metab*, **283**(4), 775–83.

Inoue, H., Nojima, H., and Okayama, H. (1990). High efficiency transformation of E*scherichia coli* with plasmids. *Gene*, **96**, 23–28.

Jin, J. B., Kim, Y. A., Kim, S. J., Lee, S. H., Kim, D. H., Cheong, G. W., and Hwang, I. (2001). A new dynamin-like protein, ADL6, is involved in trafficking from the trans-Golgi network to the central vacuole in Arabidopsis. *Plant Cell*, **13**(7), 1511–26.

Joshi, L. and Lopez, L. C. (2005). Bioprospecting in plants for engineered proteins. *Curr Opin Plant Biol*, **8**(2), 223–6.

Joyard, J., Teyssier, E., Miege, C., Berny-Seigneurin, D., Marechal, E., Block, M. A., Dorne, A. J., Rolland, N., Ajlani, G., and Douce, R. (1998). The biochemical machinery of plastid envelope membranes. *Plant Physiol*, **118**(3), 715–23.

Kanwischer, M., Porfirova, S., Bergmüller, E., and Dörmann, P. (2005). Alterations in tocopherol cyclase activity in transgenic and mutant plants of Arabidopsis affect tocopherol content, tocopherol composition, and oxidative stress. *Plant Physiol*, **137**(2), 713–23.

Kaup, M. T., Froese, C. D., and Thompson, J. E. (2002). A role for diacylglycerol acyltransferase during leaf senescence. *Plant Physiol*, **129**(4), 1616–26.

Keller, Y., Bouvier, F., d'Harlingue, A., and Camara, B. (1998). Metabolic compartmentation of plastid prenyllipid biosynthesis - evidence for the involvement of a multifunctional geranylgeranyl reductase. *Eur J Biochem*, **251**(1-2), 413–7.

Keskitalo, J., Bergquist, G., Gardestrom, P., and Jansson, S. (2005). A cellular timetable of autumn senescence. *Plant Physiol*, **139**(4), 1635–48.

Kessler, F., Schnell, D., and Blobel, G. (1999). Identification of proteins associated with plastoglobules isolated from pea (P*isum sativum* L.) chloroplasts. *Planta*, **208**(1), 107–13.

Kim, H. U., Wu, S. S., Ratnayake, C., and Huang, A. H. (2001). B*rassica rapa* has three genes that encode proteins associated with different neutral lipids in plastids of specific tissues. *Plant Physiol*, **126**(1), 330–41.

Kim, H. U., Hsieh, K., Ratnayake, C., and Huang, A. H. (2002). A novel group of oleosins is present inside the pollen of arabidopsis. *J Biol Chem*, **277**(25), 22677–84.

Kleffmann, T., Russenberger, D., von Zychlinski, A., Christopher, W., Sjolander, K., Gruissem, W., and Baginsky, S. (2004). The A*rabidopsis thaliana* chloroplast proteome reveals pathway abundance and novel protein functions. *Curr Biol*, **14**(5), 354–62.

Knoth, R., Hansmann, P., and Sitte, P. (1986). Chromoplasts of P*alisota barteri*, and the molecular structure of chromoplast tubules. *Planta*, **168**, 167–174.

Kroll, D., Meierhoff, K., Bechtold, N., Kinoshita, M., Westphal, S., Vothknecht, U. C., Soll, J., and Westhoff, P. (2001). Vipp1, a nuclear gene of A*rabidopsis thaliana* essential for thylakoid membrane formation. *Proc Natl Acad Sci U S A*, **98**(7), 4238–42.

Kuntz, M., Chen, H. C., Simkin, A. J., Römer, S., Shipton, C. A., Drake, R., Schuch, W., and Bramley, P. M. (1998). Upregulation of two ripening-related genes from a non-climacteric plant (pepper) in a transgenic climacteric plant (tomato). *Plant J*, **13**(0), 351–361.

Kyte, J. and Doolittle, R. (1982). A simple method for displaying the hydropathic character of a protein. *J Mol Biol*, **157**, 105–132.

Laizet, Y., Pontier, D., Mache, R., and Kuntz, M. (2004). Subfamily organization and phylogenetic origin of genes encoding plastid lipid-associated proteins of the fibrillin type. *J Gen Sci Tech*, **3**(1), 19–28.

Langenkamper, G., Manac'h, N., Broin, M., Cuine, S., Becuwe, N., Kuntz, M., and Rey, P. (2001). Accumulation of plastid lipid-associated proteins (fibrillin/CDSPL34) upon oxidative stress, ageing and biotic stress in solanaceae and in response to drought in other species. *J Exp Bot*, **52**(360), 1545–54.

Legget Bailey, J. and Whyborn, A. G. (1963). The osmiophilic globules of chloroplasts. ii. Globules of the spinach-beet chloroplast. *Biochim Biophys Acta*, **78**, 163–174.

Lichtenthaler, H. K. (1968). Plastoglobuli and the fine structure of plastids. *Endeavor*, **27**, 144–149.

Lichtenthaler, H. K. (1969). Zur Synthese der lipophilen Plastidenchinone und Sekundärcarotinoide während der Chromoplastenentwicklung. *Ber Dtsch Bot Ges*, **82**, 483–497.

Lichtenthaler, H. K. and Peveling, E. (1967). Plastoglobuli in verschiedenen Differenzierungsstadien der Plastiden bei A*llium cepa* L. *Planta (Berl.)*, **72**, 1–13.

Lichtenthaler, H. K. and Sprey, B. (1966). Über die osmiophilen globularen Lipideinschlüsse der Chloroplasten. *Z Naturforsch*, **21**, 690–697.

Locy, R. D., Chang, C. C., Nielsen, B. L., and Singh, N. K. (1996). Photosynthesis in salt-adapted heterotrophic tobacco cells and regenerated plants. *Plant Physiol*, **110**(1), 321–328.

Lopukhina, A., Dettenberg, M., Weiler, E. W., and Hollander-Czytko, H. (2001). Cloning and characterization of a coronatine-regulated tyrosine aminotransferase from Arabidopsis. *Plant Physiol*, **126**(4), 1678–87.

Ma, J. K., Drake, P. M., and Christou, P. (2003). The production of recombinant pharmaceutical proteins in plants. *Nat Rev Genet*, **4**(10), 794–805.

Ma, J. K., Barros, E., Bock, R., Christou, P., Dale, P. J., Dix, P. J., Fischer, R., Irwin, J., Mahoney, R., Pezzotti, M., Schillberg, S., Sparrow, P., Stoger, E., and Twyman, R. M. (2005a). Molecular farming for new drugs and vaccines. Current perspectives on the production of pharmaceuticals in transgenic plants. *EMBO Rep*, **6**(7), 593–9.

Ma, J. K., Chikwamba, R., Sparrow, P., Fischer, R., Mahoney, R., and Twyman, R. M. (2005b). Plant-derived pharmaceuticals–the road forward. *Trends Plant Sci*, **10**(12), 580–5.

Maeda, H., Sakuragi, Y., Bryant, D. A., and Dellapenna, D. (2005). Tocopherols protect S*ynechocystis sp.* strain pcc 6803 from lipid peroxidation. *Plant Physiol*, **138**(3), 1422–35.

Manac'h, N. and Kuntz, M. (1999). Stress induction of a nuclear gene encoding for a plastid protein is mediated by photo-oxidative events. *Plant Physiol Biochem*, **37**(11), 859–868.

Mandel, M. A., Feldmann, K. A., Herrera-Estrella, L., Rocha-Sosa, M., and Leon, P. (1996). *cla1*, a novel gene required for chloroplast development, is highly conserved in evolution. *Plant J*, **9**(5), 649–58.

Marano, M. R., Serra, E. C., Orellano, E. G., and Carrrillo, N. (1993). The path of chromoplast development in fruits and flowers. *Plant Sci.*, **94**, 1–17.

Matsui, M., Stoop, C. D., von Arnim, A. G., Wei, N., and Deng, X. W. (1995). Arabidopsis COP1 protein specifically interacts *in vitro* with a cytoskeleton-associated protein, CIP1. *Proc Natl Acad Sci U S A*, **92**(10), 4239–43.

McFadden, G. I. (1999). Endosymbiosis and evolution of the plant cell. *Curr Opin Plant Biol*, **2**(6), 513–9.

Menkhaus, T. J., Bai, Y., Zhang, C., Nikolov, Z. L., and Glatz, C. E. (2004). Considerations for the recovery of recombinant proteins from plants. *Biotechnol Prog*, **20**, 1001–1014.

Merzlyak, M., Solovchenko, A., and Pogosyan, S. (2005). Optical properties of rhodoxanthin accumulated in Aloe *arborescens* Mill. leaves under high-light stress with special reference to its photoprotective function. *Photochem Photobiol Sci*, **4**, 333–340.

Monte, E., Ludevid, D., and Prat, S. (1999). Leaf C40.4: a carotenoid-associated protein involved in the modulation of photosynthetic efficiency? *Plant J*, **19**(4), 399–410.

Moriguchi, T., Kita, M., Endo-Inagaki, T., Ikoma, Y., and Omura, M. (1998). Characterization of a cDNA homologous to carotenoid-associated protein in citrus fruits. *Biochim Biophys Acta*, **1442**(2-3), 334–8.

Morre, D. J., Sellden, G., Sundqvist, C., and Sandelius, A. S. (1991). Stromal low temperature compartment derived from the inner membrane of the chloroplast envelope. *Plant Physiol*, **97**(4), 1558–1564.

Motohashi, R., Ito, T., Kobayashi, M., Taji, T., Nagata, N., Asami, T., Yoshida, S., Yamaguchi-Shinozaki, K., and Shinozaki, K. (2003). Functional analysis of the 37 kDa inner envelope membrane polypeptide in chloroplast biogenesis using a ds-tagged Arabidopsis pale-green mutant. *Plant J*, **34**(5), 719–31.

Munne-Bosch, S. (2005). The role of α-tocopherol in plant stress tolerance. *J Plant Physiol*, **162**, 743–748.

Munne-Bosch, S. and Alegre, L. (2000). Changes in carotenoids, tocopherols and diterpenes during drought and recovery, and the biological significance of chlorophyll loss in Rosmarinus *officinalis* plants. *Planta*, **210**(6), 925–31.

Munne-Bosch, S. and Alegre, L. (2002). Plant aging increases oxidative stress in chloroplasts. *Planta*, **214**(4), 608–15.

Munne-Bosch, S. and Alegre, L. (2003). Drought-induced changes in the redox state of α-tocopherol, ascorbate, and the diterpene carnosic acid in chloroplasts of Labiatae species differing in carnosic acid contents. *Plant Physiol*, **131**(4), 1816–25.

Murphy, D. J. (2001). The biogenesis and functions of lipid bodies in animals, plants and microorganisms. *Prog Lipid Res*, **40**(5), 325–438.

Murray, M. G. and Thompson, W. F. (1980). Rapid isolation of high molecular weight plant DNA. *Nucleic Acids Res*, **8**(19), 4321–5.

Newcomb, E. H. (1967). Fine structure of protein-storing plastids in bean root tips. *J Cell Biol*, **33**(1), 143–63.

Newman, L. A., Hadjeb, N., and Price, C. A. (1989). Synthesis of two chromoplast-specific proteins during fruit development in C*apsicum annuum*. *Plant Physiol*, **91**, 455–458.

Nilsen, E. T., Stetler, D. A., and Gassman, C. A. (1988). Influence of age and microclimate on the photochemistry of R*hododendron maximum* leaves ii. Chloroplast structure and photosynthetic light response. *Amer. J. Bot.*, **75**(10), 1526–1534.

Niyogi, K. K., Grossman, A. R., and Bjorkman, O. (1998). Arabidopsis mutants define a central role for the xanthophyll cycle in the regulation of photosynthetic energy conversion. *Plant Cell*, **10**(7), 1121–34.

Norris, S. R., Shen, X., and DellaPenna, D. (1998). Complementation of the Arabidopsis *pds1* mutation with the gene encoding p-hydroxyphenylpyruvate dioxygenase. *Plant Physiol*, **117**(4), 1317–23.

Oksanen, E., Sober, J., and Karnosky, D. F. (2001). Impacts of elevated CO_2 and/or O_3 on leaf ultrastructure of aspen (P*opulus tremuloides*) and birch (B*etula papyrifera*) in the aspen FACE experiment. *Environ Pollut*, **115**(3), 437–46.

Ostermeyer, A. G., Ramcharan, L. T., Zeng, Y., Lublin, D. M., and Brown, D. A. (2004). Role of the hydrophobic domain in targeting caveolin-1 to lipid droplets. *J Cell Biol*, **164**(1), 69–78.

Panou-Filotheou, H., Bosabalidis, A. M., and Karataglis, S. (2001). Effects of copper toxicity on leaves of oregano (O*riganum vulgare* subsp. *hirtum*). *Ann Bot (Lond)*, **88**, 207–214.

Picher, M., Grenier, G., Purcell, M., proteau, L., and Beaumont, G. (1993). Isolation and purification of intralamellar vesicles from L*emna minor* L. chloroplasts. *New phytol*, **123**, 657–663.

Piffanelli, P., Ross, J. H. E., and Murphy, D. J. (1998). Biogenesis and function of the lipidic structures of pollen grains. *Sex Plant Reprod*, **11**, 65–80.

Porfirova, S., Bergmüller, E., Tropf, S., Lemke, R., and Dörmann, P. (2002). Isolation of an Arabidopsis mutant lacking vitamin E and identification of a cyclase essential for all tocopherol biosynthesis. *Proc Natl Acad Sci U S A*, **99**(19), 12495–500.

Possingham, J. V. and Saurer, W. (1969). Changes in chloroplast number per cell during leaf development in spinach. *Planta*, **86**(2), 186 – 194.

Pozueta-Romero, J., Rafia, F., Houlne, G., Cheniclet, C., Carde, J. P., Schantz, M. L., and Schantz, R. (1997). A ubiquitous plant housekeeping gene, PAP, encodes a major protein component of bell pepper chromoplasts. *Plant Physiol*, **115**(3), 1185–94.

Provencher, L. M., Miao, L., Sinha, N., and Lucas, W. J. (2001). *Sucrose export defective1* encodes a novel protein implicated in chloroplast-to-nucleus signaling. *Plant Cell*, **13**(5), 1127–41.

Pruvot, G., Cuine, S., Peltier, G., and Rey, P. (1996a). Characterization of a novel drought-induced 34-kDa protein located in the thylakoids of S*olanum tuberosum* L. plants. *Planta*, **198**(3), 471–9.

Pruvot, G., Massimino, J., Peltier, G., and Rey, P. (1996b). Effects of low temperature, high salinity and exogenous ABA on the synthesis of two chloroplastic drought-induced proteins in *Solanum tuberosum*. *Physiol Plant*, **97**, 123–131.

Pruzinska, A., Tanner, G., Anders, I., Roca, M., and Hörtensteiner, S. (2003). Chlorophyll breakdown: Pheophorbide *a* oxygenase is a Rieske-type iron-sulfur protein, encoded by the *accelerated cell death 1* gene. *Proc Natl Acad Sci U S A*, **100**(25), 15259–64.

Pyke, K. A. (1999). Plastid division and development. *Plant Cell*, **11**(4), 549–56.

Pyke, K. A. and Page, A. M. (1998). Plastid ontogeny during petal development in Arabidopsis. *Plant Physiol*, **116**(2), 797–803.

Rensink, W. A., Pilon, M., and Weisbeek, P. (1998). Domains of a transit sequence required for *in vivo* import in Arabidopsis chloroplasts. *Plant Physiol*, **118**(2), 691–9.

Rey, P., Gillet, B., Römer, S., Eymery, F., Massimino, J., Peltier, G., and Kuntz, M. (2000). Over-expression of a pepper plastid lipid-associated protein in tobacco leads to changes in plastid ultrastructure and plant development upon stress. *Plant J*, **21**(5), 483–94.

Reynolds, E. S. (1963). The use of lead citrate at high pH as an electron-opaque stain in electron microscopy. *J Cell Biol*, **17**, 208–12.

Rimbach, G., Minihane, A. M., Majewicz, J., Fischer, A., Pallauf, J., Virgli, F., and Weinberg, P. D. (2002). Regulation of cell signalling by vitamin E. *Proc Nutr Soc*, **61**(4), 415–25.

Sakamoto, W., Tamura, T., Hanba-Tomita, Y., and Murata, M. (2002). The VAR1 locus of Arabidopsis encodes a chloroplastic FtsH and is responsible for leaf variegation in the mutant alleles. *Genes Cells*, **7**(8), 769–80.

Sambrook, J. and Russell, D. W. (2001). *Molecular cloning: a laboratory manual*. Cold Spring Harbor Laboratory Press, Cold Spring Harbor, New York.

Sandorf, I. and Hollander-Czytko, H. (2002). Jasmonate is involved in the induction of tyrosine aminotransferase and tocopherol biosynthesis in A*rabidopsis thaliana*. *Planta*, **216**(1), 173–9.

Sattler, S. E., Cahoon, E. B., Coughlan, S. J., and DellaPenna, D. (2003). Characterization of tocopherol cyclases from higher plants and cyanobacteria. Evolutionary implications for tocopherol synthesis and function. *Plant Physiol*, **132**(4), 2184–95.

Sattler, S. E., Gilliland, L. U., Magallanes-Lundback, M., Pollard, M., and DellaPenna, D. (2004). Vitamin E is essential for seed longevity and for preventing lipid peroxidation during germination. *Plant Cell*, **16**(6), 1419–32.

Savidge, B., Weiss, J. D., Wong, Y. H., Lassner, M. W., Mitsky, T. A., Shewmaker, C. K., Post-Beittenmiller, D., and Valentin, H. E. (2002). Isolation and characterization of homogentisate phytyltransferase genes from *Synechocystis sp.* pcc 6803 and Arabidopsis. *Plant Physiol*, **129**(1), 321–32.

Schafer, E. and Bowle, C. (2002). Phytochrome-mediated photoperception and signal transduction in higher plants. *EMBO Rep*, **3**(11), 1042–8.

Schneider, C. (2005). Chemistry and biology of vitamin E. *Mol Nutr Food Res*, **49**(1), 7–30.

Schnell, D. J. and Blobel, G. (1993). Identification of intermediates in the pathway of protein import into chloroplasts and their localization to envelope contact sites. *J Cell Biol*, **120**(1), 103–15.

Schwartz, S. H., Qin, X., and Zeevaart, J. A. (2003). Elucidation of the indirect pathway of abscisic acid biosynthesis by mutants, genes, and enzymes. *Plant Physiol*, **131**(4), 1591–601.

Segrest, J. P., Jones, M. K., De Loof, H., and Dashti, N. (2001). Structure of apolipoprotein B-100 in low density lipoproteins. *J Lipid Res*, **42**(9), 1346–67.

Shinozaki, K. and Yamaguchi-Shinozaki, K. (2000). Molecular responses to dehydration and low temperature: differences and cross-talk between two stress signaling pathways. *Curr Opin Plant Biol*, **3**, 217–223.

Siegenthaler, P.-A. (1998). Molecular organization of acyl lipids in photosynthetic membranes of higher plants. In P.-A. Siegenthaler and N. Murata, editors, *Lipids in photosynthesis: structure, function and genetics*, pages 119–144. Kluwer Academic Press.

Smirnoff, N. (1993). The role of active oxygen in the response of plants to water deficit and desiccation. *New Phytol*, **125**, 27–58.

Smith, N. A., Singh, S. P., Wang, M. B., Stoutjesdijk, P. A., Green, A. G., and Waterhouse, P. M. (2000). Total silencing by intron-spliced hairpin RNAs. *Nature*, **407**(6802), 319–20.

Soll, J. and Schultz, G. (1980). 2-methyl-6-phytylquinol and 2,3-dimethyl-5-phytylquinol as precursors of tocopherol synthesis in spinach chloroplasts. *Phytochem*, **19**, 215–218.

Soll, J., Douce, R., and Schultz, G. (1980). Site of biosynthesis of α-tocopherol in spinach chloroplasts. *FEBS Lett*, **112**, 243–246.

Soll, J., Schultz, G., Joyard, J., Douce, R., and Block, M. A. (1985). Localization of synthesis of prenylquinones in isolated outer and inner envelope membranes from spinach chloroplasts. *Archives of Biochemistry and Biophysics*, **238**(1), 290–299.

Sprey, B. and Lichtenthaler, H. (1966). Zur Frage der Beziehungen zwischen Plastoglobuli und Thylakoidgenese in Gerstenkeimlingen. *Z Naturforschg*, **21b**, 697–699.

Staehelin, L. A. (1986). Chloroplast structure and supramolecular organization of photosynthetic membranes. In L. A. Staehelin and C. J. Arntzen, editors, *Photosynthetic membranes and light harvesting systems*, volume 19 of *Encyclopedia of Plant Physiology*, pages 1–72. Springer, Berlin Heidelberg.

Steinmüller, D. and Tevini, M. (1985). Composition and function of plastoglobuli. i. Isolation and purification from chloroplasts and chromoplasts. *Planta*, **163**, 201–207.

Stocker, A., Fretz, H., Frick, H., Rüttimann, A., and Woggon, W. D. (1996). The substrate specificity of tocopherol cyclase. *Bioorg Med Chem*, **4**(7), 1129–1134.

Subramanian, V., Garcia, A., Sekowski, A., and Brasaemle, D. L. (2004). Hydrophobic sequences target and anchor perilipin a to lipid droplets. *J Lipid Res*, **45**(11), 1983–91.

Targett-Adams, P., Chambers, D., Gledhill, S., Hope, R. G., Coy, J. F., Girod, A., and McLauchlan, J. (2003). Live cell analysis and targeting of the lipid droplet-binding adipocyte differentiation-related protein. *J Biol Chem*, **278**(18), 15998–6007.

Tevini, M. and Steinmüller, D. (1985). Composition and function of plastoglobuli. ii. Lipid composition of leaves and plastoglobuli during beech leaf senescence. *Planta*, **163**, 91–96.

The A*rabidopsis* G*enome* I*nitiative* (2000). Analysis of the genome sequence of the flowering plant A*rabidopsis thaliana*. *Nature*, **408**(6814), 796–815.

Thomson, W. W. and Platt, K. (1973). Plastid ultrastructure in the barrel cactus, E*chinocactus acanthodes*. *New Phytol*, **72**(4), 791–797.

Thomson, W. W. and Whatley, J. M. (1980). Development of nongreen plastids. *Ann Rev Plant Physiol*, **31**, 375–394.

Ting, J. T., Wu, S. S., Ratnayake, C., and Huang, A. H. (1998). Constituents of the tapetosomes and elaioplasts in B*rassica campestris* tapetum and their degradation and retention during microsporogenesis. *Plant J*, **16**(5), 541–51.

Tuquet, C. and Newman, D. W. (1980). Aging and regreening in soybean cotyledons. 1. Ultrastructural changes in plastids and plastoglobuli. *Cytobios*, **29**(113), 43–59.

Valentin, H. E., Lincoln, K., Moshiri, F., Jensen, P. K., Qi, Q., Venkatesh, T. V., Karunanandaa, B., Baszis, S. R., Norris, S. R., Savidge, B., Gruys, K. J., and Last, R. L. (2006). The A*rabidopsis vitamin* E *pathway gene5-1* mutant reveals a critical role for phytol kinase in seed tocopherol biosynthesis. *Plant Cell*, **18**(1), 212–24.

Van Eenennaam, A. L., Lincoln, K., Durrett, T. P., Valentin, H. E., Shewmaker, C. K., Thorne, G. M., Jiang, J., Baszis, S. R., Levering, C. K., Aasen, E. D., Hao, M., Stein, J. C., Norris, S. R., and Last, R. L. (2003). Engineering vitamin E content: from Arabidopsis mutant to soy oil. *Plant Cell*, **15**(12), 3007–19.

Vidi, P. A., Kanwischer, M., Baginsky, S., Austin, J. R., Csucs, G., Dörmann, P., Kessler, F., and Brehelin, C. (2006). Tocopherol cyclase (VTE1) localization and vitamin E accumulation in chloroplast plastoglobule lipoprotein particles. *J Biol Chem*, **281**(16), 11225–34.

Vishnevetsky, M., Ovadis, M., Itzhaki, H., Levy, M., Libal-Weksler, Y., Adam, Z., and Vainstein, A. (1996). Molecular cloning of a carotenoid-associated protein from C*ucumis sativus* corollas: homologous genes involved in carotenoid sequestration in chromoplasts. *Plant J*, **10**(6), 1111–8.

Vishnevetsky, M., Ovadis, M., Zuker, A., and Vainstein, A. (1999). Molecular mechanisms underlying carotenogenesis in the chromoplast: multilevel regulation of carotenoid-associated genes. *Plant J*, **20**(4), 423–31.

Wesley, S. V., Helliwell, C. A., Smith, N. A., Wang, M. B., Rouse, D. T., Liu, Q., Gooding, P. S., Singh, S. P., Abbott, D., Stoutjesdijk, P. A., Robinson, S. P., Gleave, A. P., Green, A. G., and Waterhouse, P. M. (2001). Construct design for efficient, effective and high-throughput gene silencing in plants. *Plant J*, **27**(6), 581–90.

Wessel, D. and Flügge, U. I. (1984). A method for the quantitative recovery of protein in dilute solution in the presence of detergents and lipids. *Anal Biochem*, **138**(1), 141–143.

Westphal, S., Soll, J., and Vothknecht, U. C. (2001). A vesicle transport system inside chloroplasts. *FEBS Lett*, **506**(3), 257–61.

Whatley, J. M. (1983). The ultrastructure of plastids in roots. *Int Rev Cytol*, **85**, 175–220.

Wu, S. S., Platt, K. A., Ratnayake, C., Wang, T. W., Ting, J. T., and Huang, A. H. (1997). Isolation and characterization of neutral-lipid-containing organelles and globuli-filled plastids from B*rassica napus* tapetum. *Proc Natl Acad Sci U S A*, **94**(23), 12711–12716.

Yang, Y., Sulpice, R., Himmelbach, A., Meinhard, M., Christmann, A., and Grill, E. (2006). Fibrillin expression is regulated by abscisic acid response regulators and is involved in abscisic acid-mediated photoprotection. *Proc Natl Acad Sci U S A*, **103**(15), 6061–6.

Ytterberg, A. J., Peltier, J. B., and van Wijk, K. J. (2006). Protein profiling of plastoglobules in chloroplasts and chromoplasts. a surprising site for differential accumulation of metabolic enzymes. *Plant Physiol*, **140**(3), 984–97.

Yu, T. S. and Li, H. (2001). Chloroplast protein translocon components atToc159 and atToc33 are not essential for chloroplast biogenesis in guard cells and root cells. *Plant Physiol*, **127**(1), 90–6.

Zimmer, S., Stocker, A., Sarbolouki, M. N., Spycher, S. E., Sassoon, J., and Azzi, A. (2000). A novel human tocopherol-associated protein: cloning, in vitro expression, and characterization. *J Biol Chem*, **275**(33), 25672–80.

Zimmermann, P., Hirsch-Hoffmann, M., Hennig, L., and Gruissem, W. (2004). Genevestigator. Arabidopsis microarray database and analysis toolbox. *Plant Physiol*, **136**(1), 2621–32.

Acknowledgments

First of all, I would like to thank Prof. Dr. Felix Kessler for giving me the opportunity to perform my Ph.D. thesis in his group at the Laboratory of Plant Physiology, University of Neuchâtel. I highly appreciated his communicative enthusiasm and his numerous motivating ideas. I am deeply grateful for his support and encouragement throughout my thesis work, as well as for the opportunities he gave me to initiate interesting collaborations.

I would also like to acknowledge Prof. Dr. Jean-Marc Neuhaus, Prof. Dr. Samuel Zeeman and Prof. Dr. Danny Schnell for accepting to serve in my thesis committee.

A special acknowledgement goes for Dr. Claire Bréhélin for advice and inspiring discussion, as well as for DNA constructs and antibodies.

I am indebted to Dr. Gabor Csucs for introducing me to confocal microscopy and to Joanne Schwaar and Christelle Joss for invaluable technical assistance. Also, I would like to thank Dr. Andreas Hiltbrunner, Dr. Petra Weibel, Dr. Birgit Agne, Sibylle Infanger, Michaël Illeguems and Gwendoline Rahim for discussion and contributions to this work.

Additional thanks go to Romain Bessire for his frequent advice regarding informatics, as well as to Jana Smutny and Marlyse Meylan for taking care of general laboratory equipment and managing the ordering.

I am grateful, too, to Dr. P. Dörmann, Prof. Dr. E. Schäfer, Prof. Dr. C. Frankhauser, Dr. M. Alvarez-Huerta, Prof. Dr. I. Small, Prof. Dr. K. Apel and Dr. S. Crafts-Brandner for kindly providing antibodies and plasmid constructs.

Last but not least, I am grateful to my parents for their support and would like to thank Joëlle for her help with LaTeX business and most importantly for her love and her patience.